A thesis on

MECHANISMS OF THE PLASTIC DEFORMATION OF MOLYBDENUM

by

Raimo Norman Orava

submitted for the degree of Doctor of Philosophy
in the University of London.

August, 1963

Department of Metallurgy,
Imperial College of Science
and Technology,
Prince Consort Road,
London, S.W.7.

ABSTRACT.

The influence of grain size, temperature and strain rate on the low temperature ($< 0.2T_m$) tensile properties of polycrystalline arc-cast molybdenum of purity >99.97% have been investigated. A model for yielding based on the multiplication and velocity characteristics of dislocations provided the best unified treatment of the grain-size, temperature and strain-rate dependence of yielding and subsequent flow behaviour.

The lattice friction stress is closely related to the single crystal yield stress and neither can be identified with the Petch parameter σ_I. In addition to the effect of grain boundaries, k_Y includes a contribution which arises from the decrease in mobile dislocation density with grain size. The value of k_f ($< k_Y$) for flow is more representative of the influence of grain boundaries on yielding than k_Y itself. Slip is probably transmitted from grain to grain by the athermal generation of fresh dislocations at or near grain boundaries. An explanation, based on the grain-size dependence of dislocation multiplication and velocity characteristics, is given for the observed contradictions in the temperature behaviour of k_Y in molybdenum and other b.c.c. transition metals.

Combining the results of the grain-size analysis and thermal activation analysis, the rate-controlling mechanism is established as one of overcoming the Peierls stress. A correction is introduced for the stress-dependence of the frequency factor ν in the equation for thermally activated yielding and flow.

The relationship between $\log \dot{\epsilon}$ and the lower yield stress of fine-grained material may be represented by several consecutive straight lines of different slopes for strain rates below $\sim 0.5 \times 10^{-4} \text{sec.}^{-1}$ Attempts have been made in the past to associate these different linear regions with different rate-controlling mechanisms. This procedure is questioned in the case of molybdenum. Evidence favours the view that they may be caused by spurious grain-boundary effects during the propagation of yielding.

TABLE OF CONTENTS.

	Page No.
TITLE PAGE	1
ABSTRACT	2
TABLE OF CONTENTS	4
LIST OF FIGURES	6
LIST OF TABLES	10
1. INTRODUCTION	
1.1 Purpose of the Investigation	11
1.2 The Yield Point Phenomenon	12
1.3 Yield Propagation	22
1.4 The Grain-size Analysis	25
1.4.1 Interpretation of k	26
1.4.2 Interpretation of σ_o	31
1.5 The Activation Analysis	33
1.6 Rate-controlling Mechanisms	38
2. EXPERIMENTAL PROCEDURE	
2.1 Selection of Experiments and Material	41
2.2 Preparation of the Material	42
2.2.1 Material	42
2.2.2 Fabrication	43
2.3 Achievement of Variation in Grain Size	44
2.4 Metallographic Technique	45
2.5 Testing Techniques	48
2.5.1 Testing Machines	48
2.5.2 Testing Temperatures	50
3. EXPERIMENTAL RESULTS	
3.1 The Effect of Grain Size on Tensile Properties	53
3.1.1 Load-elongation Curve	53
3.1.2 Yielding Characteristics	55

3.1.3 Flow Stress 57
3.1.4 Work-hardening Rate 57
3.1.5 Fracture Properties 59
3.1.6 Petch Parameters Determined by the Extrapolation Method 60
3.2 The Effect of Strain Rate on Tensile Properties 61
3.2.1 Load-elongation Curve 62
3.2.2 Yielding Characteristics 63
3.2.3 Flow Stress 67
3.2.4 Petch Parameters 71
3.2.5 Additional Observations 73
3.3 The Effect of Temperature on Tensile Properties 75
3.3.1 Yielding Characteristics 76
3.3.2 Flow Stress 77
3.4 Evaluation of the Activation Parameters 79
3.4.1 The Activation Energy, H 80
3.4.2 The Activation Volume, v^* 81
3.4.3 The Frequency Factor, ν 83

4. DISCUSSION
4.1 The Model for Yielding 85
4.2 The Yield Point 86
4.3 The Grain-size Analysis 93
4.3.1 Characteristics of k 95
4.3.2 Characteristics of σ_o 105
4.4 The Activation Analysis 107
4.5 The Strain-rate Behaviour of σ_Y 111

5. CONCLUSIONS 113

SUGGESTIONS FOR FUTURE RESEARCH 118

ACKNOWLEDGEMENTS 120

REFERENCES 121

LIST OF FIGURES.

Figure No.		Page No.
1.	Schematic representation of the force-distance relationship for thermally activated yielding or flow.	126
2.	The effect of grain size on the load-elongation curve of molybdenum at 293°K and a strain rate of 0.88×10^{-4} sec.$^{-1}$ (Ingot 1).	127
3.	The effect of testing machine on the load-elongation curve of molybdenum with a grain size of (a) 0.027 mm. and (b) 0.098 mm. at 293°K and strain rate of 0.88×10^{-4} sec.$^{-1}$ (Ingot 2).	128
4.	The effect of grain size on the yield and fracture stress of molybdenum at 293°K and a strain rate of 0.88×10^{-4} sec.$^{-1}$ (Ingot 1).	129
5.	The effect of grain size on the (a) Lüders strain and (b) yield drop of molybdenum at 293°K and a strain rate of 0.88×10^{-4} sec.$^{-1}$ (Ingot 1).	130
6.	The effect of grain size on the flow stress of molybdenum at 293°K and a strain rate of 0.88×10^{-4} sec.$^{-1}$ (Ingot 1)	131
7.	The effect of grain size on the applicability of the relation $\sigma_T = K \epsilon_T^n$ to the flow curve of molybdenum at 293°K and a strain rate of 0.88×10^{-4} sec.$^{-1}$ (Ingot 1).	132
8.	The effect of grain size on the work-hardening parameters of molybdenum at 293°K and a strain rate of 0.88×10^{-4} sec.$^{-1}$ (Ingot 1).	133

9. The effect of grain size on the reduction in cross-sectional area at fracture of molybdenum at 293°K and a strain rate of 0.88 x 10^{-4} $sec.^{-1}$ (Ingot 1). 134

10. The extrapolation method of obtaining the Petch parameters from a single stress-strain curve. 135

11. The effect of grain size on the Petch parameters for molybdenum determined by extrapolation of stress-strain curves obtained at 293°K and a strain rate of 0.88 x 10^{-4} $sec.^{-1}$ Dashed lines indicate parameters taken from the Petch plot. 136

12. The effect of strain rate on the load-elongation curve of molybdenum with a grain size of 0.027 mm. at 293°K (Ingot 2). 137

13. The effect of strain rate on the load-elongation curve of molybdenum with a grain size of 0.098 mm. at 293°K (Ingot 2). 138

14. The effect of strain rate on the lower yield stress of molybdenum with a grain size of 0.027 mm. (x) and 0.098 mm. (o) (Ingot 2). 139

15. The effect of strain rate on the upper yield stress of molybdenum with a grain size of 0.027 mm. (x) and 0.098 mm.(o). The points(⊠) represent tests conducted on a Hounsfield Tensometer. (Ingot 2). Dashed lines denote lower yield stress data. 140

16. The effect of strain rate on the Lüders strain of molybdenum with a grain size of 0.027 mm. (Ingot 2). 141

17. A typical load-elongation curve for molybdenum with a grain size of 0.027 mm. cycled between 0.88 x 10^{-4} $sec.^{-1}$ and 1.8 x 10^{-3} $sec.^{-1}$ at 293°K. 142

18. The effect of stress on the reversible change in flow stress of molybdenum with a grain size of 0.027 mm. from strain-rate factor change experiments. (Ingot 2). 143

19. The effect of strain-rate factor on the reversible change in flow stress of molybdenum with a grain size of 0.027 mm. (Ingot 2). 144

20. The effect of stress on the reversible change in flow stress of molybdenum with a grain size of 0.027 mm. from basic strain-rate change experiments at 293°K for $\dot{\epsilon}_f / \dot{\epsilon}_i = 2$. The results for $\dot{\epsilon}_f / \dot{\epsilon}_i = 20$ are given for comparison. (Ingot 2). 145

21. The effect of strain rate on the Petch parameters (a) k_Y (b) σ_I of molybdenum. Actual data points shown were obtained from Petch plots. (Ingot 2). 146

22. The effect of strain rate on the Petch relation of molybdenum at 293°K. (Ingot 2). 147

23. The effect of temperature on the yield stress of molybdenum at a strain rate of 0.88×10^{-4} sec.$^{-1}$ (Ingot 2). 148

24. The effect of temperature on the Lüders strain of molybdenum with a grain size of 0.027 mm. at a strain rate of 0.88×10^{-4} sec.$^{-1}$ (Ingot 2). 149

25. The effect of stress on the reversible change in flow stress due to a change in temperature from 293°K for molybdenum with a grain size of 0.027 mm. at a strain rate of 0.88×10^{-4} sec.$^{-1}$ (Ingot 2). 150

26. The effect of temperature on the lower yield and flow stress of molybdenum with a grain size of 0.027 mm. at a strain rate of 0.88×10^{-4} $sec.^{-1}$ (Ingot 2). 151

27. The stress-dependence of the activation energy for the yielding and flow of molybdenum. (Ingot 2). 152

28. The stress-dependence of the activation volume for the yielding and flow of molybdenum. 153

29. The stress-dependence of the activation volume for the flow of molybdenum from basic strain-rate change experiments. 154

30. The effect of strain rate on the lower yield stress of molybdenum and En2 steel at $293^{\circ}K$ 155

31. Dislocation substructure in annealed molybdenum with a grain size of (a) 0.027 mm. and (b) 0.098 mm., revealed by etch-pitting. X 500. 156

32. Dislocation substructure in molybdenum with a grain size of 0.098 mm. annealed at $1600^{\circ}C$ for 1 hour subsequent to a pre-strain of 5%, revealed by etch-pitting. X 500. 157

LIST OF TABLES.

Table No.		Page No.
1.	Effect of fabrication treatment on grain-size	44
2.	Effect of strain-anneal treatment on grain-size. Duration of anneal: 1 hour	45
3.	Effect of grain-coarsening and subsequent strain-anneal treatment on grain-size . Duration of anneal: 1 hour	46
4.	Temperature media and corresponding temperatures	51
5.	Values of the constants in the equation $\sigma_Y = \alpha + \beta \log \dot{\epsilon}$	66
6.	The strain rate at the transition points in the yield stress-strain rate curves for specimens with a grain size of 0.027 mm.	66
7.	Values of the activation energy, H, for the yielding and flow of polycrystalline molybdenum	81
8.	Values of the activation volume, v^*, for the yielding and flow of polycrystalline molybdenum	82
9.	The stress dependence of the dislocation velocity obtained from the strain-rate sensitivity of the yield stress (m') and flow stress (m), evaluated at a strain rate of 0.88×10^{-4} sec.$^{-1}$	92

1. INTRODUCTION.

1.1 Purpose of the Investigation.

The growing demand during the last decade for new and improved materials to meet the stringent requirements of the atomic and space age has stimulated considerable fundamental research into the deformation and fracture of the body-centred cubic transition metals, namely, iron, molybdenum, chromium, tungsten, niobium, tantalum and vanadium. These metals exhibit similar properties and, with the exception of tantalum, have been shown to undergo a change from ductile to brittle behaviour as the temperature is lowered. This effect, which is extremely important in structural components, seems to be closely related to the rapid increase in yield stress with decreasing temperature which precedes the onset of brittleness. Consequently, a precise knowledge of the dislocation mechanisms which control yielding and flow is essential to an understanding of the above phenomena and to the formulation of specific models for deformation and fracture.

In theory, one cannot over-emphasize the importance of using single crystals of ultra-pure materials in attempting to develop an understanding of the microscopic mechanisms which govern deformation behaviour. Neither can one ignore the fact that materials of commercial purity, in polycrystalline form, are used in nearly all practical engineering applications because of their more attractive strength properties and far greater availability. What information then, if any, can be derived from a study of the latter ? It is the aim of this investigation to

examine critically the two most widely recognized, yet controversial techniques which have been utilized in such studies to date, the grain-size analysis and the thermal activation analysis. Both will be applied to analyse the low temperature yielding and flow characteristics of a representative b.c.c. transition metal, in an attempt to resolve some of the apparent discrepancies which have arisen. Accordingly, it is proposed to consider which of the current models for yielding provides the most unified treatment of the experimental observations.

The choice of a specific metal and the selection of experiments will be discussed after the existing literature on the subject has been reviewed.

1.2 The Yield Point Phenomenon.

One of the features of the plastic deformation of annealed single crystals and polycrystals of b.c.c. metals which contain small amounts of interstitial impurities is the pronounced drop in load which occurs in the early stages of yielding. This "yield drop" results in the observation of a sharp "yield point", a phenomenon often described as "discontinuous yielding". We shall consider only yield points which are believed to arise as a direct result of an increase in the number of mobile dislocations during deformation by slip. Other effects can lead to the observation of yield drops as well, of which those due to mechanical twinning are the most familiar. However, these effects will not concern us in the investigation.

Two significant contributions have been made to an understanding of the particularly sharp yield point occuring in b.c.c. metals. The earlier theory, proposed by Cottrell[1], and Cottrell and Bilby[2], is based on the existence of elastic stress fields about dislocations and impurity atoms, which induce interactions between them. As a consequence, the strain energy of the lattice is reduced when the former take up preferred sites near dislocations. In this way, the dislocations are immobilised, "pinned", or "locked". The mechanics of pinning, and the necessary presence of interstitial impurities to ensure the immobility of dislocations of both screw and edge orientation are well established[1-6].

If dislocations are pinned in the manner just proscribed, yielding can occur when the stress acting on the dislocations is sufficient to free them from their impurity atmospheres. Since the unpinning stress is more than that required to move fresh dislocations an abrupt drop from the upper yield stress to the lower yield stress ensues to produce the yield point. This assumes that the rate of straining is too high and temperature too low for the atmospheres themselves to be mobile. Assuming a condensed atmosphere of carbon in α-iron in the form of a single line in a position close and parallel to a dislocation, with one solute atom per atomic plane, it is estimated[1,2], for example, that a concentration of 10^{-7}% by weight of carbon would be sufficient to give a full yield point for an initial dislocation density of 10^{8} lines cm^{-2}. The dependence of the magnitude and existence of the yield drop on interstitial

impurities has been conclusively demonstrated[7-9].

Another important feature of the impurity yield point model is that it provides one explanation for the temperature and strain-rate dependence of the yield stress[2,5,6,10,11]. Qualitatively, the initial stage of unpinning is envisaged as the breaking away of a small loop of dislocation, a few atomic diameters in length, from the condensed row of solute atoms. As the distance moved by the loop to an unpinned position is considered to be of the order of the wave-length of thermal vibrations, the break-away process can be thermally assisted. The higher the temperature, the greater the thermal energy available, with the result that the applied stress for yielding decreases rapidly with increasing temperature. Cottrell[6] estimates the activation energy for unpinning as

$$U = 0.9 \left(1 - \sigma / \sigma_0 \right)^3 \text{ eV} \qquad (1)$$

for the range of applied stress between 0.2 and 0.8 σ_0 where σ_0 is the true unpinning stress, i.e at temperature near $0^{\circ}K$. As thermal fluctuations with energy of order 0.3 eV(35kT) are not uncommon at $100^{\circ}K$, the observed break-away stress should fall by two-thirds of σ_0 during the first $100^{\circ}K$ rise in temperature. Thereafter, at higher temperatures, the fall should be less rapid. This is in fair agreement with experience[2].

The effect of strain rate on the yield stress is explained[6] on the basis of the probability of the occurrence of thermal fluctuations of the required magnitude in the time interval when the stress is within a given range. For example, for a high strain rate this

interval is smaller than for a low strain rate. Therefore, the probability is lower, and the yield stress is correspondingly higher.

One inadequacy of the unpinning hypothesis is its failure to account for the observation that the upper yield stress, lower yield stress and flow stress all exhibit the same temperature dependence[12,13] and the same strain-rate dependence[14,15]. This difficulty arises from the fact that the dislocations which contribute to the flow stress are most certainly free from atmospheres at low and ambient temperatures. In addition, Cochardt et al[4] cast doubt on the idea of a single line distribution and proposed a more extensive atmosphere. The direct observation by transmission electron microscopy of particles formed on dislocations in iron tends to support this view[16,17]. Under the circumstances, to release a dislocation from its atmosphere would require the nucleation of a more extensive loop. It is possible that any thermal contribution to the energy necessary to form such a loop would be negligibly small, thereby predicting a yield stress independent of temperature, which is clearly not the case in practice. This suggests that some mechanism other than unpinning must control yielding and flow.

These apparent discrepancies between theory and experiment, along with others to be outlined in following sections, directed Hahn's attention[18] to an alternative view of the yield point originally forwarded by Johnston and Gilman[19] to explain the behaviour of their lithium fluoride single crystals. They found that dislocation responsible for slip nucleated heterogenously[20] and multiplied

rapidly[21] without any evidence for the unpinning of grown-in dislocations. The yield point was accounted for in terms of the rapid multiplication of dislocations and the stress-dependence of their velocity. Johnston[22] gives a fuller quantitative outline of the theory but finds it expedient to distinguish two types of yield point, the multiplication yield point characteristic of LiF, and the sharper impurity yield point of Cottrell which occurs in materials like iron. As will become evident, this distinction is probably unnecessary.

The model for yielding derived by Hahn[18] resembles that of Johnston and Gilman except that it is based on the observed properties of dislocations in iron and steel, not LiF. Consequently, there is some justification for believing that the model may be applicable to the related b.c.c. transition metals as well, when their closely allied behaviour is taken into consideration.

The essential points of Hahn's development are as follows. The total strain rate $\dot{\epsilon}$, imposed by a testing machine in compression or tension has two components, the elastic rate, $\dot{\epsilon}_e$, of the machine and specimen, and the plastic rate, $\dot{\epsilon}_p$, of the specimen. Thus,

$$\dot{\epsilon} = \dot{\epsilon}_e + \dot{\epsilon}_p \qquad (2)$$

The plastic strain rate is maintained by the motion of L lines per unit volume of mobile dislocations of strength b at a velocity, v, so that[5]

$$\dot{\epsilon}_p = \phi\, bLv \qquad (3)$$

where $\phi \leq 0.5$ for tension. To establish an analytical relation for

the stress-strain curve, one must express L and v in terms of stress, σ, and strain, ϵ_p.

Etch-pitting[19,23] and electron microscopy[24,25] have shown that the total dislocation density, ρ, increases with strain in the manner,

$$\rho = C \epsilon_p^a \tag{4}$$

for $10^{-3} < \epsilon_p < 10^{-1}$ where C and a are constants. To take account of smaller strains

$$\rho = \rho_o + C \epsilon_p^a \tag{5}$$

is assumed valid to a first approximation. In the absence of dislocation locking ρ_o represents the grown-in dislocation density. However, when dislocations are locked, ρ_o is regardod by Hahn as the average density of unlocked dislocations which are created heterogenously at a stress level below that associated with significant mobility. Since there is no measured relation between the mobile dislocation density, L, and ρ, it is further assumed that

$$L = f \rho \tag{6}$$

with $f \simeq 0.1$ for the case of mobile dislocations freshly produced by deformation. Initially, L_o must correspond to ρ_o independent of which of the above interpretations holds for ρ_o.

The influence of stress on dislocation velocity in silicon-iron was found by Stein and Low[26] to be given by

$$v = (\sigma / \sigma_o)^m \qquad (7)$$

where σ_o is the tensile stress corresponding to unit velocity and m is a constant. Gilman and Johnston[27] find that the work-hardening in LiF closely approximates the stress increment, $\Delta\sigma$, needed to maintain a given veloctiy. Hahn accepts this as conditionally applicable to metals in order to include the influence of work-hardening. This yields a linear work-hardening law of the form

$$\Delta\sigma = q \epsilon_p \qquad (8)$$

where q is the work-hardening rate. Therefore, it follows that

$$v = (\sigma_o)^{-m} (\sigma - q \epsilon_p)^m \qquad (9)$$

A suitable combination of Equations (3)(5)(6) and (9) yields the equation

$$\sigma = q \epsilon_p + \sigma_o \left(\frac{\dot{\epsilon}_p}{\phi b f (\rho_o + c \epsilon_p^a)} \right)^{1/m} \qquad (10)$$

by neglecting the contribution to $\dot{\epsilon}_e$.

This expression enables Hahn to account for many features of b.c.c. deformation by utilizing, not dislocation unpinning, but the multiplication and velocity characteristics of dislocations. At the moment, we can deal conveniently with one of these features, namely, the yield point itself.

On Hahn's model, abrupt yielding is a consequence of the presence of a small number of mobile dislocations initially (small L_o), rapid multiplication (large a), and a low sensitivity of dislocation velocity to stress (small m). In view of the usually

large number of grown-in dislocations in metals, $10^6 - 10^8 cm.^{-2}$, it is suggested that impurity locking immobilizes them in order to satisfy the first condition. However, it is not necessary to postulate unpinning for the occurrence of a yield point, although the possibility is not excluded by Hahn. Note that in neglecting $\dot{\epsilon}_e$, the model requires a non-zero L_o for a finite yield stress.

The above treatment suffers from certain difficulties. To be consistent, ρ_o, by definition of ρ in Equation (5), should pertain to the total dislocation density at $\epsilon_p = 0$. This would immediately fix L_o as one-tenth of ρ_o, normally a high value. If grown-in dislocations are locked, then L_o would be too high. Irrespective of the definition of ρ_o, our knowledge of the magnitude of the mobile dislocation density L_o to be accorded to the upper yield point is insufficient to permit an absolute comparison between the predictions of the model and experimental observations. At best, from a series of values assumed for L_o in performing calculations, one can only select that value which gives the closest agreement between the predicted and experimentally determined upper yield stresses. Despite this uncertainty, a key point is that the subsequent yield drop follows directly from the model. Therefore, the requirement that yielding and subsequent flow be governed by the motion of free dislocations is satisfied. Finally, Hahn does not deal with the temperature and grain-size dependence, but suggests that they arise through the influence of temperature and grain size on one or more of the parameters in Equation (10). As the

role of temperature in Equation (10) is not directly known, it may be rather optimistic to term it a mechanical equation of state.

More recently, Cottrell[27] himself turned to the seemingly more satisfactory interpretation of discontinuous yielding in terms of dislocation mechanics. However, he rewrites Equation (10) in a slightly different form:

$$\sigma = q\,\epsilon_p + \sigma_o \left(\frac{\dot{\epsilon}_p}{\phi b\,(L_o + fG\,\epsilon_p^{a})} \right)^{1/m} \qquad (11)$$

thereby introducing the possibility that the mobile dislocation density need not be related initially to ρ_o by the fixed factor of 0.1. Therefore, it is suggested that sharp yield points can occur if one of three conditions is satisfied. Firstly, if

$$\rho_o = 0 \qquad (12)$$

and stress concentrations are not important, macroscopic yielding begins when the stress is able to create dislocations in the undislocated lattice. The stress then drops to the level necessary to move and multiply them. As this condition is seldom satisfied, this type of yielding is rare. Secondly, if

$$L_o = 0, \quad \rho_o > 0 \qquad (13)$$

and stress concentrations are not important, then it is not necessary to have a total absence of dislocations initially, but only that they be locked by impurities. Yielding will then begin when initial dislocations become unpinned,(weak pinning), or when new dislocations are created (strong pinning) at the upper yield

point depending on which is the easier process. Lastly, if

$$L_o > 0 \qquad (14)$$

and, additionally, the multiplication and velocity conditions are met, then the yield drop evolves by multiplication as suggested by Hahn. Thus, Cottrell[27] distinguishes, as does Johnston, between yielding by creation and yielding by multiplication of dislocations but with the reservation that unpinning in the creation process need not occur if locking is strong. Furthermore, to reduce L_o to a small value, pinning is still a primary requisite. However, Cottrell[27] agrees that a yield point by creation (or unpinning) would occur only under exceptional conditions such as these in the experiments of Hutchison[13]. That is to say, in the presence of strong pinning, stress concentrations are usually sufficient to create dislocations in their immediate vicinity at an applied stress level below the upper yield point. This, of course, leads once more to a multiplication yield point. It is revealing that Hutchison himself concludes from his own results that the temperature dependence of the upper and lower yield stress of polycrystalline iron at low temperatures results mainly from the stress required to move free dislocation and not to unpin them.

It appears, therefore, that one can reasonably conclude that the model of yielding based on the dynamical glide properties of dislocations is the most plausible one for normal b.c.c. metals tested under normal conditions.

1.3 Yield Propagation.

In many instances, the yielding of annealed impure b.c.c. transition metals, whether polycrystals or single crystals, is nucleated locally on a macroscopic scale. Consequently, positive work hardening, as shown by a load-elongation curve, does not ensue until yielding has spread over the whole of a specimen after a few percent strain, usually termed the "Lüders strain"[28] or "lower yield extension". During the course of this initial deformation, yielding is seen to propagate, without an appreciable variation in stress, by the traversal of the gauge length of one or more Lüders bands, originating from the localized regions [29].

Theories of Luders band propagation are closely allied to yield point theories. Supporters of the impurity yield point invoke dislocation unpinning as a necessary step in yield propagation whereas the ideas incorporated in a yield point theory based on dislocation mechanics can be extended to Lüders band propagation without the prerequisite of unpinning. Let us then consider the sequence of events associated with the yield process in the two approaches.

All agree that non-uniform yielding is initially a consequence of a non-uniform distribution of stress in a specimen. The true upper yield point is seldom reached in practice because non-axial loading, scratches, changes in cross-section, internal stress at corners of grains and inclusions provide stress concentrations which can set off local yielding prematurely. In detail, Cottrell believed at one time[30] that yielding is propagated as follows. In the pre-

yield region a few dislocation sources become unpinned and release an avalanche of dislocations into their planes, giving rise to the often observed pre-yield micro-strain[31,32]. Thereafter, the freed dislocations pile up at grain boundaries and the stress concentration at the tip of the pile-ups activates pinned sources in the next grain. The upper yield stress is generally regarded as the applied stress necessary to propagate yield across the first grain boundaries. As the number of points where the activation mechanism operates increases, the stress required to maintain propagation falls, resulting in the yield drop. When the yielded region has encompassed the whole cross-section, propagation proceeds as a Lüders band at the lower yield stress, until the whole specimen has yielded. At this stage, one can foresee three obvious difficulties with this concept of yield propagation. Firstly, the existence of dislocation pile-ups in b.c.c. metals has not been confirmed by direct observation. Secondly, the theory is not applicable to single crystals, in which non-uniform yielding has been observed[9,33]. Lastly, as already mentioned, the lower yield stress has a similar temperature[12,13] and strain-rate[14,15] dependence to the subsequent flow stress suggesting that unpinning may not be the controlling process in yield propagation.

As an alternative, Hahn[18] presents a unified treatment of the lower yield stress and yield propagation which appears to be more satisfactory. He argues that regions where ρ_o and stress exceed the average will yield more rapidly. The yield point still occurs

by dislocation multiplication but in a localized manner before the upper yield stress of the bulk is attained. Thereby, one or more embryonic Lüders bands are established which can propagate to cause yielding of the specimen heterogeneously and more readily than if it were necessary to initiate yielding in the undeformed matrix homogeneously. The detailed growth process itself involves the injection of dislocations generated in the band short distances into the regions immediately adjacent to the band front. Even in the event of strong locking, sufficient free dislocations are now present to satisfy the needs of further deformation so that successive steps of this kind lead to a complete yielding of the specimen. Although propagation occurs at the lower yield stress, it has no mechanistic interpretation according to Hahn. Its magnitude is merely dictated by the extension rate of the testing machine. A similar view of the non-uniform yielding process was adopted by Conrad[34] to accompany his conclusions that yielding is governed by the motion of free dislocations. In addition to the advantage that it applies to free dislocations, Hahn's approach can be applied to single crystals which do not contain grain boundaries against which dislocation may pile up. Once more it should be emphasized that pinning is still required to limit the number of mobile dislocations in normally dislocated materials.

Most recently, Cottrell[27] has expressed agreement with the basic concept of propagation by multiplication but also emphasizes the importance of the role played by pinning.

In summary, it appears that the yielding process in annealed (or strain-aged) b.c.c. metals is best interpreted in terms of the dynamical glide properties of dislocations with the provision that discontinuous and non-uniform yielding to the degree in which they are observed experimentally cannot occur without the existence of strong dislocation pinning.

1.4 The Grain-size Analysis.

The earliest technique employed in attempts to understand the dislocation mechanisms which control the yielding and flow of polycrystalline b.c.c. transition metals at low temperatures involves the study of the influence of grain size on these properties. The most information can be gained from a corresponding investigation of the effect of various testing and specimen parameters on the observed grain-size dependence.

Considerable experimental evidence suggests that the relation between the yield or flow stress, σ, and the grain diameter, l, for each of the b.c.c. transition metals takes the form

$$\sigma = \sigma_o + k l^{-\frac{1}{2}} \qquad (15)$$

where σ_o and k are empirical constants which may be functions of temperature, strain rate, strain, impurity content and distribution, and dislocation structure etc. The equation has become known as the Petch equation and σ_o and k as the Petch parameters, after one of the principal originators[35]. Only molybdenum, after neutron irradiation, has been found to deviate from this pattern of behaviour[36,48]. For Equation (15) to have any mechanistic use, σ_o

and k must be interpreted theoretically in terms of the properties of dislocations.

1.4.1 Interpretation of k.

The bulk of the work on grain-size effects has been directed at non-uniform yielding. Hall[38], Petch[35], Stroh[39] and Cottrell[30] were primarily responsible for the earliest interpretations of the grain-size parameters σ_I and k_Y in the observed relation between the lower yield stress σ_Y, and grain diameter, given by

$$\sigma_Y = \sigma_I + k_Y l^{-\frac{1}{2}} \qquad (16)$$

Their models were based on the propagation of yielding by the passage of Lüders fronts from grain to grain at the lower yield point under the action of a concentrated stress ahead of an array of like dislocations piled up at a grain boundary. However, there is one fundamental difference between the Hall-Petch treatment and the Stroh-Cottrell approach, quite apart from numerical constants. In the former, yielding can propagate when the combined stress is sufficient to emit dislocations from a solute strengthened grain boundary. As a consequence the strength of the boundary plays the dominant role in determining k_Y. In the latter, the combined stress is thought to unpin and activate Frank-Read sources in an adjacent grain and, as a result, k_Y is a measure of the unpinning stress. Since Cottrell's model more conveniently accounted for strain-ageing and the observed influence of the strength of locking on k_Y, it seemed at the time to be the more satisfactory. It also provided a useful extension to fracture phenomena. By using the expression

for the stress concentration at the tip of a pile-up developed by Eshelby et al[40] he obtained

$$k_Y = 2\sqrt{2}\,\tau_d l_d^{\frac{1}{2}} \qquad (17)$$

where τ_d is the shear stress required to unpin a dislocation source and l_d is the distance from the nearest source to the grain boundary. In agreement with this model, calculations[30] using appropriate values of k_Y and τ_d for iron gave a value of l_d in accord with the scale of a Frank-Read network. The sequence of events in the yielding process envisaged by Cottrell has been discussed in Section 1.3.

Several experimental facts are inconsistent, however, with the Cottrell model. Some of these have been outlined already, and we shall now consider those which arise directly from the grain-size analysis aspect. First, and perhaps foremost, the existence of pile-ups has not been confirmed by direct observation using electron microscopy or etch-pitting techniques. Secondly, the majority of investigations have revealed k_Y to be relatively independent of temperature[12,41,42], and strain rate[43,44]. Clearly, if k_Y is a measure of the unpinning stress, this cannot be reconciled with the theoretical analysis of the breaking-away from atmospheres[2,10,11]. In addition, the value of k ($= k_f$) for flow beyond the Lüders strain is often the same as k_Y[12,45,46]. As k_f should refer to the motion of free dislocations, it seems unlikely that $k_f \simeq k_Y$ if k_Y is associated with unpinning. Moreover, f.c.c. metals often display a dependence of yield stress on grain size[47] similar to b.c.c. metals, yet in the absence of discontinuous yielding suggestive of

little or no locking. All of this evidence rather strongly points to the fact that k_Y is not a measure of the stress required to unpin dislocations from interstitial atmospheres.

A significant contradiction does occur in the observed effect of temperature on k_Y. In some cases, for example, molybdenum[48], silicon-iron[49], steel[50,51], tantalum[52], and niobium[53], the influence of temperature on k_Y is appreciable. Surprisingly, temperature-dependent and temperature-independent behaviour has been obtained by different investigations for each of the materials, En2 steel[51,54], tantalum[52,55], and niobium[53,56].

Consequently, various alternative explanations of the effect of grain size on the yield or flow stress have been proposed in order to overcome some of these difficulties. Some workers[12,55,57-59] suggest that k_Y may reflect a difference in dislocation or precipitate structures arising from the use of different thermal treatments to obtain a variation in grain-size. Gilbert et al[55] find that when the interstitial content is less than 75 p.p.m., increasing the dislocation density decreases k_Y for tantalum. Also, Conrad and Schoeck[12] propose that k_Y could represent the stress to athermally generate dislocations from the grain boundaries or their immediate vicinity. Indeed, grain boundary sources are an integral part of Li's theoretical model[59] which provides for the observed grain-size dependence of the yield and flow stress, and its insensitivity to temperature. Alternatively, Johnson[60] relates k_Y not only to unpinning but to the extra work hardening near grain boundaries due

to the complexity of slip which occurs there. The above approaches have various short-comings and at present there is insufficient evidence to fully substantiate any one.

Very recently, however, Cottrell and Fisher[27,61] have put forward an interpretation of k_Y which is supported to a greater degree by experimental findings. For this reason it can be considered less speculative. They discard the necessity of a conventional pile-up of the Eshelby et al[40] type and think in terms of the stress concentration generated at the tip of a slip band meeting a grain boundary, acting as if it were a shear crack. The suggestion is that if pinning is strong, it is easier to create new unlocked dislocations immediately on the other side of the boundary from the slip band than to unpin sources further within the grain. Since the former process is almost temperature independent[62] then k_Y, which is a measure of the stress required to do this, is expected to be independent of temperature also. The latter process is predominant when pinning is weak, leading to a temperature-dependent[2] k_Y. Two main facts support the model. Firstly, Fisher[61] has observed the nucleation of dislocation loops in iron from grain boundaries at the Luders front when pinning is strong but not when it is weak. Similarly, Lindley and Smallman[46] found that pinned dislocations within the grains do not appear to move during deformation. Instead, dislocations are generated at or close to grain boundaries and multiply during glide. Secondly, the observed magnitude and temperature dependence of k_Y's in iron produced by different quench-ageing

treatments[61] to give different pinning strengths are in accord with the model. For example, when specimens were quenched (weak pinning) k_Y increased with decreasing temperature. Successively longer ageing times produced an increase in k_Y for a given temperature as expected for an increase in pinning strength. If the specimen was furnace-cooled, then k_Y attained a maximum value independent of testing temperature.

It seems, therefore, that k_Y is best interpreted in one of two ways, depending upon whether a state of weak or strong pinning exists. As it happens, almost all experiments are conducted on slow-cooled, strongly-locked materials which we have designated as being "normal".

The value of k_f for flow, has received little theoretical attention. It has been considered generally[45,63] as a measure of the difficulty of continuing slip across the boundaries from one grain into another and is not associated with unpinning. Cottrell[27] suggests that if the next grain cannot accommodate slip by the multiplication of its existing dislocations then a k_f approximately equal to the k_Y characteristic of strong pinning will be needed to create new dislocations. However, evidence is not entirely consistent with the requirement that $k_f \leq k_Y$[45]. Moreover, on the basis of Hahn's work[18] it seems likely that the free dislocations produced during yielding can, in fact, continue to multiply but the variation in grain size influences the multiplication and velocity characteristics.

1.4.2 Interpretation of σ_o.

Since k is relatively independent of temperature and strain rate in b.c.c. transition metals in which conventional annealing treatments normally produce strong locking, the temperature and strain rate dependence of the yield and flow stress must necessarily reside with σ_o. For this reason the interpretation of σ_o is extremely important in determining the rate-controlling mechanisms of yielding and flow.

It is now universally accepted that σ_I, for yielding, represents the resistance to movement in a glide plane that an unpinned dislocation experiences as a result of other dislocations, precipitates, solute atoms, lattice periodicity, etc, and is generally termed the lattice friction stress[30,35,64-66]. Some[38,60] identify σ_I with the yield stress of single crystals of similar composition but no data exists to support this hypothesis. Nevertheless, assuming such an identity, Johnson[60], proposes that σ_I must contain an unpinning term since single crystals show yield points and lower yield extensions[9,33]. As there is no justification for the initial assumption, and as Lüders band propagation in single crystals can readily be explained by dislocation multiplication[18], it is unlikely that pinning enters into σ_I.

In order to separate some of the effects which contribute to σ_I, Petch and his co-workers[64,65] investigated the effect of temperature and impurity on σ_I. They conclude that σ_I can be divided into two components. One, σ_I', is temperature independent, but increases with an increase in the total amount of carbon and

nitrogen in solution and varies with the presence and dispersion of precipitates. The other, σ_I'', increases with decreasing temperature in the same way as the lower yield stress but is independent of impurity content. As the temperature dependence now resides in a term which is not influenced by composition or pinning strength, Heslop and Petch[65] and Cottrell[30] propose that the temperature dependence of σ_Y arises from the high inherent resistance of the lattice itself, that is, the Peierls-Nabarro stress[67,68], which can be overcome with the assistance of thermal fluctuations. Although the evidence for a Peierls mechanism is far from incontrovertible, no satisfactory alternatives have been provided by the grain-size analysis.

In summary, the current picture of the low temperature yielding and subsequent flow of polycrystals obtained by studying grain-size effects is as follows. During the initial loading of the specimen below the upper yield stress, some dislocations are created at precipitates or inclusions[26,69] in regions of stress concentration. As the stress is increased they move and multiply by the double cross-slip mechanism[70,71] forming slip bands in a few grains to produce the pre-yield micro-strain. At the upper yield point the effective stress (combining the lattice friction stress, applied stress and stress concentration at the tip of slip bands) is sufficient to create new dislocations in adjacent grains, profuse multiplication occurs and the stress drops. At the same time, the Lüders front spreads across the specimen cross-section. At the lower yield stress, the propagation continues along the specimen by

creation and multiplication under the action of the effective stress at the Lüders front. Once the Lüders front(or fronts) has traversed the whole length of the specimen, uniform flow ensues and the rate of stress change with further deformation is determined by the dislocation multiplication and velocity characteristics. On this view, pre-yield, yielding, and flow represent the movement of free dislocations and the rate-controlling mechanism is one of overcoming the Peierls stress.

Of course, there are many limitations to the grain-size analysis, not the least of which is the fact that it is not applicable to single crystals. One's attention is then directed to other methods of investigating controlling mechanisms.

1.5 The Activation Analysis.

One of the alternative techniques which has been used with some success in the determination of the rate-controlling mechanisms involved in the plastic deformation of b.c.c. metals is thermal activation analysis. It is based on the premise that yielding or flow may by thermally assisted.

The combination of a pronounced temperature dependence and high strain-rate sensitivity of the stress required for yielding and flow leaves little doubt that thermal fluctuations can play a very important part to assist the applied stress in forcing dislocations past obstacles. Starting with this preliminary fact, Conrad and Wiedersich[72] develop an expression for the activation enthalpy, ΔH, (i.e. the so-called activation energy) for

yielding and flow in the following way. They assume, firstly, that a single activation process is rate controlling, and secondly, that ΔH does not vary appreciably from one activation site to another. One may then express the shear strain rate $\dot{\gamma}$, by an Arrhenius-type equation of the form

$$\dot{\gamma} = \nu \exp (- \Delta G/kT) \qquad (18)$$

which expands to

$$\dot{\gamma} = \nu \exp (- \Delta H/kT + \Delta S/k) \qquad (19)$$

where ΔG is the Gibbs free energy of activation, ΔS the activation entropy, k Boltzmann's constant, and T the absolute temperature. It is standard practice to omit the Δ for simplicity, with the understanding that we are dealing throughout with differences in G, H and S, not absolute values. The pre-exponential term ν, is commonly known as the frequency factor, and represents the product of the strain per successful fluctuation and the frequency ν_o at which the dislocation attempts to overcome the barrier. Therefore[73],

$$\nu = NAb\nu_o \qquad (20)$$

where N is the number of activation sites per unit volume, A the area swept out per each successful fluctuation and b the Burgers vector. Our purposes are best served by expressing ν in terms of the mobile dislocation density L, so that[74]

$$\nu = Lbs\nu_o \qquad (21)$$

where s is the distance moved by a dislocation after each successful fluctuation.

It is further assumed that G,H and S may be functions of temperature and an effective stress, τ^*, given by

$$\tau^* = \tau - \tau_\mu \tag{22}$$

with τ being the applied stress, and τ_μ the stress required to overcome thermal-insensitive long-range obstacles. The magnitude of τ_μ is influenced by temperature only through the shear modulus μ.

Thereupon, the activation energy for constant strain-rate deformation is established[74] as

$$H(T, \tau^*) = -kT^2 \frac{\left[\left(\frac{\partial \tau}{\partial T}\right)_{\dot\gamma} - \frac{\tau_\mu}{\mu}\frac{d\mu}{dT}\right]}{\left(\frac{\partial \tau}{\partial \ln \dot\gamma/\nu}\right)_T} \tag{23}$$

independent of S. Moreover, since the second term of the numerator is always negligible compared to the first for b.c.c. metals, and if τ_μ is independent of strain rate, Equation (23) may be written

$$H(T, \tau^*) = -kT^2 \frac{\left(\frac{\partial \tau}{\partial T}\right)_{\dot\gamma}}{\left(\frac{\partial \tau}{\partial \ln \dot\gamma/\nu}\right)_T} \tag{24}$$

Another way of expressing H results from a suitable differentiation of Equation (19) to give

$$H(T, \tau^*) = -k\left(\frac{\partial \ln \dot\gamma/\nu}{\partial\, 1/T}\right)_{\tau^*} \tag{25}$$

It should be noted that this is only true if both H and S are

regarded as functions of the two variables, T and τ^*. Alternatively[75], one can now derive Equation (24) from (25) if the material obeys an equation of state which introduces a rational functional relationship between $\dot{\gamma}/\nu$, T and τ^* of the form

$$f(\dot{\gamma}/\nu, T, \tau^*) = 0 \tag{26}$$

As a result, the expression

$$\left(\frac{\partial \tau^*}{\partial T}\right)_{\dot{\gamma}} \left(\frac{\partial \ln \dot{\gamma}/\nu}{\partial \tau^*}\right)_T \left(\frac{\partial T}{\partial \ln \dot{\gamma}/\nu}\right)_{\tau^*} = -1 \tag{27}$$

holds and the identity of (24) and (25) is established. No change in the assumptions is required and the two expressions must necessarily yield identical results.

The potential energy barrier to dislocation movement may be represented by a hypothetical force-distance curve of the type illustrated in Figure 1. Part of the energy necessary to enable a dislocation segment of length L^* to surmount the barrier is furnished by the effective stress, τ^*, and the rest, H, by thermal fluctuations, shown as the shaded portion in the figure. Since the work done by τ^* is given by $\tau^* bL^* (x_2 - x_1)$ from dislocation theory[5] and H^* is taken as the total area under the curve between the initial and final equilibrium positions of the segment, x_1 and x_2, fixed by τ^*, then

$$H = H^* - \tau^* bL^* (x_2 - x_1) \tag{28}$$

The quantity $bL^*(x_2 - x_1)$ is defined as the "activation volume", v^*, so that

$$H = H^* - v^* \tau^* \tag{29}$$

As x_1 and x_2 are functions of τ^*, the parameters H^* and v^* must be functions of τ^* also. By differentiating the integral

$$H = \int_{F^* = \tau^* bL^*}^{F_{max}} \left[f_2(F) - f_1(F) \right] \, dF \tag{30}$$

with respect to τ^*, Conrad[34] obtains

$$v^* = - \left(\frac{\partial H}{\partial \tau^*} \right)_T \tag{31}$$

where $f_1(F)$ and $f_2(F)$ denote the curve on either side of F_{max} in Figure 1. A direct differentiation of H from Equation (29) with respect to τ^* also yields Equation (31) since it can be shown from the model that

$$\left(\frac{\partial H^*}{\partial \tau^*} \right)_T - \tau^* \left(\frac{\partial v^*}{\partial \tau^*} \right)_T = 0 \tag{32}$$

In both cases, it must be assumed that the shape and height of the energy barrier is unaffected by changes in stress. Provided that one regards the entropy in Equation (19) as relatively independent of stress, then the activation volume may be written as

$$v^* = kT \left(\frac{\partial \ln \dot{\gamma}/\nu}{\partial \tau} \right)_T \tag{33}$$

if in addition τ_μ is independent of strain rate.

In practice, H and v^* are calculated from the measured dependence of stress on temperature and strain rate, with the

assumption that ν is relatively insensitive to stress. However, neither Conrad nor others who have used these or similar expressions have been able satisfactorily to justify this last point on experimental or theoretical grounds.

The frequency factor is determined from the approximation

$$H = kT \ln \nu/\dot{\gamma} \qquad (34)$$

to the Arrhenius relation, as the slope of a plot of H against T for a constant strain rate. That ν turns out to be constant is probably only a consequence of the fact that it was assumed so in the initial calculation of the H values, but certainly does not constitute a proof that this assumption is valid.

Moreover, the neglect of the entropy term in Equation (34) and its stress-dependence in (33) is a necessary step in the application of these equations. Whether the effects so ignored are appreciable or not is an extremely complicated problem which still awaits solution.

1.6 Rate - controlling Mechanisms.

In summary, numerous mechanisms have been proposed to account for the strong temperature and strain-rate dependence of the yield and flow stress of the b.c.c. transition metals at low temperatures. These are:

1. Unpinning from interstitial atmospheres[1,2,10,11,76-78]
2. Overcoming the Peierls stress[34,58,65,74,79-83]
3. Non-conservative motion of jogs[84,85]

4. Conservative motion of jogs[86,87]

5. Cross-slip[32]

6. Overcoming interstitial precipitates[88]

7. Overcoming solute atoms[13]

Most of the determinations are based on the activation analysis and, clearly the greatest recent support is for overcoming the Peierls stress. This is in agreement with the conclusions reached by the method of grain-size analysis. A critical appraisal of the results does not indicate any systematic relation between the type of material used and the mechanism proposed. In fact, Conrad[81,82] shows that overcoming the Peierls barrier is consistent with the experimental observations for all of the b.c.c. metals. In general, he obtains[82] $H \simeq 0.1\mu b^3$ at $\tau^* = 1$ kg.mm.$^{-2}$, $v^* \simeq 50b^3$ at $\tau^* =$ 2 kg.mm.$^{-2}$ and $\nu = 10^6 - 10^{12}$ sec.$^{-1}$ with the higher values of ν being associated with purer materials. Both H and v^* increase with decreasing stress in a manner independent of impurity content, structure, and whether yielding or flow is considered. It is suggested that these facts are not in accord with any mechanism but that of overcoming a Peierls stress. Physically, Conrad proposes that the Peierls barrier can be surmounted by the nucleation of kinks in dislocations. At low stresses, the magnitude of H and the variation of H with stress are in agreement with those predicted by Seeger's model[89] for kink nucleation.

No apparent criticism can be attached to the conclusions reached by Conrad from an exhaustive series of calculations

utilizing a wide range of experimental data. What can be questioned, however, is the extent of the validity of the assumptions used in the development and subsequent application of the activation equations. Consequently, it would probably be well to treat the activation analysis in its present form with some reserve.

2. EXPERIMENTAL PROCEDURE.

2.1 Selection of Experiments and Material.

The present investigation constitutes part of a more extensive programme initiated in this Department some years ago with the aim of gaining some understanding of the contribution of lattice defects to the mechanical and physical properties of the b.c.c. transition metals.

The grain-size analysis was the only comprehensive method of treating deformation and fracture data at the time that Johnson[90] and Wronski[37] carried out their studies on niobium and molybdenum. As a result, their work was concentrated on the grain-size dependence of the lower yield stress and fracture stress, and the corresponding effect of temperature on the Petch parameters. Now, it is possible, in addition, to consider observations in the light of the more recent activation analysis, and also of the view that discontinuous yielding may be a consequence of dislocation multiplication and velocity characteristics instead of unpinning from impurity atmospheres. Information necessary for the application of these ideas was obtained in the current work by conducting experiments not only on the grain-size dependence, but also on the temperature and strain-rate dependence of tensile yielding and flow characteristics in a range where temperature has the greatest influence on these properties.

The major prerequisite of a material to be used for the investigation is a high sensitivity to changes in grain-size, temperature and strain rate. From this point of view, molybdenum

is one of the most suitable of the transition metals. At the same time, molybdenum has certain other advantages over, say, tungsten. It is readily available in bulk form of sufficiently good purity to be ductile down to about 200°K in normal tensile tests. Thus, its machining properties at room temperature are favourable. Moreover, mechanical working and heat treatments are not complicated by phase changes as in iron, for example.

2.2 Preparation of the Specimens.

2.2.1 Material.

Arc-cast molybdenum for the investigation was supplied by Mr. J.M. Clyne of the Armaments Research and Development Establishment, Woolwich. In order to ensure the absence of intergranular brittleness, deoxidation during melting was effected by the addition of carbon. Typical molybdenum produced in this manner at A.R.D.E. contains nominally 0.01% iron and 0.002% silicon. An analysis for interstitial impurities in the second of two ingots (1 and 2) produced in an identical manner, revealed 80 p.p.m. carbon, 12 p.p.m. nitrogen, 6 p.p.m. oxygen and 4 p.p.m. hydrogen, but A.R.D.E. did not quote the limits of accuracy. However, in view of the enormous inconsistencies[37,48] in the results of analyses of material from a single ingot carried out by independent laboratories on eight different ingots used by Wronski, the present author felt that a separate analysis for Ingot 1 would serve no useful purpose. Instead, both ingots were considered to be impure ($>99.97\%$) with the major interstitial impurity being carbon. Any integration of

specimens from the two different ingots during any specific phase of the investigation was avoided completely.

2.2.2 Fabrication.

All of the specimens were obtained from Ingots 1 and 2, which were given different thermal and mechanical treatments at A.R.D.E. to provide various grain sizes.

Initially, each ingot was reduced to a bar of one inch square cross-section by a series of rolling and intermediate annealing operations at 1350°C, followed by recrystallization in pure hydrogen for one hour at 1350°C. Subsequently, each bar was divided into three parts and then rolled to a 5/8 inch square cross-section at 1350°C. Thereafter, to obtain consistently fine grain sizes, all parts of Ingot 1 were swaged to a final diameter of 1/4 inch at 800°C and recrystallized for one hour at 1350°C in hydrogen. On the other hand, a finer grain size was produced in two-thirds of Ingot 2, by swaging also at 800°C, but reducing the annealing temperature to 1250°C. The remainder of Ingot 2 was swaged at 1000°C and annealed at 1600°C.for three hours to yield a coarse grain size. The final swaging and annealing treatments with the resulting grain sizes are summerized in Table 1.

Hounsfield-type tensile specimens of gauge diameter 0.1 inch and gauge length 0.75 inch were machined from the as-received 1/4 inch diameter rods. After machining, additional grinding and buffing operations served to reduce surface irregularities to a minimum. Stresses developed during cold-working were relieved by annealing

at 1250°C for one hour in a vacuum of about 10^{-5}mm. of mercury. A final electrolytic polish ensured a microscopically smooth, oxide-free surface.

Table 1. Effect of fabrication treatment on grain size.

Ingot	Swaging Temperature	Recrystallization Temperature & Time	Grain Diameter (mm.)
1	800°C	1 hour - 1350°C	0.026 - 0.054
2	800°C	1 hour - 1250°C	0.024 - 0.029
	1000°C	3 hours - 1600°C	0.077 - 0.12

2.3 Achievement of Variation in Grain Size.

A study of grain size effects necessitates the use of as wide and as complete a range of grain sizes as possible. A strain-anneal technique similar to that described by Savitskii[91] was used previously by Wronski[37,48] with limited success. He encountered no difficulty in obtaining grains of diameter less than 0.06 mm. or coarse grains in a narrow range centred about 0.25 mm. However, all but one or two attempts at growing grains of intermediate diameters were thwarted by the intervention of non-uniform grain growth. A similar pattern was observed in the strain-anneal characteristics of the present material, as shown in Table 2. The incidence of non-uniform grain growth was rare. Consequently, it became evident that the technique required refinement in order to complete the range of grain sizes. A detailed investigation of several possibilities lead to the eventual adoption of a procedure which

involved an initial grain-coarsening anneal followed by a strain-anneal treatment. The results are given in Table 3.

Table 2. Effect of strain-anneal treatment on grain size. Duration of anneal: 1 hour.

Ingot	Pre-strain (%)	Annealing Temperature (°C)	Grain Diameter (mm.)
1	-	-	0.026 - 0.054
	$\frac{1}{2}$	1500	0.047 - 0.052
	3	1500	0.052
	3	1600	0.060
	5	1600	0.047 - 0.073
	7	1650	0.25 - 0.31
2	-	-	0.024 - 0.029
	3	1600	0.029 - 0.043
	4	1600	0.029 - 0.038
	5	1600	0.049, 0.51, 0.17 - 0.25

2.4 Metallographic Technique.

Three types of metallographic study were necessary: grain size measurements; fractography; and substructure determination.

Grain size measurements were made on transverse sections after testing. When a specimen had not received a strain-anneal treatment, the section was cut from a shoulder. In other instances it was taken from a region of the gauge length adjacent to the shoulder remote from the fracture surface or portion where necking had occurred. Each section was mounted in bakelite, polished and etched chemically.

Table 3. Effect of grain-coarsening and subsequent strain-anneal treatment on grain size. Duration of final anneal: 1 hour.

Ingot	Grain-coarsening Anneal	Pre-strain (%)	Annealing Temperature(°C)	Grain Diameter(mm.)
I	1650°C - 3 hrs.	-	-	0.049 - 0.060
		2	1600	0.060
		3	1600	0.073 - 0.077
		3½	1600	0.098
		4	1600	0.087 - 0.092 1.7
		5	1500	0.098
		5	1525	0.092 - 0.098
		5	1550	0.092, 0.047 - 0.057
		5	1575	0.054 - 0.060
		5	1600	1.7, 0.063
		6	1650	1.7, single crystal
2	1600 - 3 hrs.	-	-	
		5	1600	0.054, single crystal
		7	1600	1.7

Polishing was carried out on wet silicon carbide-papers. Only for fine grain sizes was it necessary to apply a fine polish on an automatic wheel using diamond paste as an abrasive. Chemical etching was done in a 1:1 solution of nitric acid and water. Grain counts were made with a Reichert projection microscope using the linear intercept method. This entailed counting the number of boundary

intersections along approximately equally spaced parallel chords on the circular surface of a section in each of two directions oriented 90° to each other. The average was taken of not less than 20 readings. An examination of both types of afore-mentioned section from the same specimen revealed a barely detectable difference in the value of the reciprocal square root of the grain diameter, $l^{-\frac{1}{2}}$, the grain size parameter of interest. This is not surprising since it can easily be shown that the percentage increase in $l^{-\frac{1}{2}}$ is about one quarter of the plastic strain expressed in percent. Moreover, shoulder constraints prevent large strains in the region from which a gauge length section was obtained. Therefore, one would rarely expect the measured value of $l^{-\frac{1}{2}}$ to exceed the true value by more than 2%. Since the probable error in the measurement of $l^{-\frac{1}{2}}$, in the grain size range where the effect of strain is the largest, is about 2%, it was considered unwise to make a correction for prior deformation.

The fractography generally assumed two forms. Firstly, the fracture surfaces of unmounted specimens were examined to determine whether fracture occurred by cleavage or in a fibrous manner. Secondly, in order to ascertain the extent of grain boundary failure, longitudinal sections were mounted, polished and etched, as described above, to provide a profile view roughly normal to the fracture surface.

The nature of the dislocation substructure was investigated by an etch-pitting technique. Annealed, unmounted specimens were initially polished electrolytically in concentrated sulphuric

acid using a platinum cathode. Although the polishing conditions were not exceedingly critical, the best results were obtained for a current density of $1\frac{1}{2}$ - 2 amperes per cm.^{2} at 3 - 4 volts at a temperature of 30°C. A total of about 50 was removed from the surface before a stable etch-pit density was achieved with additional polishing. Of three etchants[92,93,94], which are known to pit dislocations in molybdenum, a chemical etchant[92] with the composition:

$K_3 Fe(CN)_6$	10 gm.
KOH	10 gm.
H_2O	100 c.c.

proved most satisfactory.

2.5 Testing Techniques.

2.5.1 Testing Machines.

Conventional tensile tests were conducted on either a modified Hounsfield Tensometer or an Instron testing machine. All strain-rate and temperature cycling experiments were performed on the Instron.

The Hounsfield Tensometer was mounted vertically and driven automatically by a fractional horse-power motor. By means of suitable combinations of two gearboxes (500:1 and 30:1 reduction) and two sets of four standard bicycle gears (52,26,18 and 13 teeth) it was possible to vary the strain rate in discrete steps from 0.72×10^{-6} to 0.88×10^{-4} sec.$^{-1}$ Higher strain rates, of course, could also be obtained but were not used because the lack of an automatic method of load observation appreciably reduced the reliability of load-elongation data above about 10^{-4} sec.$^{-1}$

Ordinarily, load measurements on a Hounsfield are made from a mercury column which moves in a capillary tube under the influence of the pressure from a piston operated by a deflected load beam. Because the meniscus changes shape when the load passes through an extremum, this method does not always provide an accurate picture of the initial and final stages of plastic deformation. Therefore, an optical system was devised by Wronski[37] to increase the sensitivity of measurement. Briefly, two optical levers were mounted on the load beam. Light from a slit source was reflected five times at the two mirrors and then observed on a translucent metre scale suitably displaced from the mirrors. Thus, any deflection of the load beam produced a deflection of the light beam, without the extensive "backlash" experienced with the mercury column. Consequently, the sensitivity of load detection was considerably enhanced. Due to the necessity of calibrating this system against the mercury scale before each test the absolute accuracy of the load measurement was not increased. Both a 0.5 ton and a 500 lb. load beam were used.

Tests on the Hounsfield at temperatures other than room temperature were performed in a rigid steel frame designed[90] in such a way that the specimen could be immersed in a liquid maintained at a constant temperature in a dewar flask during the experiment while at the same time maintaining an axiality of loading.

The Instron testing machine[95], Model TT-CM, had a capacity of 5000 kg. The standard pen recorder was replaced by one with $\frac{1}{4}$-second full-scale response. A quick-change push-button unit

supplied with the instrument allowed a rapid change of cross-head speeds to be made before or during a test. With the insertion of a decade speed reducer into the drive gear system, the cross-head speed could be varied in discrete steps from 0.005 to 50 cm.min.$^{-1}$, which corresponded to strain rates from .44 x 10^{-4} to 0.44 sec.$^{-1}$

To avoid changing the shape and size of the specimens, stainless steel adaptors were designed to accommodate the Hounsfield specimen grips. For tests at other than room temperature, a frame to fit on the bottom of the lower, mobile cross-head was constructed from mild steel and subsequently nickel plated to increase its resistance to corrosion. The whole frame was immersed in a liquid during the test. A mild steel nickel-plated rod transmitted the load from the specimen, through the lower cross-head to a universal coupling fixed to a load cell in the upper stationary cross-head. The coupling served to maintain the axiality of loading. A 500 or 5000 kg. capacity load cell was used for all tests.

2.5.2 Testing Temperature.

A range of temperatures from 190^{o}K to 450^{o}K was required for the investigation. To ensure long term stability during cycling experiments, four fixed temperatures were taken as those listed in Table 4. Although the deviation from 293^{o}K, or room temperature, is given as $\pm$ 1^{o}K, the variation was never found to be greater than $\pm$ 0.5^{o}K during the course of a single test.

Below 293^{o}K, any specific temperature was achieved by bubbling cooled nitrogen gas through a suitable liquid. The flow system was

Table 4. Temperature media and corresponding temperatures.

FIXED TEMPERATURES.

Medium	Fixed Point	Temperature ^{o}K
$CHClF_2$ and solid CO_2	Sublimation	193 ± 0.5
$CHClF_2$	Boiling	233 ± 0.5
Air	Ambient	293 ± 1
Water	Boiling	99.5 ± 0.5

CONTINUOUS RANGE OF TEMPERATURES.

Medium	Temperature Range ^{o}K
$CHClF_2$	$190 - 233, \pm 1$
CCl_2F_2	$233 - 293, \pm 1$
Silicone oil	$293 - 450, \pm 1$

set up in the following manner. First, an on-off type solenoid valve, activated by the voltage from a temperature controller, permitted the flow of gas from a compressed nitrogen cylinder through a needle valve which controlled the actual volume of flow. The solenoid valve opened when the temperature detected by a chromel-alumel thermocouple rose approximately $2^{o}K$ above a preset valve and closed again when the required temperature was regained. Thereafter, the gas was dried with anhydrous calcium chloride before being passed through a copper coil immersed in liquid nitrogen and finally bubbled through one of the coolants recorded in Table 4.

Above 293^{o}K, a continuous range of temperatures was obtained by the controlled heating of a silicon oil bath. A standard system consisting of a chromel-alumel thermocouple, temperature controller and a resistance wire heating element was used. The latter was located at the bottom of the dewar flask.

3. EXPERIMENTAL RESULTS.

3.1 The Effect of Grain Size on Tensile Properties.

Specimens from Ingot 1 covering a wide range of grain sizes were used specifically for the detailed investigation of the effect of grain size on the tensile properties of arc-cast molybdenum to be described in this particular section. All tests were performed to fracture on the Hounsfield tensometer at 293°K and a strain rate of 0.88×10^{-4} sec.$^{-1}$ Unless otherwise specified, stresses are henceforth given as tensile stresses, and grain sizes in terms of the grain diameter, l, in mm.

3.1.1 Load-elongation Curve.

Load-elongation curves for seven typical specimens are shown in Figure 2. It is apparent that the grain size has a pronounced effect on the tensile behaviour. An increase in grain size towards 0.28 mm. is accompanied, in general, by a decrease in overall strength and ductility, and a decrease in the tendency to exhibit a yield point, a Lüders strain, and necking. At 0.28 mm., only an inflexion occurs in the load-elongation curve at yielding, and the elongation to fracture, which occurred in the rapid work-hardening region, is only about 5%. Below 0.28 mm., the yield point and Lüders strain return, and ductility increases whereas the strength decreases, until for a single crystal the curve appears very much similar to that for a fine-grained specimen, but on a greatly reduced scale.

In several instances, a pronounced Lüders strain was observed in the absence of a yield point for specimens with an intermediate

grain size, e.g. 0.092 mm. It was felt that this behaviour might not necessarily be characteristic of the specimen but could instead be a machine effect. When the Instron became available, it was possible to make a comparison of the load-elongation curves obtained using the Hounsfield with those using the Instron. Figure 3 illustrates this effect of the testing machine on the observed tensile behaviour of four specimens from Ingot 2, two of which had a fine grain size, 0.027 mm., and the other two an intermediate grain size, 0.098 mm.

Apart from the expected experimental scatter, the main distinction between the two tensile curves for the fine-grained material is the lack of detail in the Lüders strain region of the Hounsfield curve. The difference in yielding behaviour, however, appears to be more marked for specimens with an intermediate grain size. In this case, the yield point is masked entirely in the Hounsfield test which then leads to the observation of the absence of a yield point but existence of a measurable Lüders strain. The Instron curve, on the other hand, shows the reverse behaviour. A yield point without a detectable Lüders strain was observed on every occasion in over one hundred Instron tests on sepcimens from Ingot 2 with grain sizes of 0.51, ∽ 0.25, and 0.098 mm. under various conditions of temperature and strain rate. One must regard the latter results as the more reliable for two reasons. Firstly, calibration experiments indicate that the Instron is about twice as hard as the Hounsfield and consequently better capable of following sudden drops in load. Secondly, the automatic recording device

of the Instron can detect load drops which may be missed by the optical lever system of the Hounsfield. Therefore, more caution should be exercised in regard to the weight given to measurements of the upper yield stress, yield drop and Lüders strain taken from Hounsfield than Instron data, particularly for material of intermediate and coarse grain size.

3.1.2 Yielding Characteristics.

The yield stress, Lüders strain, and yield drop were measured from the load-elongation curves in order to establish the effect of grain size on the characteristics of yielding.

It was necessary to define the yield stress in three ways. When a yield point was present, the lower yield stress was used. In the absence of a yield point, the yield stress was taken as either that stress corresponding to the horizontal Lüders strain region, or, in the absence of a Lüders strain also, as the stress at the proportional limit. The yield stress is shown plotted in Figure 4 against the reciprocal square root of the grain diameter, $l^{-\frac{1}{2}}$, in $mm.^{-\frac{1}{2}}$ Clearly the points do not lie on a single straight line as predicted by the theories discussed in the introduction. However, for values of $l^{-\frac{1}{2}} \geqslant 2\ mm.^{-\frac{1}{2}}$, $(l \leqslant 0.25\ mm.)$, the relationship between the yield stress and $l^{-\frac{1}{2}}$ does appear to be linear and the points were fitted, therefore, to a straight line by the method of least squares. A measure of the scatter about this line can be expressed statistically as the standard error, having a value in this case of 1.0 $kg.mm.^{-2}$ On this basis, the average slope, k_Y, with the corresponding limits,

is 4.3 ± 0.5 kg.mm.$^{-3/2}$ and the stress-intercept, σ_I, by extrapolation, 9.3 ± 2.0 kg.mm.$^{-2}$ On the other hand, the yield stress of specimens with a grain size ≥ 0.25 mm. was practically independent of grain size. Although there seems to be a tendency for the yield stress to decrease slightly towards $l^{-\frac{1}{2}} = 0$, such a small positive slope cannot be treated with much confidence because of the experimental scatter. The average single crystal yield stress is about 40% greater than the upper limit set on σ_I.

The Lüders strain, ϵ_L, and the yield drop, $\Delta\sigma$, for each specimen were plotted against $l^{-\frac{1}{2}}$ (Figure 5). The scatter in the experimental results was very large so that only a trend is perceivable. Nevertheless, the results are portrayed better in this way than in table form. Taken together with the load-elongation curves of Figure 2, and those of Figure 3 for specimens from Ingot 2, it appears from these results that the yield drop reaches a minimum, which is not necessarily zero, at about 0.25 mm. Furthermore, the presence of a yield point does not imply the existence of a measurable Lüders strain; the latter is effectively zero for a range of grain sizes from 0.1 to 1.0 mm.

It is well known that the existence of a yield point and the magnitude of the Lüders strain are very sensitive to the type of testing machine used, axiality of loading, and the size, shape, previous history, and surface condition of the specimen. As a consequence, the absolute values of ϵ_L and $\Delta\sigma$ given in Figure 5 are to be regarded with some reserve. The only real significance

to be attached to these observations is the tendency for the values to pass through a minimum at certain coarse grain sizes.

3.1.3 Flow Stress.

The true flow stress beyond the Lüders strain was calculated for each specimen at various strains from 0.02 to 0.10. To do this it was necessary to assume that the volume within the gauge length remained constant with deformation in this range. Such an assumption was proved to be valid by measuring the diameter after various elongations. Two sets of typical flow stress data, at strains of 0.02 and 0.05 are plotted against $l^{-\frac{1}{2}}$ in Figure 6(a). The whole series is presented in Figure 6(b) along with the yield stress curve for comparison.

It would be conceivable to draw a straight line through the points corresponding to a strain of 0.02. However, it is clear that such a simple relationship no longer holds at strains greater than 0.02. Although a sharp transition such as appears in the yield s tress relation is not evident in the flow stress results, an apparent change in the grain-size dependence of the flow stress occurs in the region of 0.25 mm.

3.1.4 Work-hardening Rate.

The work-hardening rate, defined in the usual way as the slope of the true stress-true strain curve, was determined for each specimen. To simplify the calculations, an attempt was made to fit the true homogeneous flow curves to a standard analytical relation of the form[96]

$$\sigma_T = K \epsilon_T^{\,n} = K \left[\ln(L/L_o)\right]^{n} \qquad (35)$$

where σ_T is the true stress based on the assumption of constant volume, ϵ_T is the true strain, L the instantaneous specimen gauge length, and L_o the original gauge length. The parameters K and n are termed the work-hardening constant and work-hardening exponent, respectively. If Equation (35) is obeyed by molybdenum, then

$$\log \sigma_T = \log K + n \epsilon_T^{\,n} \qquad (36)$$

should be a straight line for any given specimen. Figure 7 shows that the above relation is a good representation of the flow curve for fine-grained specimens, up to strains of 0.14, but begins to break down at about 0.1 mm. Eventually, at 1.7 mm. and for a single crystal the points seem to fall on two separate straight lines which indicates that the flow curve can be represented by two parabolae. Previous workers have noted similar behaviour in iron[96-98], tantalum[55,99], and vanadium[46].

Differentiation of Equation (35) gives the work-hardening rate as

$$d\sigma_T/d\epsilon_T = n\sigma_T/\epsilon_T \qquad (37)$$

When the flow curve did not yield unique values of n, that is, at coarse grain sizes, care was taken to use a value of n characteristic of the strain of interest. The work-hardening rates are shown plotted against $l^{-\frac{1}{2}}$ in Figure 8(a) for two strains, 0.03 and 0.06. In the range 0.027 to 0.10 mm. there is no systematic variation in the work-hardening rate with grain size; the average values are 270 kg.mm.$^{-2}$($\sim \mu/60$) for 0.03 and 160 kg.mm.$^{-2}$($\sim \mu/100$) for

0.06. From previous observations of load-elongation curves and yielding characteristics, there appears to be some justification for taking the results for grain sizes above 0.10 mm. at face value and drawing the best fitting curve through them as shown. Even if this were not done, it seems that the work-hardening rate at $l^{-\frac{1}{2}}$ = 1.9 mm.$^{-\frac{1}{2}}$(0.28 mm.) is greater than the fine-grained average, drops to a minimum at 0.8 mm.$^{-\frac{1}{2}}$ (1.7 mm.), and increases again at the single crystal configuration to a value about 20% less than that at fine grain sizes.

The parameters n and K were also plotted against $l^{-\frac{1}{2}}$, in Figure 8(b) and (c). At coarse grain sizes, their values were taken from the portion of the log σ_T - log ϵ_T curve corresponding to low strains. Their grain-size dependence is consistent with that obtained for the work-hardening rate.

3.1.5 Fracture Properties.

The fracture stress of each specimen was calculated by measuring the cross-sectional area of the fracture surface (Figure 9) and dividing this into the load at fracture. The results are shown plotted against $l^{-\frac{1}{2}}$ in Figure 4. With the exception of the single crystal fracture stresses, the data were fitted to an inverse square root law by the method of least squares, irrespective of the large scatter.

The fracture surfaces of fine-grained specimens were fibrous with a few cleavage facets. An increase in the grain size was generally accompanied by an increase in the tendency to fracture

by cleavage. About 50% of the fracture surfaces at 0.098 mm. consisted of cleavage facets and for $l \gtrsim 0.25$ mm. fracture occurred entirely by cleavage. Metallographic examination of longitudinal sections through fracture surfaces revealed that fractures were basically transcrystalline in character although cracks were occasionally seen to follow grain boundaries over very short distances.

3.1.6 Petch Parameters Determined by the Extrapolation Method.

The parameters σ_I and k_Y of the Petch relation are normally taken as the stress-intercept and slope of a plot of yield stress against $l^{-\frac{1}{2}}$. However, this method has two main shortcomings. A large number of specimens must be tested to obtain accurate values of σ_I and k_Y. In addition, since different thermal or mechanical treatments are required to give different grain sizes, the possibility exists that different internal or sub-grain structures are produced concurrently. To overcome these difficulties, Cottrell[30] has proposed an alternative method of finding σ_I and k_Y. This entails extrapolating that part of the true stress-true strain curve which corresponds to homogeneous plastic flow, to the elastic range (Figure 10). The stress at the point of intersection, σ_1, is then considered to be the lattice friction stress, σ_I. The difference, σ_2, between the lower yield stress, σ_Y, and σ_1 is a measure of the contribution to the resistance to yielding provided by grain boundaries. From an appropriate comparison with the Petch relation (Equation 16) it follows that

$$k_Y = \sigma_2 / l^{-\frac{1}{2}} \qquad (38)$$

Mathematically, the stress σ_1 is found by solving simultaneously the equation for the plastic region, (35), and that for the elastic range, namely

$$\sigma = E\epsilon \tag{39}$$

where E is Young's Modulus. To a very good approximation σ and ϵ can be considered to be the true stress and true strain, respectively. The solution gives, therefore,

$$\sigma_1 = (K\epsilon^{-n})^{1/1-n} \tag{40}$$

Using $E = 3.3 \times 10^4$ kg.mm.$^{-2}$ for molybdenum at room temperature and the values of K and n from Section 3.1.4, the magnitudes of σ_1, σ_2 and $\sigma_2/1^{-\frac{1}{2}}$ were calculated for each specimen. Figure 11, a plot of the results, illustrates the significant discrepancy in the magnitude of the Petch parameters obtained by the two methods. In particular, σ_1 and $\sigma_2/1^{-\frac{1}{2}}$ are not independent of grain size as required, and the magnitude of σ_1 at fine grain sizes is nearly twice that of σ_I.

3.2 The Effect of Strain Rate on Tensile Properties.

The effect of strain rate on the tensile properties of molybdenum was investigated in detail at two temperatures, 243°K and 293°K, for two grain sizes, 0.027 mm. and 0.098 mm. All of the specimens tested came from Ingot 2. Both the Hounsfield and Instron were employed to obtain a range of strain rates from 0.72×10^{-6} sec.$^{-1}$ to 1.8×10^{-1} sec.$^{-1}$, as outlined in Section 2.5.1.

A number of tests were also conducted at 373°K in the higher strain rate range, but the results were used chiefly to calculate

activation parameters. In addition, a series of experiments was carried out to examine the applicability of the Petch relation at four different strain rates in the above range.

3.2.1 Load-elongation Curve.

The load-elongation characteristics at 293°K for various strain rates are shown in Figure 12 and Figure 13 for typical specimens with a fine and an intermediate grain size, respectively. At the lower strain rates, tests were concluded shortly after the Lüders strain or lower yield point. The most pronounced effect of an increase in strain rate is the increase in overall strength, more specifically, the upper and lower yield stress, and flow stress up to the onset of necking. At the same time, the extent of uniform deformation in the fine-grained specimens decreases with increasing strain rate above 10^{-4} sec.$^{-1}$, as does the total elongation to fracture for both grain sizes. However, it is apparent that the Lüders strain, yield drop and initial work-hardening rate do not seem to vary in a systematic way with strain rate. It will be recalled (Section 3.1.1, Figure 3) that the use of different tensile machines imposes an abrupt discontinuity in the presence and magnitude of the yield drop, and possibly Lüders strain also. This accounts for the sudden disappearance of the yield point in the curves for specimens with a grain size of 0.098 mm. The flow portions of the load-elongation curves for both grain sizes closely parallel one another for different strain rates.

3.2.2 Yielding Characteristics.

The choice of a yield stress criterion presented little difficulty in the case of the fine-grained specimens. Since a yield point was always observed, the lower yield stress was invariably used. However, due to the detail brought out in the Lüders strain region during the more sensitive Instron test it was then necessary to define the lower yield stress itself in some consistent manner; it was taken as the lowest stress attained during the lower yield extension. Similarly, the lower yield stress was chosen for specimens with an intermediate grain size whenever possible, but only one of the specimens tested on the Hounsfield at low strain rates exhibited a yield point, and often no Lüders strain, as can be seen in Figure 13. In these instances, the yield stress was defined as in Section 3.1.2. Nevertheless, in view of the fact that such behaviour did not bear any obvious relation to the strain rate, it was felt that the yield stress determined in one of the two alternative ways would be reasonably representative of the lower yield stress had a harder machine been used. As a consequence, the yield stress was specified throughout as the lower yield stress, σ_Y, thereby distinguishing it from the upper yield stress.

The values of σ_Y for $l = 0.027$ and 0.098 mm. obtained at the three temperatures, 243, 293, and 373°K, are shown plotted against the common logarithm of the strain rate, $\dot{\epsilon}$, in Figure 14. Unfortunately, a large number of tests is a requisite of investigations

of this kind. Consequently, even though the fullest possible use was made of each specimen, the limited amount of material in a single ingot prevented the extension of the data at 373°K to the full range of strain rates. Conceivably, a change to another ingot would have raised the problem of introducing material with a different impurity content thereby precluding reliable comparison of experimental data. Each point represents the average of 2 to 16 tests with an experimental scatter from the mean usually less than 3%, and only once exceeding 5% slightly. One can, in fact, account for as much as 3% scatter solely from a variation of the grain size from the average value(cf. Table 1).

The strain-rate behaviour of specimens with an intermediate grain size is strikingly different to that of the fine-grained material. In the former case, all of the data at each temperature can be fitted satisfactorily to a single straight line over the whole range of strain rates examined. However, in the latter case there appear to be four distinctly linear regions at 293°K and three at 243°K, the existence of which cannot be explained on the basis of experimental scatter alone. The regions are numbered from I to IV as shown in the figure. The method of least squares was used for curve fitting and one can represent each of the straight line portions analytically by a simple expression of the form

$$\sigma_Y = \alpha + \beta \log \dot{\epsilon} \qquad (41)$$

where α is the stress-intercept at $\dot{\epsilon} = 1$ sec.$^{-1}$, and the slope, β is a measure of the strain-rate sensitivity of the lower yield stress.

The various values of α and β are given in Table 5, with β, the most important parameter for our purpose, being accurate to about $\pm$ 4%.

In addition to the decrease in σ_Y of nearly 30%, the net effect of an increase in temperature from 243°K to 293°K is to shift the transition points in the $\sigma_Y - \log\dot{\epsilon}$ plots for the fine grain size to higher strain rates (Table 6). Whereas the slopes of the respective stages remain roughly independent of temperature in this range, except in the case of Region III, it is evident from the available data that the strain-rate sensitivity in Region I of the fine-grained specimens has been significantly reduced, as has that of the coarser grained material above a strain rate of 0.4×10^{-4} sec.$^{-1}$, by increasing the temperature to 373°K.

An interesting feature of the yielding behaviour of molybdenun is the fact that a change in strain rate of five orders of magnitude does not lead to a systematic variation in the value of the yield drop. This is effectively demonstrated by plotting the upper yield stress, σ_U, against $\log\dot{\epsilon}$ in Figure 15 for 243°K and 293°K. In spite of the large scatter, a comparison with the lower yield stress curves, which are included, reveals the closely parallel behaviour. It should be emphasized again that the switch from the Instron to the Hounsfield below 0.44×10^{-4} sec. does produce an unavoidable discontinuity in the values of σ_U, so that the results from the two machines should be considered separately. No comparison can be made between σ_U and σ_Y for specimens with a grain size of 0.098 mm.

Table 5. Values of the constants in the equation

$$\sigma_Y = \alpha + \beta \log \dot{\epsilon}.$$

Grain size = 0.027 mm.

Region	α (kg.mm.$^{-2}$)			β (kg.mm.$^{-2}$(log sec.$^{-1}$)$^{-1}$)		
	243°K	293°K	373°K	243°K	293°K	373°K
I	77.0	65.8	41.6	6.75	7.56	5.04
II	45.7	33.9	*	0	0	*
III	106	69.7	*	12.0	7.40	*
IV	*	27.8	*	*	0	*

Grain size = 0.098 mm.

I	61.5	49.1	27.8	6.30	6.40	3.92

Table 6. The strain rate at the transition points in the yield stress - strain rate curves for specimens with a grain size of 0.027 mm.

Region	Transition Strain Rate (sec.$^{-1}$)		
	243°K	293°K	373°K
I - II	0.22×10^{-4}	0.56×10^{-4}	$\sim 0.9 \times 10^{-4}$
I - III	0.50×10^{-5}	1.4×10^{-5}	*
III -IV	*	2.0×10^{-6}	*

since only one specimen tested on the Hounsfield exhibited a yield point. Therefore, the solid line is intended to indicate that $\sigma_U = \sigma_Y$, i.e. $\Delta\sigma = 0$.

The scatter in the measurements of the Lüders strain of fine-grained specimens, shown plotted against $\log \dot{\epsilon}$ in Figure 16 for

243°K and 293°K, is even greater than that of the yield drop. Although there appears to be a slight tendency for ϵ_L to increase with an increase in strain rate it is clearly difficult to place any confidence in this trend. One can merely note the relative insensitivity of ϵ_L to strain rate changes in the range used. The specimens with an average grain size of 0.098 mm. did not exhibit a Lüders strain.

3.2.3 Flow Stress.

The experimental approach to the investigation into the influence of strain rate, and also temperature, on the flow stress of molybdenum differed from that used in Section 3.1.3 to study the effect of grain size. In the latter case, the flow stress was measured directly from a straightforward true stress-true strain curve, and the results for various grain sizes compared at a constant strain. One had to ignore the possibility that the same strain in specimens with different grain sizes did not necessarily represent the same dislocation structure due to their inherently different dislocation creation and multiplication characteristics up to the strain in question. In consequence, the observed variation in flow stress with grain size may not be solely a reflection of the influence of grain size per se. A similar argument holds for temperature or strain rate changes. Whereas a solution to the problem is not readily apparent in the grain size case. Cottrell and his co-workers[100,101] employed an alternative testing technique to reveal the effect of a change in temperature on flow stress which is equally applicable to strain-rate changes. This method entails making a temperature or strain-rate change at a fixed plastic strain during

the course of a test on a single specimen, thereby permitting a comparison of the flow stress at two different temperatures or strain rates for a constant dislocation configuration. The resulting flow stress change is, in effect, a change in the thermal component, τ^*, of the flow stress, discussed in Section 1.5 of the Introduction. Furthermore, if the change to the second temperature or strain rate, and back to the initial one, could be made instantaneously then the load would return to the initial value and the flow curve would continue as if the change had never been made. For this reason the changes in flow stress obtained by temperature or strain-rate cycling experiments have become known as reversible changes in flow stress.

In detail, two types of strain-rate cycling experiments were conducted. On one hand, a series of specimens were strained repeatedly at the same basic rate, $\dot{\epsilon}_i$, partially unloaded, and then strained at a second, higher rate, $\dot{\epsilon}_f$, which was different for each test. On the other hand, a series of tests were carried out in which $\dot{\epsilon}_i$ and $\dot{\epsilon}_f$ were both changed in such a way that their ratio, $\dot{\epsilon}_f/\dot{\epsilon}_i$, termed the strain-rate factor, remained constant at a value of two. To distinguish between them, the first type was designated a strain-rate factor change experiment, and the second, a basic strain-rate change experiment. A typical load-elongation curve produced by strain-rate cycling is shown in Figure 17.

The method of evaluation of the stress change was identical to that used by other workers[79,88], that is, the values of the stress

corresponding to two strain rates were extrapolated linearly to the same plastic strain as illustrated in Figure 17. All measurements were made for an increase in strain rate, and therefore, an increase in flow stress.

A number of preliminary experiments established the following facts. Flow stress changes were independent of whether the strain rate was changed instantaneously or subsequent to unloading. Since the latter method permitted more accurate extrapolation, it was adopted. The amount and duration of unloading were not critical variables. Moreover, intermediate stages of load relaxation by suddenly stopping the Instron did not seem to affect the outcome of the results, and a continuation of the test at the same strain rate brought the load back to the same point on the flow curve from which it had fallen. Yield points were never observed after reloading at the same or a different strain rate, or after load relaxation. These observations tended to support the view that the reversible changes in flow stress were not measures of unloading or relaxation effects to any appreciable extent.

Strain-rate cycling was carried out at three temperatures, 243,293 and 373°K, using only fine-grained material with $l = 0.027$ mm. The principle reason for this choice, instead of the coarser grain size, lay in the fact that its generally greater ductility enabled one to cycle over a wider range of strain at the lowest temperature and higher strain rates. Having chosen the fine grain size for this work the selection of the range of strain rates and the minimum value

of the basic strain rate was determined by two considerations. Since the lowest cross-head speed of the Instron sets a lower limit of 0.44×10^{-4} sec. on the strain rate, the only region within which cycling could be performed without the risk of running into another stage was Region I. This, in turn, fixed the minimum of ϵ_i at 0.88×10^{-4} sec.$^{-1}$

A typical series of results produced by strain-rate factor change experiments are shown in Figure 18 where the reversible change in the flow stress, $\Delta\sigma_T$, is plotted against the stress σ, at which the change was made to a higher strain rate. Stresses are given as true values calculated on the assumption of constant volume. Cycling was discontinued at the onset of plastic instability because a suitable correction could no longer be made for the reduction in area. It is evident that in every case $\Delta\sigma_T$ decreases with increasing stress (or strain) in an approximately linear manner. Moreover, this stress-dependence of the strain-rate sensitivity at 293°K and 373°K becomes more pronounced as the strain-rate factor is increased. However, at 243°K a change in the strain-rate factor produces no apparent change in the stress-dependence of $\Delta\sigma_T$. In general, the strain-rate sensitivity at 243°K for low strains is similar to that at 293°K, but falls off noticably at 373°K. This can be seen by plotting $\Delta\sigma_T$ against $\log \dot{\epsilon}_f / \dot{\epsilon}_i$, i.e. $\Delta \log \dot{\epsilon}$, as in Figure 19. As $\Delta\sigma_T / \Delta \log \dot{\epsilon}$ is in all cases dependent on σ, the value of $\Delta\sigma_T$ corresponding to the yield stress of the specimen was taken. To a first approximation this is equivalent to

selecting $\Delta\sigma_T$ at zero strain. The initial slopes, given by $\Delta\sigma_T/\Delta\log\dot{\epsilon}$ are 6.35, 6.35 and 4.05 kg.mm.$^{-2}$ sec. for 243°, 293° and 373°K, respectively, and can be compared with the values of β appearing in Table 5 for Region I yielding of specimens with l = 0.027 mm.

An increase in the basic strain rate, for a constant strain rate factor of 2, results in an increase in overall strain-rate sensitivity and an increase in the dependence of $\Delta\sigma_T$ on σ (Figure 20). In comparison, the plot for $\dot{\epsilon}_r/\dot{\epsilon}_i$ = 20 illustrates the relatively smaller effect of a basic strain-rate change of two orders of magnitude.

3.2.4 Petch Parameters.

Since the strain-rate dependence of the lower yield stress was determined for two appreciably different grain sizes over a wide range of strain rates, one has, in theory at least, the two points required to establish the Petch relation at each strain rate. Correspondingly, the values of σ_I and k_Y derive directly and their strain-rate dependence can be found. This dependence at 243, 293 and 373°K is shown in Figure 21 for σ_I and k_Y calculated on the basis of the mean curves drawn for σ_Y versus $\log\dot{\epsilon}$ in Figure 14. The purpose of using the curves themselves instead of the actual data points is two-fold. In the first place, each curve was considered to be more truly representative of the average strain-rate dependence of the lower yield stress than a series of results, at individual strain rates, which show a certain amount of scatter from the least square lines. In the second place, their use enabled the determination of

a continuous spectrum of values of σ_I and k_Y as functions of strain rate.

The results of Figure 21 indicate that the choice of strain rate has a considerable influence on the Petch parameters. At high strain rates corresponding to Region I yielding in the fine-grained material, σ_I and k_Y both increase linearly with a logarithmic increase in strain rate, although the change in k_Y is relatively small. At the same time, the strain-rate dependence of σ_I is greatest at 243°K and least at 373°K, and of k_Y, greatest at 293°K and least at 243°K. It is also interesting to note that σ_I and k_Y apparently increase with a decrease in temperature for a given strain rate, but again, the change in k_Y is very small. On the other hand, the existence of the various regions for the fine-grained material leads to a rather odd effect of strain rate on the Petch parameters at the lower strain rates. By comparing Figures 14 and 21 it is a simple matter to correlate the transition points with the extrema in the k_Y curves, and the horizontal Regions II and IV with the steepest slopes of the σ_I curves. Of particular significance is the fact that σ_I becomes negative on decreasing the strain rate below 10^{-5} sec.$^{-1}$

Now, the whole procedure which was used to establish the Petch plot experimentally on the basis of only two data points is, of course, open to severe criticism. Nevertheless, it can be justified to a reasonable degree, and the most obvious way of doing so is to carry out Petch-type experiments for a series of strain rates and

temperatures. In practice, the inherent enormity of such a task prohibited the selection of all but a few critical strain rates at a single temperature. In the end four were used, namely, 1.6×10^{-6}, 1.3×10^{-5}, 0.88×10^{-4}, and 1.8×10^{-2} sec.$^{-1}$ at a temperature of 293°K. Grain sizes were obtained by strain-annealing (Tables 2 and 3). The results are given in Figure 22, where the yield stress was defined as in Section 3.1.2. Corresponding values of σ_I and k_Y determined from the linear portions associated with the finer grain sizes are shown as data points in Figure 22. More specifically, σ_I and k_Y at 0.88×10^{-4} sec.$^{-1}$ are 10.7 ± 2.0 kg.mm.$^{-2}$ and 4.0 ± 0.5 kg.mm.$^{-3/2}$ respectively, which agree very well with the values for Ingot 1, within the assigned error. Consequently, it appears from these results that an appreciable discrepancy does not arise by determining σ_I and k_Y from the two grain sizes only.

Furthermore, it is of interest that the single crystal and coarse-grained results at the two lowest strain rates most decidedly confirm that a transition must occur in the Petch plot in order to obtain finite positive strengths in the large grain-size region. Even at the highest rate of 1.8×10^{-2} sec.$^{-1}$ there is evidence for this transition.

3.2.5 Additional Observations.

The work-hardening rate of molybdenum has been found to increase with decreasing temperature[78]. It is therefore expected that an increase in strain rate would also give an increase in work-hardening rate. Calculations showed this to be the case. Typically, a

variation from 0.72×10^{-6} to 0.44×10^{-1} sec.$^{-1}$ resulted in an increase in the rate of work hardening from $\sim\mu/65$ to $\sim\mu/40$ for specimens with a 0.098 mm. grain size. Although this variation is not readily apparent from the tensile curves of Figure 13, it can be discerned easily in strain-rate cycling experiments. In these, the higher strain rate is always accompanied by a higher work-hardening rate for the range of strain rates used.

An attempt to detect possible differences in work-hardening rates in various stages did not yield positive results on account of the extensive scatter in the results.

The strain-rate dependence of the ductile fracture stress was examined for the relatively few specimens which were deformed to fracture. It was found that an increase in strain rate, in the range above 0.4×10^{-4} sec.$^{-1}$ did not affect the ductile fracture stress as much as the yield stress, but did lead to a detectable increase of about 4.8 kg.mm.$^{-2}$(log sec.$^{-1}$)$^{-1}$ for both grain sizes, 0.027 mm. and 0.098 mm. However, at 243°K the strain-rate sensitivity dropped to practically zero.

From the point of view of ductility, there was a general tendency for the total elongation to decrease with increasing strain rate for both grain sizes at 243°K and 293°K. This decrease was accompanied by a decrease in the reduction in area to fracture, except in the case of fine-grained specimens tested at 293°K. Here, the early onset of plastic instability resulted in a measured increase instead of a decrease. In view of recent observations by Wronski[48]

on the grain-size dependence of the ductile-brittle transition temperature for polycrystalline molybdenum, it was not surprising that at 243°K, the onset of brittleness occurred at a lower strain rate for the fine-grained than coarser-grained material. For example, three out of four of the former were brittle at 1.8×10^{-3} sec.$^{-1}$ whereas brittleness was not encountered in the latter at 0.88×10^{-2} sec.$^{-1}$

The extrapolation technique (Figure 10) of determining the Petch parameters was applied to specimens from Ingot 2 with a grain size of 0.027 mm. and 0.098 mm. tested at 293°K at various strain rates. At 0.88×10^{-4} sec.$^{-1}$ the values fell on the curve of Figure 11 for Ingot 1 specimens. However, their strain-rate dependence did not follow a systematic pattern similar to that in Figure 21 as found by the conventional method of Petch. Consequently, the extrapolation method was discarded.

3.3 The Effect of Temperature on Tensile Properties.

Unlike the case of strain-rate effects, the influence of changes in testing temperature on the tensile properties of polycrystalline molybdenum is reasonably well documented[15,48,102-104] except for reversible changes in flow stress, which have not been reported. The main reason then, for investigating the effect of temperature on the upper yield stress, lower yield stress, yield drop, Lüders strain, and flow stress in the present work is to establish the characteristics of the present material for purposes of correlation with the rest of the data.

All of the tests were conducted on specimens with a grain size of 0.027 and 0.098 mm. using the Instron testing machine at a strain rate of 0.88×10^{-4} sec.$^{-1}$ Temperatures in the range from 190°K to 450°K were obtained as described in Section 2.4.2.

3.3.1 Yielding Characteristics.

Since a yield point was invariably observed, the lower yield stress, σ_Y, was defined as in Section 3.2.2. A plot of the values of σ_Y against temperature in Figure 23 shows that the yield stress for both grain sizes is very sensitive to changes in temperature, particularly below 350°K. The linear portion below 320°K represents a temperature sensitivity of approximately 0.3 kg.mm.$^{-2}$ deg.$^{-1}$ As the temperature sensitivity is practically independent of grain size there is a suggestion that k_Y may be relatively independent of temperature for this material. Although this observation was not confirmed by conducting Petch-type experiments at the lower temperatures, it is not inconsistent with the relatively small effect of temperature on k_Y found in the strain-rate experiments of Section 3.2.4.

Whereas the experimental points for 0.098 mm. at all temperatures, and the ones for 0.027 mm. above 200°K represent an average of 2 to 16 tests, with a scatter less than 5%, the onset of brittleness in the fine-grained material precluded the attainment of a good average below 200°K without an excessive wastage of specimens. In fact, the result given for 195°K is from one test, obtained after four attempts. As a consequence, it is not

considered particularly reliable. Taken together with the lack of embrittlement in the coarser-grained specimens down to 190°K, these observations support previous evidence that the ductile-brittle transition temperature of molybdenum is higher for finer grain sizes[48].

In Figure 23 are also plotted the upper yield stresses, σ_U, for the two grain sizes. The results closely parallel those for σ_Y although the yield drop for specimens with a 0.027 mm. grain size has a tendency to increase slightly with decreasing temperature.

The Lüders strain plotted in Figure 24, appears to increase very slowly with increasing temperature, for the fine-grained material, but remains zero throughout for the 0.098 mm. grain size.

3.3.2 Flow Stress.

The influence of temperature on the flow stress was determined by conducting temperature cycling experiments on material with a grain size of 0.027 mm.

Initially all specimens were deformed past the Lüders strain at the basic temperature of 293°K and then unloaded to about 10 kg. to maintain axiality. Thereafter, the temperature was changed to 190°, 243° or 373°K by immersion in the appropriate bath as described in Section 2.5.2. After allowing not more than ten minutes for temperature stabilisation, the specimen was reloaded at the same strain rate and deformed approximately 1% at the new temperature, unloaded again, and reloaded at 293°K. This cycle was repeated

several times up to onset of necking. In order to ensure that 293°K be reached consistently and reasonably rapidly, a water bath at this temperature was used. The general features of the load-elongation curve obtained by temperature cycling did not differ appreciably from the typical one shown in Figure 17 for strain-rate cycling. Moreover, irregularities such as yield points subsequent to unloading or load relaxation were never seen. As a result, the observed change in flow stress at a given strain was considered to be a measure of the influence of temperature at a constant dislocation configuration. The change in flow stress was evaluated in a similar manner to that described in Section 3.2.3.

Figure 25 shows the reversible change in flow stress $\Delta\sigma_{\dot{\epsilon}}$, plotted against the stress σ, at which the temperature is decreased. It is apparent that within the experimental accuracy, $\Delta\sigma_{\dot{\epsilon}}$ is independent of stress (or strain) for temperature changes between 293°K to 190°K. However, as the secondary cycling temperature is increased, there is an increasing tendency for $\Delta\sigma_{\dot{\epsilon}}$ to decrease linearly with σ.

A comparison of the temperature-dependence of the flow stress with that of the lower yield stress is given in Figure 26. The values of $\Delta\sigma_{\dot{\epsilon}}$ found by extrapolation to the lower yield stress (i.e. zero strain) are plotted against the secondary cycling temperature and the lower yield stresses for $l = 0.027$ mm. are shown as differences, $\sigma_T - \sigma_{293}$, between σ_Y at a temperature T and that at 293°K. It is evident that there is no appreciable difference between the temperature dependence of the lower yield stress and the thermal

component of the flow stress. If the values of σ_U were plotted in the same manner, one would not detect an appreciable deviation from the curve.

3.4 Evaluation of the Activation Parameters.

For purposes of application, Equation (24),(33) and (34) were written in terms of tensile stress and tensile strain rate, neglecting the stress variation of ν, as

$$H = -kT^2 \frac{\left(\frac{\partial \sigma}{\partial T}\right)_{\dot{\epsilon}}}{\left(\frac{\partial \sigma}{\partial \ln \dot{\epsilon}}\right)_T} \qquad (24a)$$

$$v^* = 2kT \left(\frac{\partial \ln \dot{\epsilon}}{\partial \sigma}\right)_T \qquad (33a)$$

$$H = kT \ln (\nu / 0.7\dot{\epsilon}) \qquad (34a)$$

where $\sigma = 2\tau$ and $\dot{\gamma} = 0.7\dot{\epsilon}$.

The magnitude of σ_μ which is required to establish the effective stress σ^* ($= \sigma - \sigma_\mu$) is normally taken experimentally as the observed yield stress at the temperature, T_o, where the temperature dependence begins to reside completely with the shear modulus. In this work, experiments were not conducted at sufficiently high temperatures to permit a direct determination of σ_μ. However, an extrapolation of the yield stress-temperature curves

beyond 450°K by a comparison with the results of other workers (collated by Conrad and Hayes[80]) gave values for σ_μ of 16.1, and 5.4 kg.mm.$^{-2}$ for a grain size of 0.027 mm., and 0.098 mm., respectively, at $T_o = 600 \pm 50$°K. The error, estimated at not greater than $\pm$ 1 kg.mm.$^{-2}$, in finding σ_μ by the above method is not considered significant as σ^* is used only for plotting results.

3.4.1 The Activation Energy, H.

Values of the activation energy for yielding and flow were calculated, using Equation (24a), from the measured dependence of the upper yield stress, lower yield stress and flow stress on temperature at a strain rate of 0.88×10^{-4} sec.$^{-1}$ (Region I) and on the strain rate at 243, 293 and 373°K for the two grain sizes, 0.027 mm. and 0.098 mm. The flow stress data corresponding to strains of zero, 0.025 and 0.10 were found from the results of strain-rate factor change experiments. A record of the activation energies is given in Table 7. Figure 27 shows the same values of H plotted against σ^*, with the omission of those for flow at $\epsilon = 0.05$ and 0.10.

The dashed curve in Figure 27 represents activation energies determined from results which were obtained by a combined extrapolation and interpolation of the direct measurements of the temperature and strain-rate dependence of the lower yield stress. Since one cannot place absolute confidence in such values, the curve is intended only as a prediction of the way in which the activation energies shown as the actual data points might tie together.

Table 7. Values of the activation energy, H, for the yielding and flow of polycrystalline molybdenum.

Grain Size (mm.)	Temp. (°K)	* (kg.mm.$^{-2}$)	Activation Energy, H, in eV				
			Upper Yield	Lower Yield	Flow		
					Strain		
					0	0.05	0.10
0.027	243	33.1	0.58	0.48	0.47	0.53	0.55
	293	20.2	0.75	0.62	0.64	0.82	0.87
	373	5.2	-	0.24	0.26	0.48	0.66
0.098	243	30.1	0.50	0.50	-	-	-
	293	17.5	0.71	0.71	-	-	-
	373	6.5	-	0.37	-	-	-

There is no doubt, however, of the fact that H for this material, as calculated using Equation (24a), increases with decreasing stress at high stresses, and drops to a low value at low stresses. In addition, it is clear that H is independent of grain size and not significantly different for upper yield, lower yield or subsequent flow. In all cases, H for flow increases as the strain increases, and in turn, the strain-dependence appears to increase with increasing temperature.

3.4.2 The Activation Volume v^*.

Activation volumes were calculated, using Equation (33a), from the measured dependence of the upper yield stress, lower yield stress and flow stress on strain rate at 243, 293 and 373°K for the two

Table 8. Values of the activation volume, v^*, for the yielding and flow of polycrystalline molybdenum.

Grain Size (mm.)	Region	Temp. (°K)	σ^* (kg.mm^{-2})	Act'n vol. v^* in units of b^3			
				Upper and Lower Yield	Flow		
					Strain		
					0	0.05	0.10
0.027	I	243	29.6-42.5	11.5			
			33.1		12.3	12.8	13.3
		293	17.8-44.4	12.4			
			20.2		14.8	16.4	17.4
		373	5.2-31.2	23.7			
			5.2		26.5	33.9	39.7
0.098	I	243	17.6-43.0	12.3			
		293	5.3-35.8	14.6			
		373	5.3-14.3	30.5			
0.027	II	243	29.6	∞			
		293	17.8	∞			
	III	243	21.1-29.6	6.5			
		293	11.7-17.8	12.7			
	IV	273	11.7	∞			

grain sizes, 0.027 mm. and 0.098 mm. Table 8 gives the results for yielding corresponding to the various regions of Figures 14 and 15 for l = 0.027 mm. and the single region (designated I) for l = 0.098 mm. Also listed in Table 8 are the values of v^* for flow at ϵ = 0, 0.05 and 0.10, as determined from the results of strain-rate factor change experiments. The activation volumes for Region I yielding, and flow at ϵ = 0 are plotted against σ^* in Figure 28. In the case of yielding the constant slopes of the yield stress-log (strain rate)

curves over wide ranges of strain rate necessarily lead to constant values of v^* over wide ranges of σ^*. It is evident from the figure that, in general, v^* is not appreciably different for upper and lower yield, and subsequent flow, for a given grain size and temperature. On the other hand, v^* tends to be somewhat greater for the coarser-grained material at all three twmperatures with the difference increasing as the temperature increases. However, it is doubtful whether the difference can be considered to be significant at 243 and 293°K.

The effect of stress, and strain, on the activation volume for flow is better illustrated in Figure 29 in which are plotted values of v^* for $\epsilon = 0$ and 0.10 obtained from results of basic strain-rate change experiments conducted at 243, 293 and 373°K. It can be seen that v^* increases with decreasing stress at a given strain and with increasing strain at a given stress. A curve corresponding to $\epsilon = 0.05$ would lie symmetrically between the ones for $\epsilon = 0$ and 0.10.

3.4.3. The Frequency Factor, ν.

The magnitude of the frequency factor at a strain rate of 0.88×10^{-4} sec.$^{-1}$ was calculated assuming that Equation (34a) is a true representation of the relation between temperature and the activation energy. It should be noted that only the data for 243°K and 293°K could be used effectively in view of the abnormally low values of H at 373°K. On this basis, ν was found to be about 2×10^{6} sec.$^{-1}$ independent of grain size and irrespective of whether the upper yield, lower yield or flow was considered.

If one were to ignore the high temperature values of H (and there is no justification whatever for doing so) then Equation (34a) provides the only means at our disposal for estimating H (= H_o) at T_o (i.e. where $\sigma^* = 0$). Taking $\dot{\gamma} = 2 \times 10^{-6}$ sec.$^{-1}$ and $T_o = 600^\circ$K, H would be 1.26 eV or 0.082 μb^3. This would compare favourably with Conrad's value[82] of 0.080 μb^3 for polycrystalline molybdenum tested at a strain rate of 10^{-4} sec.$^{-1}$ Under the circumstances, however, there is every reason to believe from the current work that H approaches zero as T approaches T_o (or as σ^* approaches zero).

4. DISCUSSION.

4.1 The Model for Yielding.

Certain results of this investigation are particularly fundamental with regard to the selection of a model for yielding which might provide the most satisfactory unified treatment not only of the yielding but, as an extension, the subsequent flow behaviour of polycrystalline molybdenum.

Firstly, it has been shown that in the temperature range below 320°K down to the onset of brittleness at ~195°K, the upper yield stress, lower yield stress, and subsequent flow stress of material with a grain size of 0.027 mm. exhibit a nearly identical temperature dependence when tested at a strain rate of 0.88×10^{-4} sec.$^{-1}$ Moreover, this temperature-dependence is not significantly different to that of the upper and lower yield stresses of the coarser-grained (0.098 mm.) material. Secondly, closely allied to the temperature behaviour is the fact that there is no appreciable difference in the pronounced strain-rate sensitivity of the upper yield stress, lower yield stress and flow stress at 243°K or 293°K, irrespective of the grain-size, for strain rates corresponding to Region I yielding. Therefore, in all probability, the dislocation mechanism which determines the temperature and strain-rate dependence of yielding is the same one that governs flow behaviour in molybdenum. It will be recalled that one model of low temperature yielding is based on the unpinning of dislocations from dilute impurity atmospheres. Yet it is unlikely that unpinning can be important in the homogeneous

flow stage where there are already large numbers of dislocations able to move outside the influence of conventional pinning by stationary atmospheres. Consequently, one takes the view that the rate-controlling mechanism is one which affects the properties of free dislocations. From this stand-point, Hahn's model for yielding[18] is adopted and the experimental observations are discussed in terms of their consistency with this model.

4.2 The Yield Point.

The upper yield stress, σ_U, was found to have a strain-rate dependence which is equivalent, within the accuracy of measurement, to that of the lower yield stress, σ_Y, over a range of 10^{-6} to 10^{-1} sec.$^{-1}$ in strain rate. Therefore, one can write for the yield stress in general that

$$\sigma = \alpha_0 + \beta \log \dot{\epsilon} \qquad (42)$$

where β has the same value for σ_U and σ_Y in any particular region. On the one hand, Conrad[34,82] favours such a semi-log relation to describe the strain-rate dependence of the yield stress of b.c.c. metals. On the other hand, Hahn[18] suggests that the emphirical relation

$$\log \sigma = \log B + r \log \dot{\epsilon} \qquad (43)$$

is a satisfactory representation of the experimental facts. Each investigator obtains a reasonably good straight line by fitting results from the literature to the respective relations. As the source of data is the same in several instances, it is uncertain which of the two representations is the more correct. It is

immediately evident on examination that any clear distinction is precluded by the narrowness of the stress and strain-rate ranges covered by each set of experiments. This is also true here for the fine-grained material, where several distinctly linear regions appear for σ_Y (or σ_U) whether plotted on a semi-log scale, as in Figure 14, or on a log-log scale. However, when a log-log plot is used for the σ_Y values of the coarser-grained material, as in Figure 30, a pronounced curvature is readily apparent which is absent in the semi-log plot of Figure 14. Included in Figure 30 is an independent set of results for the lower yield stresses of En 2 steel[105]. In this case, the log-log fit for strain rates greater than $\sim 3 \times 10^{-5}$ sec.$^{-1}$ is considerably better than the semi-log one which exhibits a distinct curvature. Furthermore, Fourdeux and Wronski[106] find that the yield stress of niobium of good purity conforms to a log-log relation over the range 10^{-5} to 1 sec.$^{-1}$ This presents no contradiction to the semi-log plot of Sargent et al[107] for less pure niobium since their range of stress is insufficient to make a distinction between semi-log and log-log behaviour.

Using Equation (10), Hahn predicted that for a constant strain

$$\log \sigma = \log A + 1/m \log \dot{\epsilon} \qquad (44)$$

which is identical to the experimental relation (43) providing A is a constant. Is, therefore, the linear semi-log strain-rate dependence of σ_U (and σ_Y) for molybdenum consistent with Hahn's model for yielding ? From Equation (42) we have, experimentally,

that,

$$\partial \log \dot{\epsilon} / \partial \sigma = 1/\beta \tag{45}$$

and thus

$$\partial \log \dot{\epsilon} / \partial \log \sigma = \sigma \ln 10/\beta \tag{46}$$

where the left-hand side is denoted by m'. However, since A in Equation (44) is given by $(1/\phi bL)^{1/m}$ then a suitable differentiation of (44) yields

$$\partial \log \dot{\epsilon} / \partial \log \sigma = m + \partial \log L / \partial \log \sigma \tag{47}$$

By combining (46) and (47) it can be seen that a semi-log dependence is compatible with Hahn's theory if

$$\partial \log L / \partial \log \sigma = \sigma \ln 10/\beta - m \tag{48}$$

In fact, Hahn did point out that L may be a function of stress as well as strain on the basis of evidence by Li[108] and Guard[109], available at the time, but a specific functional relationship was not given. Subsequently, Johnston and Stein[110] have found that $\Delta \log \dot{\epsilon} / \Delta \log \sigma$ for lithium fluoride and silicon-iron increases with strain (or stress) in strain-rate cycling tests through a roughly linear increase of $\partial \log L / \partial \log \sigma$ with strain. They obtained an expression similar to (47) where m, independent of strain (or stress), is equal to $\Delta \log \dot{\epsilon} / \Delta \log \sigma$ at zero strain. A replot of the current cycling data for molybdenum revealed a linear increase of $\Delta \log \dot{\epsilon} / \Delta \log \sigma$ with stress. If one assumes that $\Delta \log \dot{\epsilon} / \Delta \log \sigma = m$ at zero strain for molybdenum also, and that m is independent of stress (or strain) as for polycrystalline

silicon-iron, then $\partial \log L / \partial \log \sigma$ increases linearly with stress. Whereas the slope evaluates to 0.62, the slope of Equation (48), given by $\ln 10/\beta$, is 0.31 for the same conditions. This agreement, which is surprisingly good in view of the fact that two different types of test are involved in the calculations, provides reasonable grounds for believing that the modile dislocation density varies with the upper or lower yield stress in a manner specified by Equation (48) when the strain rate is changed. Unfortunately, there are no direct measurements to confirm this point. Indirectly, one piece of evidence is favourable. The results of Brown and Ekvall[32] imply that the mobile dislocation density of iron increases with decreasing temperature because of an observed increase in the pre-yield microstrain. Hence, due to the parallel effects experienced on decreasing the temperature or increasing the strain rate, one is justified to some extent in presuming that an increase in strain rate will cause an increase in the pre-yield strain and, by implication, the mobile dislocation density. It is concluded, therefore, that a model for yielding which is based on dislocation multiplication and velocity characteristics can readily lead, under certain circumstances, to a semi-log relation between σ_U(or σ_Y) and strain rate. Also of significance is the fact that neither Hahn's model, nor the activation analysis used extensively by Conrad, necessarily predicts a specific strain-rate dependence. Conrad uses the semi-log relation only as a matter of convenience in the calculation of the activation parameters. Accordingly, it seems that the increase in the yield stress of molybdenum which accompanies an increase in

strain rate is not only a consequence of the increase in stress required to move dislocations at higher velocities but is reduced by the fact that more mobile dislocations become available to meet the deformation requirements as the strain rate increases.

The observed relative insensitivity of the yield drop to changes in strain rate follows directly from a similar argument if, again, $\partial \log L / \partial \log \sigma$ is considered to be linear with stress. The yield drop occurs when the number of mobile dislocations has increased to such an extent that any further increase results in a decrease in the average velocity necessary to maintain the imposed strain rate. Correspondingly, the stress falls also.

It would be advantageous to know how closely one can predict the stress-strain curve for molybdenum from Hahn's equation. An attempt to do this was not completely successful because of the lack of accurate information on multiplication rates and velocity characteristics for molybdenum in general, and this material in particular. Nevertheless, the exercise proved invaluable inasmuch as it served to clarify two important points. On the one hand, our knowledge of the dynamical glide properties of dislocations and the contribution of work-hardening must be precise and pertinent to the specific material under consideration before an equation such as Hahn's can be fully tested. On the other hand, it became obvious that an upper yield stress and a yield drop which agree very well indeed with those observed experimentally can be obtained by this method.

In the past, the strong temperature dependence of the upper (and lower) yield stress has often been interpreted in terms of the temperature dependence of the stress required to unpin dislocations. However, as pointed out, this concept is not completely consistent with the experimental facts. Hahn suggests that the temperature dependence of the yield stress may arise through the influence of temperature on one or more of the parameters in Equation (10). Ignoring for the moment the rate-controlling mechanism itself, let us examine what magnitude of temperature dependence of σ_U one might expect purely from the observed variation of m, σ_o and L with temperature. Writing for the upper yield stress

$$\ln \sigma_U = \ln \sigma_o + 1/m \ln (\dot{\epsilon}/C.5bL_o) \qquad (49)$$

and differentiating with respect to temperature, one obtains

$$\frac{1}{\sigma_U}\frac{\partial \sigma_U}{\partial T} = \frac{1}{\sigma_o}\frac{\partial \sigma_o}{\partial T} + \ln\left(\frac{\dot{\epsilon}}{0.5bL_o}\right)\frac{\partial\, 1/m}{\partial T} - \frac{1}{m}\frac{\partial \ln \sigma_o}{\partial T} \qquad (50)$$

Now, substituting σ_o = 35 kg.mm.$^{-2}$, $\dot{\epsilon}$ = 0.88 x 10^{-4} sec.$^{-1}$, b = 2.73 x 10^{-8}cm., L_o = 3 x 10^{5}cm.$^{-2}$, m = 10, $\partial \sigma_o / \partial T$ =-0.266, $\partial (1/m)/\partial T = \partial(1/m')/\partial T$ = 0.00056 (from Table 9), and $\partial \ln L_o / \partial T$ = 0.0056, all for a grain size of 0.098 mm., into Equation (50) gives

$$\frac{1}{\sigma_U}\frac{\partial \sigma_U}{\partial T} = - 0.0076 - 0.0022 + 0.0006$$
$$= - 0.0092$$

Experimentally,

$$\frac{1}{\sigma_U}\ \frac{\partial \sigma_U}{\partial T} = -\ 0.0105$$

Bearling in mind that there are large uncertainties associated with the above data, the agreement between the predicted and observed temperature-dependence of the upper yield stress is still exceedingly good and encourages the belief that the influence of temperature can be accounted for in terms of its effect on the properties of mobile dislocations, without recourse to unpinning.

Table 9. The stress dependence of dislocation velocity obtained from the strain-rate sensitivity of the yield stress (m') and flow stress (m), evaluated at a strain rate of 0.88×10^{-4} sec.$^{-1}$

Grain Size (mm.)	Yielding (m')			Flow (m)		
	243°K	293°K	373°K	243°K	293°K	373°K
0.027	18.1	13.1	10.9	14.5	13.1	7.6
0.098	12.6	9.3	7.1	-	10.0	-

In order to establish whether the observed insensitivity of the yield drop to changes in temperature is in accord with the predictions of the model, it is necessary to show that the estimated temperature dependence of the lower yield stress is not significantly different from that of the upper yield stress. In the determination of the temperature dependence of σ_Y, we are beset by two main difficulties. The first involves the lack of a measurement of the dislocation

multiplication rate for this material. As a result, one for a zone-refined single crystal of molybdenum[94] was used, given by $3.6 \times 10^{7} \epsilon^{0.94}$, which is comparable to rates quoted by Hahn[18] for iron and steel. The second problem is more serious and concerns the contribution of work-hardening to the lower yield stress. As a first approximation, the temperature dependence of the macroscopic work-hardening rate evaluated at the lower yield strain using Equation (37) was considered. Thus, using Equation (10), one can write

$$\frac{1}{\sigma_Y}\frac{\partial \sigma_Y}{\partial T} = \frac{\epsilon_p}{\sigma_Y}\frac{\partial q}{\partial T} + \frac{1}{\sigma_o}\frac{\partial \sigma_o}{\partial T} + \ln\left(\frac{\dot{\epsilon}}{0.5bL}\right)\frac{\partial 1/m}{\partial T} - \frac{1}{m}\frac{\partial \ln L}{\partial T} \qquad (51)$$

which evaluates to - 0.0108. As a result, $\partial \sigma_Y / \partial T$ becomes - 0.25 which compares favourably with the value of - 0.24 for $\partial \sigma_U / \partial T$. Thus, as in the case of the insensitivity of the yield drop to changes in strain rate, the properties of free dislocations can be used effectively to account for its insensitivity to temperature.

4.3 The Grain-size Analysis.

Previously, changes in the mechanical properties of molybdenum which has undergone neutron irradiation[36,37] or a variation of testing temperature[48] have often been treated on the basis of changes in the Petch parameters. The results of this investigation leave little doubt that at 293°K and a strain rate of 0.88×10^{-4} sec.$^{-1}$, the lower yield stress of arc-cast molybdenum in the annealed and unirradiated state obeys a Petch relation of the form

$$\sigma_Y = \sigma_I + k_Y l^{-\frac{1}{2}} \qquad (16)$$

in the grain size range from 0.027 to 0.25 mm. The corresponding values of σ_I and k_Y, 9.3 kg.mm.$^{-2}$ and 4.3 kg.mm.$^{-3/2}$, respectively, for Ingot 1, and 10.7 kg.mm.$^{-2}$ and 4.0 kg.mm.$^{-3/2}$ for Ingot 2 are in agreement with those found by Johnson[111](11.0 and 5.5) and Wronski[48](10.2 and 3.7) for material produced in a similar manner and tested under the same conditions. The value of σ_I is comparable to that for other b.c.c. metals but the k_Y value for molybdenum is the highest reported for the b.c.c. transition metals[45,46] being over ten times greater than that for niobium.

Two features of fundamental importance, which have not been reported hitherto for any of this group of materials, are evident from the yield stress-grain size plot in Figure 4 for molybdenum. Firstly, σ_Y is practically independent of grain size above 0.25 mm. This indicates that the hardening effect of grain boundaries in molybdenum does not become significant until some critical grain size, l_c, is attained, in this case $\sim$0.25 mm. Secondly, the lower yield stress of single crystals can clearly not be identified with the value of σ_I, as found by the extrapolation of the data for finer grain sizes. Since this identity constitutes one of the basic assumptions in the modified theory of Johnson[60], its applicability to the deformation behaviour of molybdenum is open to serious criticism. Irradiated molybdenum exhibits similar behaviour in that σ_Y does not become dependent on grain size until some critical grain size is reached, although the transition occurs at a much smaller grain size, namely, $\sim$0.06 mm.

4.2.1 Characteristics of k.

It is pointed out in Section 1.4 that k_Y as a measure of the grain-size dependence of σ_Y, could reflect, to some extent, a possible variation in the dislocation substructure which may arise when different thermal or mechanical treatments are used to produce different grain sizes. For example, tantalum[55,112] and vanadium[46] appear to be particularly susceptible to such variations when the annealing temperature is changed. Satisfactory data is not available for molybdenum although Johnson and Wronski[37,113] claimed that in their material the sub-grain size was independent of grain size. This may indeed be true, but the present author found that the same metallographic technique used by the above workers gave misleading results for the current material. The apparent sub-grain size agreed favourably with that reported by Johnson and Wronski but it was clearly seen to be a surface etching characteristic and bore no relation to the dislocation substructure. Consequently, an etch-pitting technique, described in Section 2.4, was used to reveal individual dislocations in typical specimens from Ingot 2 with a grain size of 0.027 mm. and 0.098 mm. Within the experimental scatter, their yield stresses fell on the Petch plot for $l < 0.25$ mm. Figures 31(a) and (b) show that there is no appreciable difference in the dislocation density and distribution for the two grain sizes, and that sub-boundaries are absent in both cases. The distribution was found to be fairly homogeneous, with a density of about 3×10^7 cm.$^{-2}$, therefore within the range $10^6 - 10^8$ cm.$^{-2}$ usually associated with annealed metals. It would be unwise to place much

faith in the absolute value of the dislocation density determined by etch-pitting, especially since the pit density in molybdenum varies markedly with orientation[94]. Nevertheless, one can obtain suitable relative values by making the comparison for similar pit shapes since the shape also varies with orientation.[94] In order to demonstrate that substructure can play an important role in determining σ_Y, and therefore k_Y in molybdenum, several specimens with $l = 0.098$ mm. were pre-strained 5% and then annealed at 1600°C for one hour. A change in grain size was not detected, yet the yield stress invariably increased about 35%. If one were to use the σ_Y value for $l = 0.027$ mm., this could lead to an observed k_Y of approximately 1.7 kg.mm.$^{-3/2}$, a reduction of over 50%. Since the same anneal for specimens without a pre-strain produced no appreciable change in grain size, and a slight decrease in yield stress, the difference in behaviour cannot be attributed to the introduction of impurities during annealing. Instead, the increase in σ_Y must be attributed to a difference in substructure. Figure 32 shows the increase in dislocation density and introduction of sub-boundaries resulting from the above strain-anneal treatment. One concludes, therefore, that the k_Y value determined from the present Petch analysis is a true measure of the influence on σ_Y of grain size per se, but that a variation in dislocation substructure with grain size can have a pronounced effect on the magnitude of k_Y. Furthermore, it is suggested that little variation from a true k_Y will be experienced provided grain growth occurs to "mop up" some of the dislocations introduced initially by pre-straining or during fabrication. This

would account for the similarity in k_Y for Ingot 1 specimens where the grain sizes were obtained by strain-annealing and k_Y for Ingot 2 where the grain size was varied by changing the fabrication treatment. Any difference in k_Y from that found by other workers[48,111] is not large enough to be considered significant.

In order to overcome the complication of a possible variation in substructure with grain size, some investigators advocate the use of the extrapolation method to find the true values of the grain size parameters. Figure 11 shows that for grain sizes less than $\sim$0.16 mm., k_Y by extrapolation is less than that obtained from the Petch plot, and σ_I is greater. In addition, the extrapolated value of k_Y increases with increasing grain size whereas σ_I decreases. These facts clearly indicate that the two methods yield results which cannot be identified with each other in the case of impure molybdenum. Johnson[114] reaches the same conclusion except that his values do not vary with grain size for similar material. This difference in the two sets of results is understandable when one considers that Johnson's extrapolations were performed graphically using load-elongation curves. The analytical extrapolation applied here to true stress-true strain data is the more accurate.

Usually the difference in k_Y obtained by the two methods, and the increase in the extrapolated value with increasing grain size is explained on the basis of a decrease in dislocation density or substructure with grain size. This could occur when increasingly higher annealing temperatures are employed to achieve an increase

in grain size[112]. The implication is that if the impurity content is low enough, the strength of locking increases as the dislocation density decreases thereby causing a corresponding increase in k_Y[115]. These arguments break down in the present case for two main reasons. Firstly, it has already been shown that the dislocation density does not vary appreciably with grain size. Secondly, the interstitial impurity concentration of the molybdenum used here would be sufficient to make the strength of locking independent of any variation in dislocation density over the range expected in fully annealed material[1,2]. Since the k_Y value determined by the grain-size method is believed to be a true value, it becomes difficult to attach any specific significance to the extrapolated parameters, at least for molybdenum.

The following considerations point to a serious shortcoming when the extrapolation method is applied to niobium. Recently, Lindley and Smallman[115], and Gilbert et al[55] found reasonable agreement between the two methods for relatively impure vanadium, and tantalum containing a large amount (147 p.p.m.) of oxygen. However, for electron beam melted niobium[115], k_Y by extrapolation was 5 to 8 times higher than the Petch value and increased with increasing grain size. This was attributed to the decreasing dislocation density and accompanying increase in strength of locking because of the high purity. However, if this is the explanation, one should also get a decrease in the lattice friction stress with increasing grain size, whereas, in fact, σ_I was found to be independent of grain size. Another inconsistency is apparent when

one recalls that k_Y by the grain-size method is also exceedingly small for much less pure niobium[36]. Since any variation in dislocation density of the order expected should not result in any change in locking strength when a large amount of impurity is present, the preceding arguments necessarily lead to a prediction of identical low k_Y's by the two methods. Even if this were true, the small k_Y would still present a problem from the locking viewpoint in that its small magnitude is incompatible with the pronounced yield points observed for niobium[60]. Further, Evans et al[116], also working with niobium of good purity, found k_Y by extrapolation to be only twice the Petch value. On the other hand, after neutron irradiation, the former showed a general decrease, and a marked decrease with increasing grain size, while the latter remained constant. This apparent weakening of locking is contrary to the current view of the effect of radiation introduced defects on yielding [116,117].

The preceding discussion further suggests that our understanding of the meaning of the extrapolated parameters is far from complete and care should be exercised in the use of the extrapolation method in the determination of the grain size parameters.

Until recently, k_Y was generally interpreted[30] as a measure of the unpinning stress (cf. Equation (18)). Fisher[61] has since demonstrated that this interpretation is feasible only in the case of weak dislocation locking. For strongly-locked materials he suggested that k_Y is probably a measure of the stress required to generate fresh dislocations athermally at or near grain boundaries

while heavily locked dislocations remain inactive in yielding. Under these circumstances, one would expect k_Y to be independent of temperature and strain rate. Since the molybdenum used in the present investigation is relatively impure and well annealed, with a dislocation density less than $10^8 cm.^{-2}$, its dislocations must be considered as strongly locked. The relative unimportance of unpinning in yielding is reflected not only in the previously mentioned similarity of the temperature or strain-rate dependence of the yield and flow stress, but also in insensitivity of the yield drop and Lüders strain to temperature and strain rate[30]. Yet, the k_Y value in Figure 21 does appear to increase slightly with decreasing temperature and increasing strain rate in Region I. However, on closer examination, k_Y increases from 4.0 $kg.mm.^{-3/2}$ at 293°K to 4.8 $kg.mm.^{-3/2}$ at 243°K for a strain rate of 0.88×10^{-4} $sec.^{-1}$ but when a probable error of $\pm$ 0.5 $kg.mm.^{3/2}$ is taken into consideration the ranges of magnitude overlap. On the other hand, the results of experiments on the temperature dependence of σ_Y (Figure 23) show that k_Y is not detectably affected by temperature changes in the range 200 to 320°K in which the influence of temperature on σ_Y is the greatest. Therefore, the combined evidence from the temperature and strain-rate experiments suggests that k_Y is not appreciably sensitive to temperature. Moreover, Figure 22 illustrates that the strain-rate sensitivity of k_Y for Region I shown in Figure 21 is not clearly detectable from the Petch plots. One would be hard pressed to explain such small, if not zero, effects of temperature and strain rate on k_Y if, in fact, k_Y were a reflection of thermally

assisted unpinning of dislocations from dilute impurity atmospheres. Consequently, we shall regard k_Y, in this case, to be independent of unpinning effects per se.

Two possible explanations may account for the appreciably smaller temperature dependence of k_Y observed here ($\backsim 0.01$ kg.mm.$^{-3/2}$ deg.$^{-1}$) to that found by Wronski and Johnson[48] (0.022 kg.mm.$^{-3/2}$ deg.$^{-1}$). Figure 21 indicates the importance of the choice of strain rate for investigating the temperature dependence of the Petch parameters. It may be that in their material, the various regions are so situated that in going from one temperature (293°K) to the other (196°K) one changes regions. As this would be expected to give a smaller change in k_Y with temperature to that observed, this explanation is unlikely. More probably, the answer lies in the variation of one or more of the parameters in Equation (10) with grain size. This could influence the temperature dependence of σ_Y as given by Equation (51) in a manner which would lead to the observation of either a temperature sensitive or insensitive σ_Y. For example, the temperature variation of m (approximated by m') is seen from Table 9 to be different for the two grain sizes, 0.098mm. and 0.027mm. In addition, the amount of pre-yield micro-strain is known[118] to increase with increasing grain size in iron, suggestive of a corresponding increase in the mobile dislocation density at the upper and lower yield point. One can reasonably expect a similar tendency in molybdenum, a fact which is consistent, on the multiplication yield point hypothesis, with the observed

decreases in yield drop with decreasing grain size. Another factor which could be important is the variation in the initial total dislocation density and configuration with grain size which could arise during the production of different grain sizes. In this work, no such variation was found whereas Wronski and Johnson[48] did not determine the dislocation substructure of their material. Whether k_Y is temperature dependent or independent is dictated by the balance between the above factors. As it happens, the balance is such that a decrease in temperature leads to little or no change in k_Y for the material used here, and a significant increase for that of Wronski and Johnson[48]. A similar argument prevails for the strain-rate dependence of k_Y. One can now understand the apparent contradictions in the observed temperature behaviour of the k_Y for other b.c.c. metals, discussed in Section 1.4.1. Any detraction from k_Y as a grain size parameter is not implied. Although the above approach is largely speculative at this stage, it brings to light the extreme complexity of the grain size analysis as a whole and of its application to the fundamental understanding of various phenomena such as strain-ageing, irradiation hardening and fracture.

The relatively larger values of k_Y/μ for the Group VIA metals (Mo,W,Cr) than those for the Group VA metals (Nb,Ta,V) metals[46] has been attributed[45,46] to the inferior stress concentrating ability of the more extensive slip bands in the former. Present evidence showed that up to strains of 3% the density of dislocation etch pits in molybdenum increased fairly homogeneously within individual grains. Any localised mass of pits which could be

likened to dislocation pile-ups, slip bands or "forced slip"[60] was not found. This is in accord with the above explanation.

The theoretical development of the yield stress-grain size equation is based on the propagation of Lüders bands. In practice, specimens of molybdenum in the grain size range 0.01 - 0.25 mm. yielded without a detectable Lüders strain. This uniformity of yielding was confirmed directly by etch-pitting. Their lower yield stresses, however, fell on a Petch plot which could be established solely from data for finer grain sizes for which Lüders strains were observed. Both an etch-pitting and brittle lacquer technique showed up the non-uniform propagation of yield. Hence, it seems that the model used in the development is not of particular significance but that the grain-size dependence of the yield stress is nevertheless caused by some grain size dependent boundary accommodation effect. Without further evidence, we must regard k_Y with Fisher[61], as a measure of the stress required to transmit deformation across grain by the athermal generation of fresh dislocations at or near the boundaries.

The increase in the yield drop and Lüders strain for molybdenum with decreasing grain size presents an interesting and pertinent problem. Using dislocation mechanics, the following tentative explanation is forwarded to account for the above observation. Let us ignore, for the moment, the concept of the k parameter and consider generally the different behaviour of coarse and fine grain sizes. The amount of pre-yield microstrain in the former is assumed

to exceed that in the latter[118]. This is regarded by some[118,119] as a consequence of the fact that the density of sources per grain decreases with decreasing grain size. Additional multiplication within coarse grains is probably enhanced by the smaller influence of boundary constraints. Whatever the explanation, the net result is that the mobile dislocation density is greater and dislocations more evenly distributed throughout the gauge length in the coarse grain size case. At the same time, the effect of such macroscopic stress concentrators as shoulders is relatively unimportant. Consequently, macroscopic yielding occurs uniformly, with or without the appearance of a yield point depending on the value of L_o. By contrast, the mobile dislocation density builds up less rapidly in the finer grain sizes and macroyielding finally occurs at a higher stress while L_o is still fairly low. At these higher stress levels, macroscopic stress concentrations become more important in two ways; firstly, in their effect on providing initially a sufficient variation of the mobile dislocation density in the specimen to encourage the localized nucleation of yielding; secondly, in assisting the applied stress in the nucleation process. As the mobile dislocation density at the upper yield point decreases with decreasing grain size, the magnitudes of the upper yield stress and the yield drop increase accordingly[18,27]. The value of the lower yield stress at which propagation occurs is dictated by the combined necessity for the average velocity of the available mobile dislocations at the Lüders front to conform to the requirement imposed by the extension rate[18] and the propagation difficulties imposed by the presence of grain

boundaries. Therefore, the increase in the yield propagation stress, σ_Y, with decreasing grain size is seen to be due partly to the decrease in the number of mobile dislocations at the front and partly to the increase in grain boundary resistance. However, the contribution of each is rather difficult to assess. One would expect the Lüders strain to increase with decreasing grain size for the same reasons.

A direct corollary of the preceding argument is that the k value for flow, k_f, is more representative of the general effect of grain boundaries on the yield stress than k_Y itself. Figure 6 shows that k_f tends to vary slightly with grain size but an average value would be less than k_Y and reasonably independent of strain. Empirically, this result is expected in view of the insensitivity of the work-hardening rate to grain size and the increase in Lüders strain with decreasing grain size. If one could eliminate the effects of the variation in the mobile dislocation density with grain size which are encountered in the early stages of yielding, then k_Y would reflect only the influence of grain boundaries on σ_Y. Accordingly, k_Y would approach k_f as opposed to k_f approaching k_Y. The added implication here is that k_Y for molybdenum has a more complex meaning from the mechanistic point of view than has hitherto been supposed.

4.3.2 Characteristics of σ_o.

The results of this investigation introduce certain difficulties with respect to the interpretation of the conventional σ_I for

molybdenum. The observation that σ_Y is relatively insensitive to grain size above 0.25 mm. so that the yield stress of single crystals never falls to the value of σ_I does not by itself constitute a significant contradiction to the consideration of σ_I as a lattice friction stress. What does seem incompatible with giving σ_I any mechanistic meaning is the fact that it is negative (Figure 21) under certain testing conditions. Consequently, in the case of molybdenum, it seems more reasonable to identify the lower yield stress of single crystals, or slightly less accurately, of specimens with a grain size of $\sim$0.25 mm., with the lattice friction stress σ_I. Since k_Y is not very sensitive to temperature or strain-rate, one can regard the temperature or strain-rate dependence of σ_I as being closely approximated by that of σ_Y for a grain size of 0.098 mm. for which the behaviour has been well documented.

Now, as k_Y is very nearly independent of temperature or strain rate, the major part of the temperature and strain-rate dependence of σ_Y resides with σ_I. No attempt has been made in this work to separate the lattice friction stress into the two components[64,65] σ'_I and σ''_I, defined in Section 1.4.2. Nevertheless, the identical temperature dependence of the yield stress and flow stress, where the latter must be governed mainly by σ'_I, suggests that most of the temperature dependence, and accordingly, strain-rate dependence of σ_Y rests in particular, with σ'_I. Since σ'_I is independent of the amount and distribution of impurities[65], one is forced to rule out overcoming precipitates and solute atoms as rate-controlling mechanisms in impure molybdenum. Moreover,

unpinning has already been eliminated. At this point, however, the grain-size analysis can provide no further conclusive information concerning controlling mechanisms. Although Heslop and Petch[65] and Cottrell[30] propose that the Peierls stress is the controlling mechanism, one cannot safely disregard the possibility that the motion of jogs or cross-slip may be controlling. As a consequence, we go to the thermal activation analysis.

4.4 The Activation Analysis.

Except for one major point, and minor differences in detail, the results of the activation analysis for the yielding and flow of molybdenum do not differ substantially from the findings of Conrad and Hayes[81], and Conrad[82]. Taking the analysis at face value, the apparent activation energy, H_o (i.e. at $\sigma^* = 0$) of $0.082\,\mu b^3$ agrees very well with that of Conrad ($0.080\,\mu b^3$) as does the stress-dependence of H for effective stresses greater than ~ 14 kg.mm.$^{-2}$ In addition, the observed stress-dependence of the activation volume, v^*, does not differ appreciably from that found previously, increasing from $\sim 8b^3$ at $\sigma^* = 40$ kg.mm.$^{-2}$ to nearly $30b^3$ at $\sigma^* = 5$ kg.mm.$^{-2}$ The range of the experiments does not permit comparison below $\sigma^* = 5$ kg.mm.$^{-2}$ The magnitude of v^* at 5 kg.mm.$^{-2}$ from Conrad's data is $\sim 45b^3$. Since small errors in σ^* at low values can lead to large variations in v^*, this discrepancy is not considered to be particularly significant. Good agreement exists between the frequency factor ($\nu \approx 10^{-6}$ sec.$^{-1}$) determined here and that given by Conrad and Hayes[81] as the low range of $10^4 - 10^{11}$ sec.$^{-1}$ and by Conrad[82], of $10^6 - 10^{12}$ sec.$^{-1}$

As in the case of former investigations, the activation energy is the same for yielding and flow which indicates that the rate-controlling mechanism is probably the same for both. Any variation in H with strain can be attributed to the strain-dependence of ν. Moreover, if one were to take the activation volume for yielding and flow at the same effective stress, then their values of v^* would agree reasonably well. However, the fact that v^* for yielding is independent of stress over large ranges of stress is somewhat disturbing when, by definition, v^* should increase with decreasing stress. To clarify this point, let us examine the possibility of determining the stress-dependence of ν where ν is given as Lbs ν_o (Equation (21)). Assuming that the stress-dependence of S and ν_o is negligible[74] compared to that of L, then $\partial \ln \nu / \partial \sigma^* \approx \partial \ln L / \partial \sigma^*$. Using Equation (48), we obtain, for a constant temperature,

$$\frac{\partial \log L}{\partial \log \sigma^*} = \frac{\sigma \ln 10}{\beta \sigma^*} - m \qquad (52)$$

Substitution into

$$v^* = 2kT \left(\frac{\partial \ln (\dot{\epsilon}/\nu)}{\partial \sigma^*} \right)_T$$

gives the activation volume as

$$v^* \approx \frac{2kT}{\sigma^*} \left(m - \sigma_\mu \ln 10 / \beta \right) \qquad (53)$$

Thus v^* is no longer independent of stress but approximately inversely proportional to it, in accord with the experimental observations for flow in Figure 29. A new evaluation of v^* leads to an elimination of the discontinuities in Figure 28 for yielding as enforced by changes in temperature. Instead, a continuous curve results, irrespective of the temperature used in the evaluation. The magnitude of v^* increases from $6\ b^3$ at 40 kg.mm.$^{-2}$ to $40b^3$ at 5 kg.mm.$^{-2}$, again in close agreement with the flow curve for zero strain. Since the latter is thought[110] to be free of variations in L, then the correction utilised for the stress-dependence of ν is believed to be a reasonable first approximation.

The decrease in $\Delta\sigma_T$ and $\Delta\sigma_\varepsilon$ with strain (or stress) in the cycling experiments is simply attributed to an increase in the mobile dislocation density with strain (or stress). This increase is reflected in the derived increase in v^* with strain. When a correction for the stress-dependence of L is incorporated in the stress-dependence of ν then v^* assumes the level at zero strain, and becomes independent of strain.

As the general level of v^*, at the stresses where H has been evaluated, has not changed appreciably by making the above correction for yielding, it is evident that no significant change in the magnitude of H is expected in the present case. This introduces, however, the aforementioned major point of difference between these results and those of other workers[81,82], namely, the decrease in H with a decrease in stress below $\sigma^* \simeq 14$ kg.mm.$^{-2}$

Mathematically, of course, one can foresee this behaviour from Equation (24a) if the temperature-dependence of the yield or flow stress approaches zero more rapidly than the strain-rate dependence as the temperature is raised to T_o. In the present work, low effective stresses were achieved by making measurements at a high temperature. In view of the possibility that H may be a function of temperature as well as stress, temperature may be more important at high temperatures and a correction should be made for it to obtain the true H - σ^* curve. Otherwise, from the mechanistic point of view, the low values of H at low stresses or high temperatures would be difficult to understand. Ideally, low σ^* values should be obtained by lowering the strain rate at a constant temperature but the scope of the current experiments do not permit the evaluation of H in this region because the temperature dependence was only established for a single, relatively intermediate, strain rate. Before this is done, it would be unwise to regard the low H values as a reflection of an inadequacy in the activation analysis. Tentatively, we are forced to take H_o as $0.082\,\mu b^3$.

In summary, all of the available evidence indicates that the activation energy and volume for plastic deformation are insensitive to structure (i.e. amount of strain and grain size), whether yielding or flow is considered. The only known rate-controlling mechanism which meets these requirements is that of overcoming the inherent resistance of the lattice i.e. the Peierls stress. Another convincing reason for discarding cross-slip and the non-conservative motion of jogs as possible controlling mechanisms is the similarity

of H and v^* for yielding and flow to those for the mobility of edge dislocations[82] since edges cannot cross-slip and contain jogs which can move conservatively. A mechanism based on the conservative motion of jogs[86,87] does not contradict the Peierls mechanism since one can visualise this as a way in which dislocations overcome the Peierls barrier.

It is not the specific aim of this investigation to study the causes of the high Peierls stress for the b.c.c. lattice, or the precise means by which dislocations can surmount the barrier. Suffice it to say that the present results agree on most points with those of other workers[81,82] who found that the value of H_o and the stress-dependence of H are consistent with the predictions of Seeger's model[89] for the nucleation of kinks.

4.5 The Strain-rate Behaviour of σ_Y.

Heretofore, most of the discussion has been restricted to results for experimental conditions which pertain to Region I yielding. A word is warranted on the interpretation to be attached to the other linear portions of the $\sigma_Y - \log\dot{\epsilon}$ plot for fine-grained material. Their existence has also been observed for impure niobium and tantalum and were interpreted[107] as being representative of different rate-controlling mechanisms due to abrupt changes in v^*. On this view, the infinite v^* for Regions II and IV is indicative of the unimportance of thermal fluctuations. That this should be legitimately so when Region II, in particular, is bounded by two others which have relatively low activation volumes seems unlikely.

The explanation may be that more than one mechanism is controlling, thereby invalidating the analysis. The single region for l = 0.098 mm. further points out that the significance of the presence of Regions II and IV should not be over-rated in regard to the determination of mechanisms. As it stands, the author feels that without additional evidence, identifying each of the linear portions with a different rate-controlling mechanism is somewhat premature in the case of molybdenum.

Alternatively, one can regard the existence of Regions II and IV as a direct consequence of the non-uniform yielding in fine-grained specimens. Should a change occur in the way in which yielding is transmitted from grain to grain during Lüders front propagation when the strain rate is lowered, the result could be reflected as a strain-rate insensitive propagation stress. Meanwhile, the primary rate-controlling mechanism remains unchanged. Evidence that this may be true is derived from the similarity of the slopes, and hence activation volumes, for the neighbouring Regions I and III. Whether the rapid increase in k_Y in Regions II and IV supports the preceding argument is open to question since it is difficult to separate cause from effect. All in all, the reason for the sudden change in the strain-rate sensitivity of σ_Y is not clearly understood at this stage.

5. CONCLUSIONS.

The principal conclusions which can be drawn from this investigation are as follows:

(1) The influence of grain size, temperature, and strain rate on the yielding and flow behaviour of polycrystalline arc-cast molybdenum is best treated in a unified manner by the adoption of a model for yielding based on the multiplication and velocity characteristics of gree dislocations. The similar temperature dependence and strain-rate dependence of the upper yield stress, lower yield stress, and flow stress governed the initial selection of the model, since the impurity yield point theory is necessarily ruled out. Strong dislocation locking is still required to reduce the initial density of mobile dislocations to a reasonable value.

(2) The strain-rate dependence of the upper yield stress, σ_U, is identical to that of the lower yield stress, σ_Y, irrespective of grain size and testing temperature. This dependence can be expressed generally as $\sigma = \alpha_o + \beta \log \dot{\epsilon}$. The adopted model for yielding correctly predicts the strain-rate dependence of σ_U and σ_Y where the mobile dislocation density, L, increases with stress in the manner $\partial \log L / \partial \log \sigma = \sigma \ln 10/\beta - m$, where m is a measure of the stress-dependence of dislocation velocity. Accordingly, the observed insensitivity of the yield drop to strain rate changes is also consistent with the model.

(3) An effective comparison of predicted with experimental stress-strain curves is only possible if our knowledge of the glide

properties of dislocations is precise. Nevertheless, approximate data can be used to illustrate that the model can lead to an upper yield stress and yield drop of the observed magnitude.

(4) The reversible change in flow stress with a change in strain rate $\Delta\sigma_T$, or change in temperature, $\Delta\sigma_{\dot{\epsilon}}$, decreases with increasing strain (or stress) as a result of an increase in the mobile dislocation density with stress, or strain.

(5) The strong temperature-dependence of σ_U, and flow stress σ_Y can be attributed to the temperature dependence of the multiplication and velocity characteristics of free dislocations without recourse to unpinning of dislocations from dilute impurity atmospheres. The predicted temperature dependence for σ_U and σ_Y of - 0.24 and - 0.25 kg.mm.$^{-2}$ deg.$^{-1}$, respectively, compares favourably with the observed dependence of 0.27 kg.mm.$^{-2}$ deg.$^{-1}$ The observed insensitivity of the yield drop to changes in temperature is in accord with the model.

(6) The lower yield stress at 293^{o}K for a range of strain rates increases with decreasing grain size, l, according to the relation $\sigma_Y = \sigma_I + k_Y l^{-\frac{1}{2}}$ when $l \leq 0.25$ mm. where σ_I and k_Y evaluate to 9.3 kg.mm.$^{-2}$ and 4.3 kg.mm.$^{-3/2}$, respectively, for Ingot 1 and 10.7 kg.mm.$^{-2}$ and 4.7 kg.mm.$^{-3/2}$ for Ingot 2 at a strain rate of 0.88×10^{-4} sec.$^{-1}$ The difference between the values for the two Ingots is not considered to be significant.

(7) For grain sizes greater than 0.25 mm., σ_Y is relatively independent of grain size. As a consequence, σ_I cannot be identified with the yield stress of single crystals.

(8) The values of σ_I and k_Y determined by the extrapolation of the uniform flow portion of individual stress-strain curves to zero plastic strain cannot be identified with the values taken from Petch plots. Care should be exercised in the use of the extrapolation method since the meaning of the resulting parameters is not fully understood.

(9) The quoted value of k_Y can be considered as representative of the effect of grain size on σ_Y since the initial dislocation substructure did not vary with grain size.

(10) The parameter k_Y is not appreciably affected by changes in temperature or strain rate above a strain rate of $\sim 0.5 \times 10^{-4}$ sec.$^{-1}$ Any slight increase in k_Y with decreasing temperature or increasing strain rate can be attributed to a grain-size dependence of the dislocation multiplication and velocity characteristics. The same explanation can be applied to resolve the contradictory observations of temperature-dependent and independent k_Y values for molybdenum and other b.c.c. transition metals.

(11) The parameter k_Y can be interpreted as being a consequence of two factors, namely, a decreasing mobile dislocation density and increasing grain boundary resistance with decreasing grain size. The transmission of yielding from grain to grain probably occurs by the athermal generation of fresh dislocations at or near grain boundaries. A corresponding increase in the Lüders strain with decreasing grain size is also determined by the above two factors.

(12) The increase in the yield drop with decreasing grain size

can be attributed to a decrease in the mobile dislocation density, ρ_0, with decreasing grain size.

(13) The average value of k (= k_f) for the flow stress at a constant strain is more representative of the influence of grain boundaries per se on the yield stress than k_Y itself.

(14) It is impossible to identify σ_I with the lattice friction stress. Instead, the latter is more reasonably associated with σ_Y for single crystals, or slightly less accurately, for material with a grain size of $\backsim$0.25 mm.

(15) Almost all of the temperature dependence of σ_Y resides in the lattice friction stress, and in turn, in a term which is independent of impurity content and distribution, thereby ruling out the overcoming of solute atoms and precipitates as rate-controlling mechanisms.

(16) The activation energy, H, and activation volume, v^*, are independent of structure (i.e. amount of strain and grain size) whether yielding or flow is considered. The rate-controlling mechanism for strain rates greater than 0.5×10^{-4} sec.$^{-1}$ is established as an overcoming of the Peierls stress. The substantial agreement of the present results with those of other workers tentatively supports their view that the Peierls barrier is surmounted by the nucleation of kinks in dislocation.

(17) The activation energy is thought to be more sensitive to temperature at high temperatures than hitherto supposed. The result may be reflected in the observed decrease in H with decreasing stress

below $\sigma^* \lesssim 14$ kg.mm.$^{-2}$ Without further evidence this does not provide grounds for questioning the validity of the activation analysis. Using the value of 2×10^{-6} sec.$^{-1}$ obtained for ν, and $T_o = 600^\circ C$, H_o (at $\sigma^* = 0$) is tentatively taken as $0.082\,\mu b^3$. The activation volume for yielding and flow at $\sigma^* = 5$ kg.mm.$^{-2}$ is $30\text{-}40b^3$ dropping to $6\text{-}8b^3$ at $\sigma^* = 40$ kg.mm.$^{-2}$

(18) Using the stress-dependence of the mobile dislocation density, a correction for the stress-dependence of ν is now possible, changing the expression for v^* to $2kT/\sigma^* (m - \sigma\mu \ln 10/\beta)$. This brings v^* for yielding into line, in magnitude and stress-dependence, with v^* for flow at zero strain, where variations of L with stress are neglibible.

(19) The association of each of the three or four different linear regions in the $\sigma_Y - \log\dot{\epsilon}$ relation, for a fine grain size of 0.027 mm., with different rate-controlling mechanisms is questionable, in view, mainly, of their absence for a grain size of 0.098 mm. Existing evidence suggests that the rate-controlling process may be masked by spurious grain-boundary effects which arise during the propagation of yielding.

SUGGESTIONS FOR FUTURE RESEARCH.

This investigation introduces considerable scope for future work in the field of the plastic deformation of the b.c.c. transition metals.

Prior to this investigation, no attempt has been made to treat, in a unified way, the detailed grain-size, temperature and strain-rate dependence of yielding and subsequent flow behaviour of b.c.c. metals in terms of the glide properties of free dislocations. The present treatment suffers somewhat from the lack of a precise knowledge of these properties in molybdenum. Necessarily, one of the next steps is to improve this state of knowledge using such techniques as transmission electron microscopy and dislocation etch-pitting. In this respect, a study of the stage preceding macroscopic yielding is particularly important. Meanwhile, it would be profitable to extend the approach to iron for which the data is more complete, and thereafter, to the other b.c.c. metals as well.

One of the main reasons for studying the strong temperature dependence of the yield stress is to gain an understanding of the important brittle fracture phenomenon. Some of the results obtained here lend themselves to a cursory treatment of fracture in terms of dislocation properties, but a more extensive experimental programme is desirable.

In view of the inadequacies of the technique for impurity analysis available to the author[37,48] no serious attempt could be made to investigate the influence of impurities, in particular

carbon and nitrogen, on dislocation properties, or on the general tensile behaviour of molybdenum. When better techniques such as neutron activation analysis become available, a more conclusive study would be feasible.

The results of the activation analysis suggest that experiments should be extended to include an investigation of the temperature dependence of the yield and flow stress over a wide range of strain rates.

The various regions in the strain-rate dependence of the lower yield stress for fine-grained material should be examined more carefully in the light of dislocation and grain boundary properties. Temperature and strain-rate cycling experiments in the strain-rate insensitive regions should prove particularly useful.

ACKNOWLEDGEMENTS.

The author is indebted to Mr. J.M. Clyne of A.R.D.E., Woolwich, for fabricating the molybdenum rods and supplying the impurity analysis. Thanks are due to Dr. A.A. Johnson for suggesting the grain-size experiments, and for advice and guidance during the initial stage of the investigation. The continual interest and encouragement of Professor J.G. Ball is gratefully acknowledged. The author was assisted by discussions with Professor H.W. Paxton, Dr. L.M. Brown, and his own colleagues of the Lattice Defects Group especially Mr. F. Guiu. Helpful comments on the manuscript were rendered by Professors J.G. Ball and H.W. Paxton.

The author is extremely grateful to the Ontario Research Foundation, Toronto, Canada, for the award of a research scholarship. This work was financed by the Central Electricity Generating Board, which was responsible for personal financial assistance during the last four months of the work.

REFERENCES.

1. Cottrell, A.H., Bristol Conference Report on the Strength of Solids, Phys. Soc., (1948) 30.
2. Cottrell, A.H., and Bilby, B.A., Proc. Phys. Soc., A62 (1949) 49.
3. Crussard, C., Met. et Corr., 25 (1950) 203.
4. Cochardt, A.W., Schoeck, G., and Wiedersich, H., Acta Met., 3 (1955) 533.
4. Cottrell, A.H., "Dislocations and Plastic Flow in Crystals", Oxford, (1953).
6. Cottrell, A.H., Conference on High Rates of Strain, I. Mech. E., (1957).
7. Low, J.R., Jr., and Gensamer, M., Trans. A.I.M.M.E., 158 (1944)207.
8. Wood, D.S., and Clark, D.S., Trans. A.S.M., 44 (1952) 726.
9. Paxton, H.J., and Bear, I.J., Trans. A.I.M.E., 203 (1955) 989.
10. Yokobori, T., Phys. Rev., 88 (1952) 1423.
11. Fisher, J.C., Trans. A.S.M., 47 (1955) 451.
12. Conrad, H., and Schoeck, G., Acta Met., 8 (1960) 791.
13. Hutchison, M.M., Phil. Mag., 8 (1963) 121.
14. Manjoine, M.J., Trans. A.S.M.E., 66 (1944) A-211.
15. Carreker, R.P., and Guard, R.W., Trans. A.I.M.E., 206 (1956) 178.
16. Doremus, R.H., and Kock, E.F., Trans. Met. Soc. A.I.M.E., 218 (1960) 591.
17. Metal Treatment and Drop Forging, 28 (1961) 279.
18. Hahn, G.T., Acta Met., 10 (1962) 727.
19. Johnston, W.G., and Gilman, J.J., J.Appl. Phys., 30 (1959) 129.
20. Gilman, J.J., and Johnston, W.G., "Dislocations and Mechanical Properties of Crystals", Wiley, (1957) 116.
21. Gilman, J.J., J. Appl. Phys., 30 (1959) 1584.
22. Johnston, W.G., J. Appl. Phys., 33 (1962) 2716.
23. Hahn, G.T., Trans. Met. Soc. A.I.M.E., 224 (1962) 395.
24. Keh, A.S., cf. Ref. 18.
25. Keh, A.S., and Weissman, S., Conference on "The Impact of Transmission Electron Microscopy on Theories of the Strength of Crystals", held at Berkeley (1961). To be published by Interscience.

26. Stein, D.F., and Low, J.R., Jr., J. Appl. Phys., 31 (1960) 362.
27. Cottrell, A.H., Private Communication, (1963)
28. Luders, W., Dinglers, J., 155 (1860) 18.
29. Butler, J.F., J. Mech. Phys. Sol., 10 (1962) 313.
30. Cottrell, A.H., Trans. Met. Soc. A.I.M.E., 212 (1958) 192.
31. Vreeland, T., Wood, D.S., and Clarke, D.S., Acta Met., 1 (1953) 414.
32. Brown, N., and Ekvall, R.A., Acta Met., 10 (1962) 1101.
33. Biggs, W.D., "The Brittle Fracture of Steel"., MacDonald and Evans, (1961) 93.
34. Conrad, H., J. Iron Steel Inst., 198 (1961) 364.
35. Petch, N.J., J. Iron Steel Inst., 174 (1953) 25.
36. Johnson, A.A., J. Less-Common Met., 2 (1960).
37. Wronski, A.S., Ph.D. Thesis, University of London (1961).
38. Hall, E.O., Proc. Phys. Soc., B64 (1951) 747.
39. Stroh, A.N., Phil Mag., 46 (1955) 960.
40. Eshelby, J.D., Frank, F.C., and Nabarro, F.R.N., Phil Mag., 42 (1951) 351.
41. Petch, N.J., Phil. Mag., 3 (1958) 1089.
42. de Kazinczy, F., Backofen, W.A., and Kapadia, B., "Fracture", Wiley, (1959) 65.
43. Heslop, J., and Petch, N.J., Phil Mag., 3 (1958) 1128.
44. Campbell, J.D., and Harding, J., "Response of Metals to High Velocity Deformation", Interscience, (1962)
45. Armstrong, R., Codd, I., Douthwaite, R.M., and Petch, N.J., Phil. Mag., 7 (1962) 45.
46. Lindley, T.C., and Smallman, R.E., Acta Met., 11 (1963) 361.
47. Baldwin, W.M., Jr., Acta Met., 6 (1958) 139.
48. Wronski, A.S., and Johnson, A.A., Phil.Mag., 7 (1962) 213.
49. Hull, D., Acta Met., 9 (1961) 191.
50. Owen, W.S., Cohen, M., and Averbach, B.L., Trans. A.S.M. 50 (1958) 517.
51. Hull, D., and Mogford, I.L., Phil. Mag., 3 (1958) 1213.
52. Koo, R.C., J. Less-Common Met., 4 (1962) 138.
53. Adams, M.A., Roberts, A.C., and Smallman, R.E., Acta Met., 8 (1960) 328.

54. Petch, N.J., "Fracture", Wiley, (1959) 54.
55. Gilbert, A., Hull, D., Owen, W.S., and Reid, C.N., J. Less-Common Met., 4 (1962) 399.
56. Johnson, A.A., Acta Met., 8 (1960) 737.
57. Wronski, A.S., Private Communication, (1963).
58. Christian, J.W., and Masters, B.C., Private Communication, (1961).
59. Li, J.C.M., Trans.Met. Soc. A.I.M.E., 227 (1963) 239.
60. Johnson, A.A., Phil. Mag., 7 (1962) 177.
61. Fisher, R.M., Ph.D. Thesis, University of Cambridge, (1962).
62. Frank, F.C., Symposium on "Plastic Deformation of Crystalline Solids", O.N.R., (1950) 60.
63. Tjerkstra, H.H., Acta Met., 9 (1961) 259.
64. Cracknell, A., and Petch, N.J., Acta Met., 3 (1955) 186.
65. Heslop, J., and Petch, N.J., Phil. Mag., 1 (1956) 866.
66. Codd, I., and Petch, N.J., Phil. Mag., 5 (1960) 30.
67. Peierls, R.E., Proc. Phys. Soc., 52 (1940) 34.
68. Nabarro, F.R.N., Proc. Phys. Soc., 59 (1947) 256.
69. Holden, J., Acta Met., 8 (1960) 424.
70. Koehler, J.S., Phys. Rev., 86 (1952) 52.
71. Orowan, E., "Dislocations in Metals", A.I.M.E., (1954) 103.
72. Conrad, H., and Wiedersich, H., Acta Met., 8 (1960) 128.
73. Seeger, A., Phil. Mag., 46 (1956) 1194.
74. Conrad, H., and Frederick, S., Acta Met., 10 (1962) 1013.
75. Sleeswyk, A.W., and Helle, J.N., Acta Met., 11 (1963) 187.
76. Louat, N.F., Proc. Phys. Soc., B69 (1956) 454.
77. Louat, N.F., Proc. Phys. Soc., B71 (1958) 444.
78. Lawley, A., Van den Sype, J., and Maddin, R., J. Inst. Met. 91 (1962-63) 23.
79. Basinski, Z.S., and Christian, J.W., Austl. J.Phys., 13 (1960) 299.
80. Conrad, H., and Hayes, W., Trans. A.S.M., 56 (1963) 125.
81. Conrad, H., and Hayes, W., Trans. A.S.M., 56 (1963) 249.
82. Conrad, H., Private Communication, (1963).
83. Conrad, H., "High Purity Iron and its Dilute Solid Solutions", A.I.M.E., To be published by Interscience / Wiley.
84. Schoeck, G., Acta Met., 9 (1961) 382.

85. Gregory, D.P., Acta Met., 11 (1963) 455.
86. Rose, R.M., Ferris, D.P. and Wulff, J., Trans. Met. Soc. A.I.M.E., 224 (1962) 981.
87. Mordike, B.L., Zeit. Metallk., 53 (1962) 586.
88. Mordike, B.L., and Haasen, P., Phil.Mag., 7 (1962) 459.
89. Seeger, A., Phil. Mag., 1 (1956) 651.
90. Johnson, A.A., Ph.D. Thesis, University of London, (1961)
91. Savitskii, E.M., Doklady Akad. Nauk. S.S.S.R., 113 (1957) 1010.
92. Aust. K.T., and Maddin, R., Acta Met., 4 (1956) 632.
93. Hahn, G.T., Private Communication, (1963).
94. Guiu, F., Private Communication, (1963).
95. Hindman, H. and Burr, G.S., Trans. A.S.M.E., Oct. (1949).
96. Jaoul, B., I.U.T.A.M., Madrid Colloquium, "Deformation and Flow of Solids", Springer-Verlag, Berlin, (1956).
97. Jaoul, B., J. Mech. Phys. Sol., 9 (1961) 69.
98. Mogford, I.L., and Hull, D., J.Iron Steel Inst., 201 (1963) 55.
99. Rosenfield, A.R., J. Inst. Met., 91 (1962-63) 104.
100. Adams, M.A., and Cottrell, A.H., Phil.Mag., 46 (1955) 1187.
101. Cottrell, A.H., and Stokes, R.J., Proc.Roy. Soc., A233 (1955) 17.
102. Bechtold, J.H., and Scott, H., J. Electrochem. Soc., 98(1951) 495.
103. Bechtold, J.H., Trans. A.I.M.E., 197 (1953) 1469.
104. Pugh, J.W., Trans. A.S.M., 47 (1955) 984.
105. Sargent, G.A., and Orava, R.N., Unpublished results, (1962).
106. Fourdeux, A., and Wronski, A., Private Communication, (1963).
107. Sargent, G.A., Sherwood, P.J., and Johnson, A.A., Nature, 195 (1962) 374.
108. Li, J.C.M., J. Appl. Phys., 32 (1961) 593.
109. Guard, R.W., Acta Met., 9 (1961) 163.
110. Johnston, W.G., and Stein, D.S., Acta Met., 11 (1963) 317.
111. Johnson, A.A., Phil. Mag., 4 (1959) 194.
112. Hull, D., McIvor, I.D., and Owen, W.S., J. Less-Common Met., 4 (1962) 409.
113. Wronski, A.S., and Johnson, A.A., Phil. Mag., 7 (1962) 1429.
114. Johnson, A.A., Acta Met., 10 (1962) 975.

115. Lindley, T.C., and Smallman, R.E., Acta Met., 11 (1963) 626.

116. Evans, P.R.V., Weinberg, A.F., and Van Thyne, R.J., Acta Met., 11 (1963) 143.

117. Wronski, A.S., and Johnson, A.A., Phil. Mag., 8 (1963) 1067.

118. Brown, N., and Lukens, K.F., Jr., Acta Met., 9 (1961) 106.

119. Suits, J.C., and Chalmers, B., Acta Met., 9 (1961) 854.

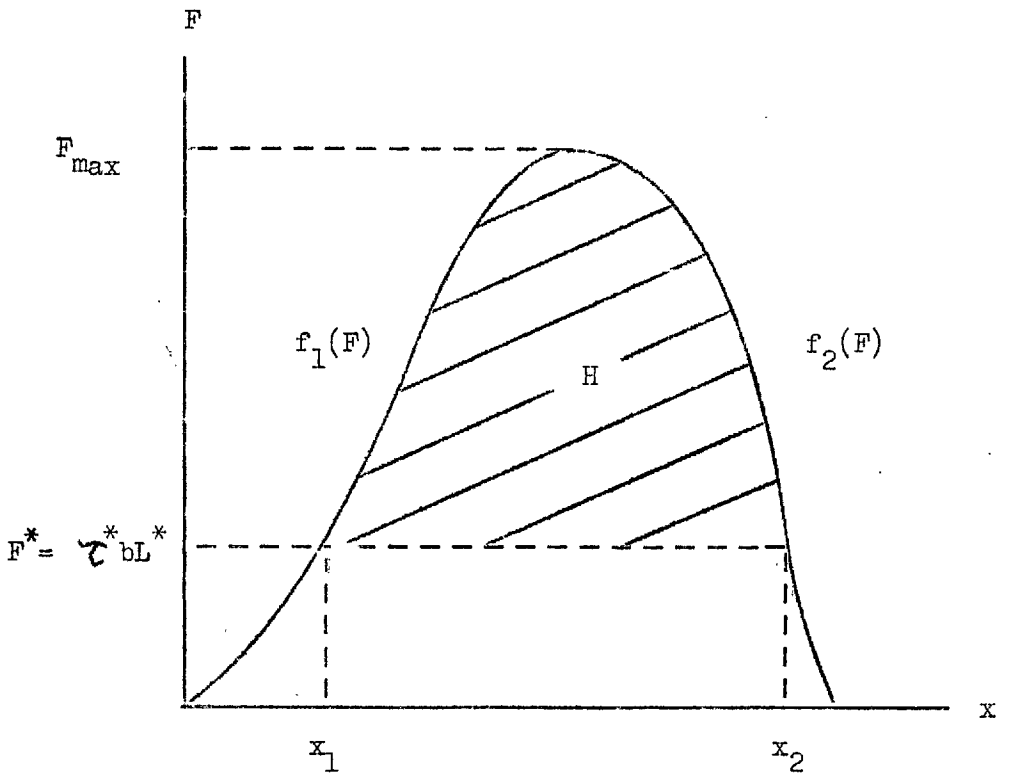

Schematic representation of the force-distance relationship for thermally activated yielding or flow.

FIG. 1

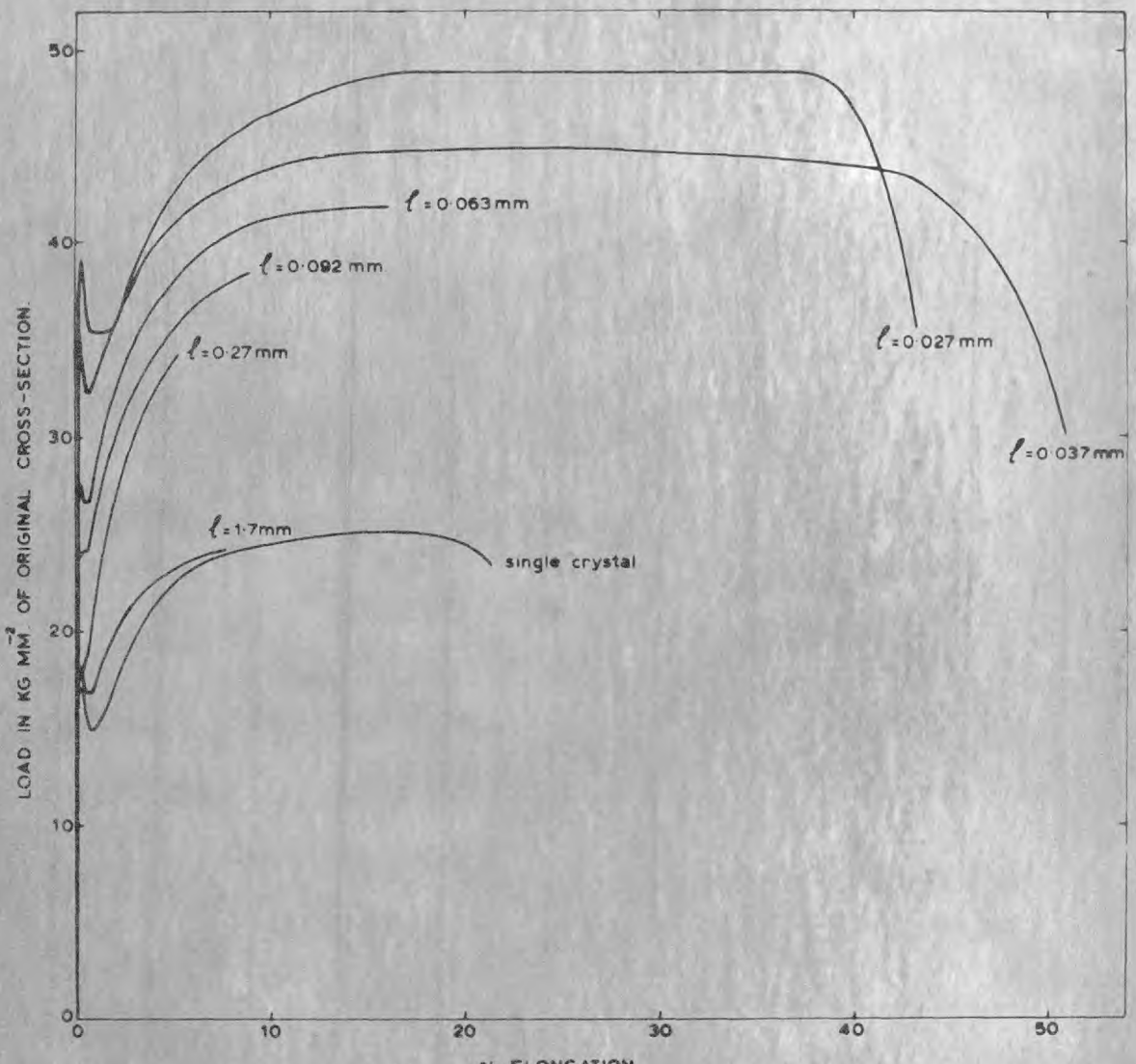

THE EFFECT OF GRAIN SIZE ON THE LOAD-ELONGATION CURVE OF MOLYBDENUM AT 293°K AND A STRAIN RATE OF $0{\cdot}88 \times 10^{-4}$ sec^{-1} (INGOT 1)

FIG.2

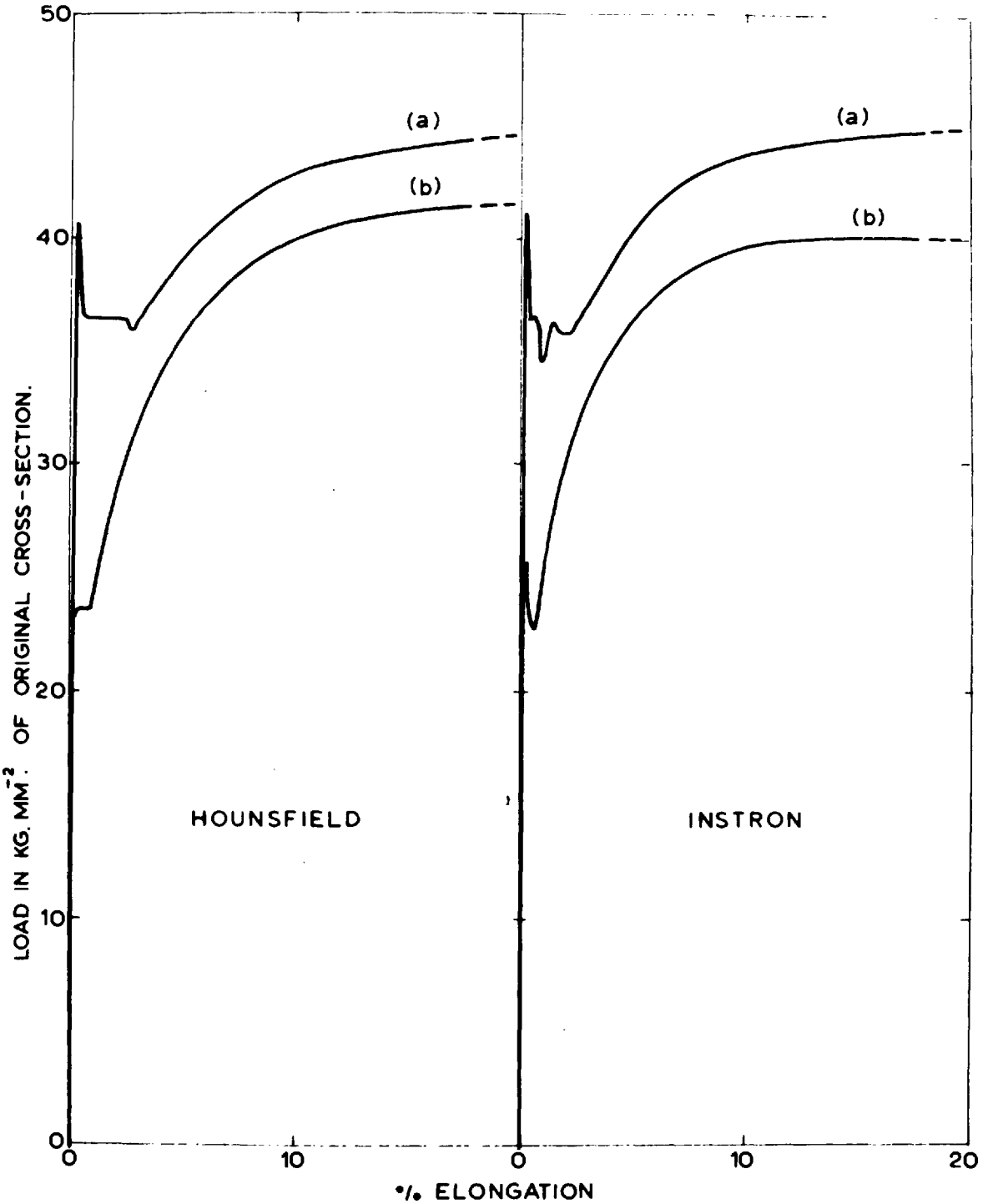

THE EFFECT OF TESTING MACHINE ON THE LOAD-ELONGATION CURVE OF MOLYBDENUM WITH A GRAIN SIZE OF (a) 0·027 mm AND (b) 0·098 mm, AT 293°K AND A STRAIN RATE OF $0{\cdot}88 \times 10^{-4}$ sec^{-1} (INGOT 2)

FIG. 3

THE EFFECT OF GRAIN SIZE ON THE YIELD AND FRACTURE STRESS OF MOLYBDENUM AT 293°K AND A STRAIN RATE OF $0{\cdot}88 \times 10^{-4}\ sec^{-1}$ (INGOT 1)

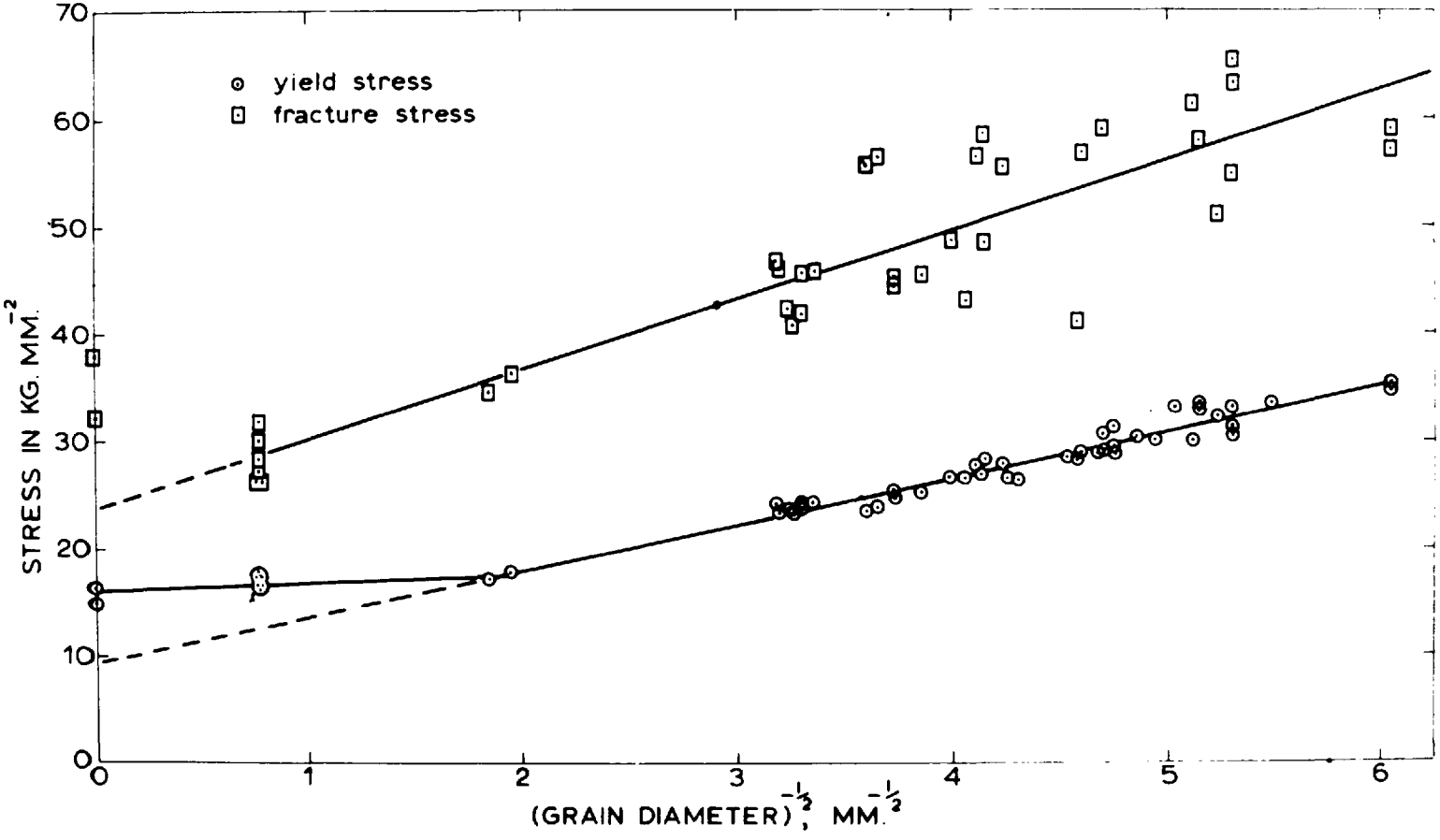

FIG.4

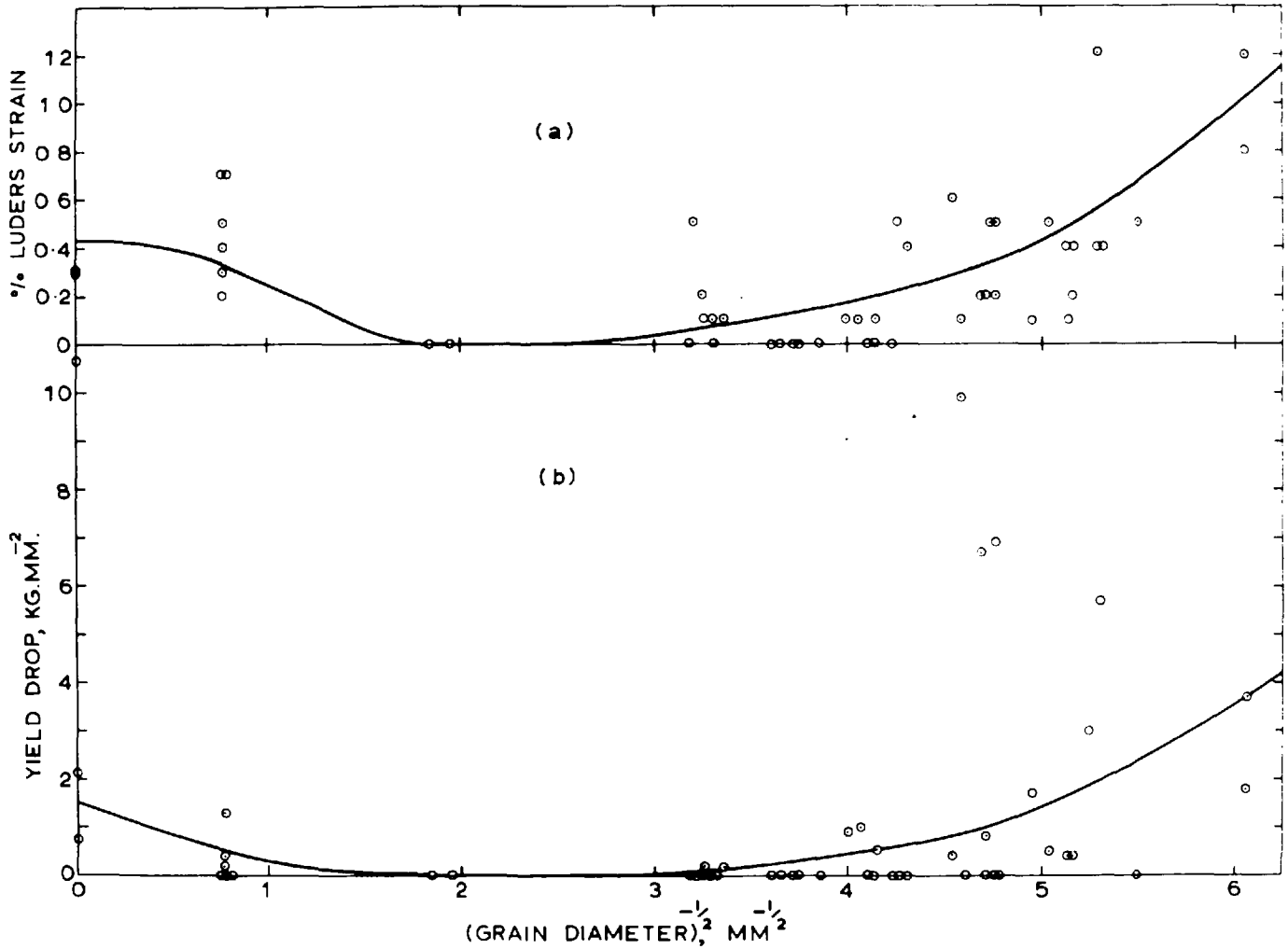

THE EFFECT OF GRAIN SIZE ON THE (a) LÜDERS STRAIN (b) YIELD DROP OF MOLYBDENUM AT 293°K AND A STRAIN-RATE OF 0.88×10^{-4} sec^{-1} (INGOT 1)

FIG.5

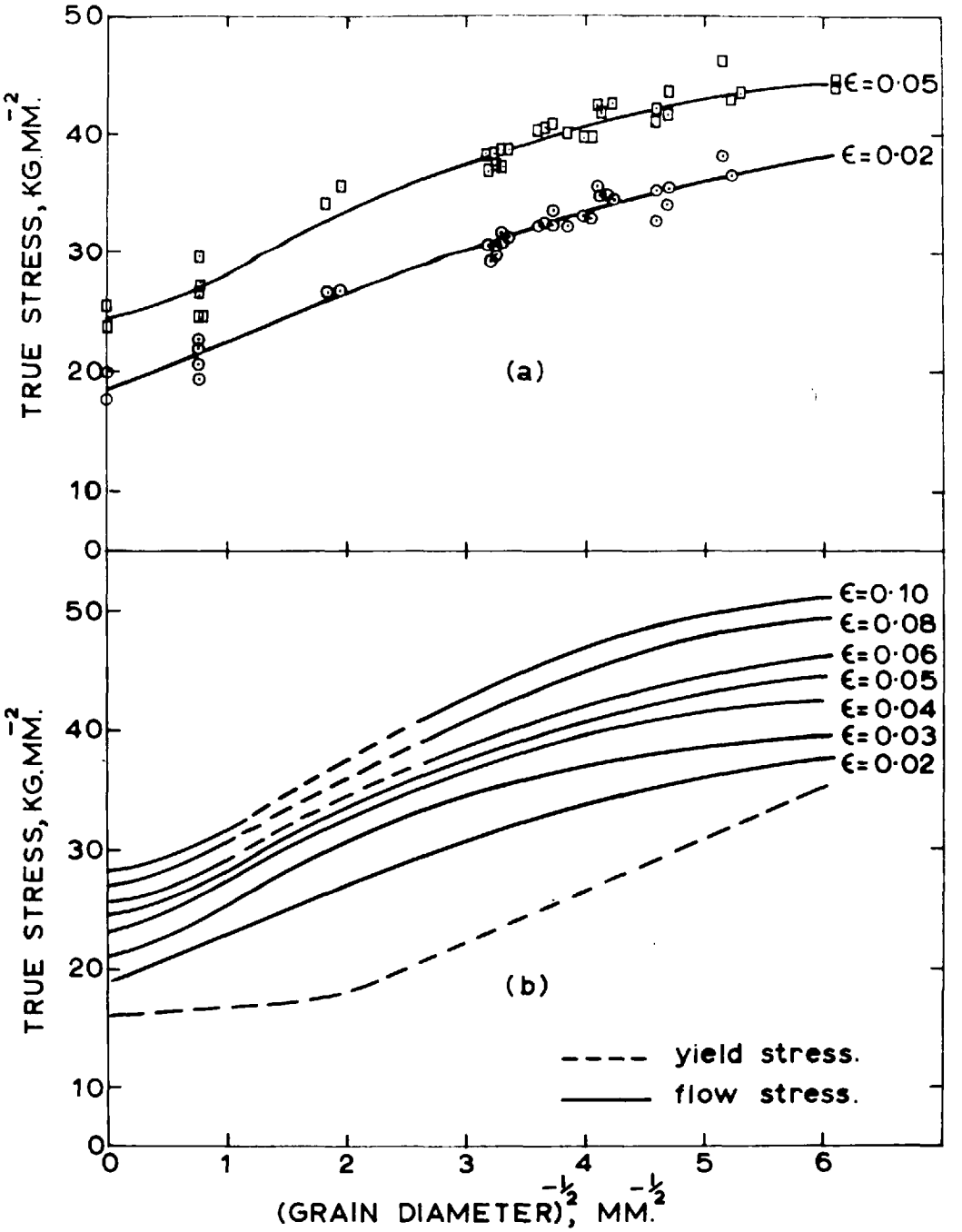

THE EFFECT OF GRAIN SIZE ON THE FLOW STRESS OF MOLYBDENUM AT 293°K AND A STRAIN-RATE OF $0 \cdot 88 \times 10^{-4}$ sec^{-1} (INGOT 1).

FIG.6

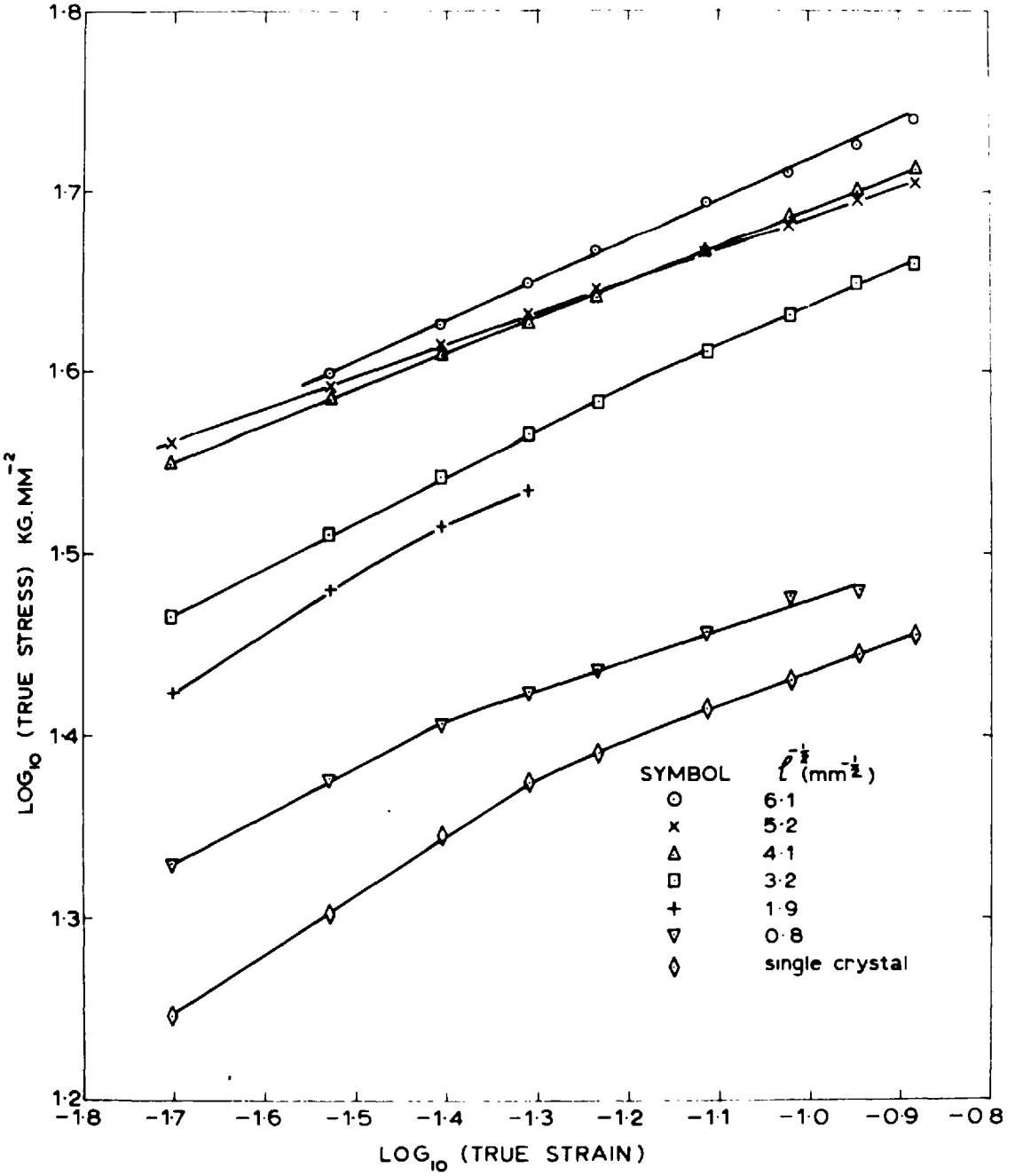

THE EFFECT OF GRAIN SIZE ON THE APPLICABILITY OF THE RELATION $\sigma_T = K\epsilon_T^n$ TO THE FLOW CURVE OF MOLYBDENUM AT 293°K AND A STRAIN RATE OF $0{\cdot}88 \times 10^{-4}\ sec^{-1}$ (INGOT 1).

FIG.7

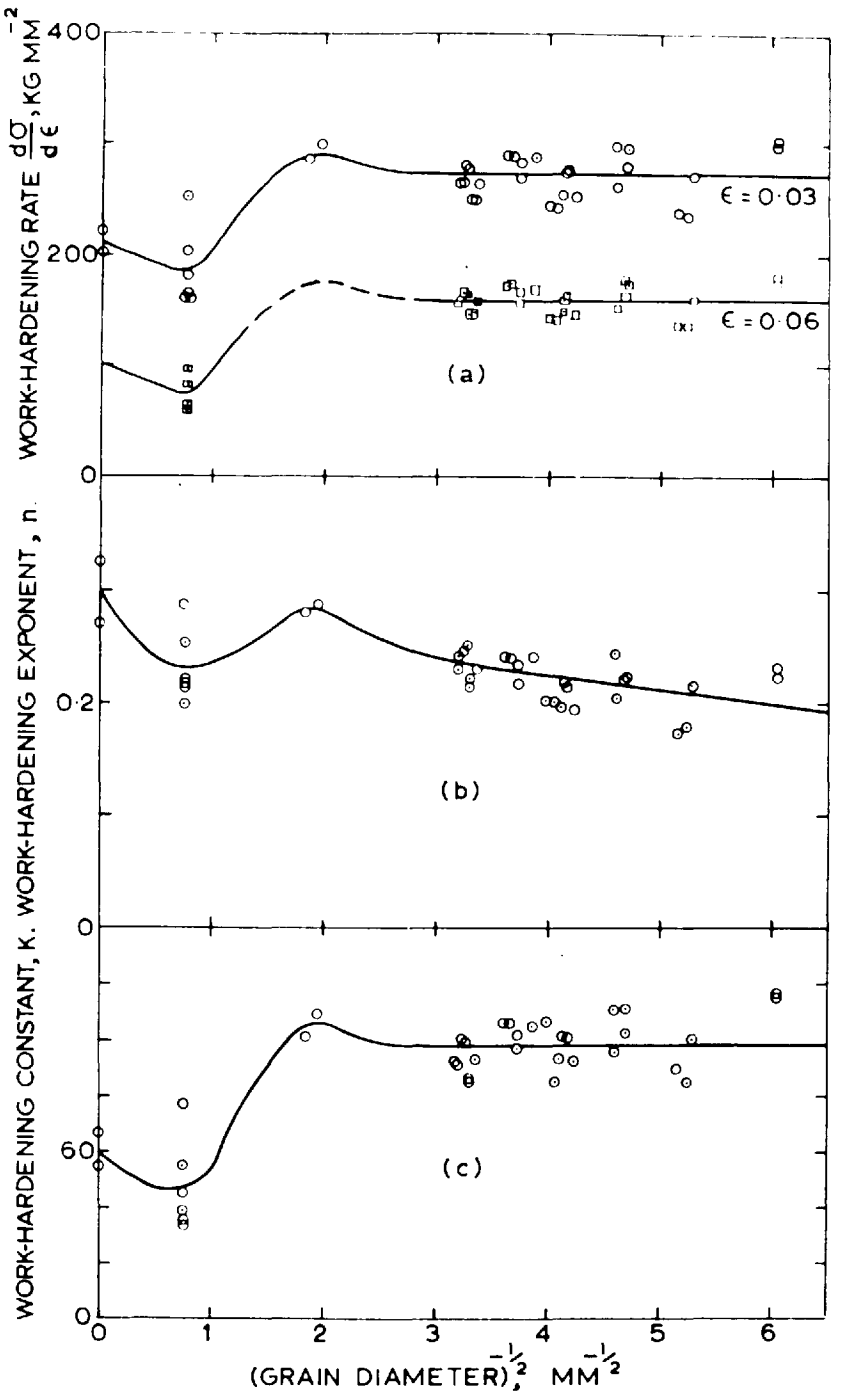

THE EFFECT OF GRAIN SIZE ON THE WORK-HARDENING PARAMETERS OF MOLYBDENUM AT 293°K AND A STRAIN-RATE OF $0{\cdot}88\times10^{-4}$ sec^{-1} (INGOT 1)

FIG.8

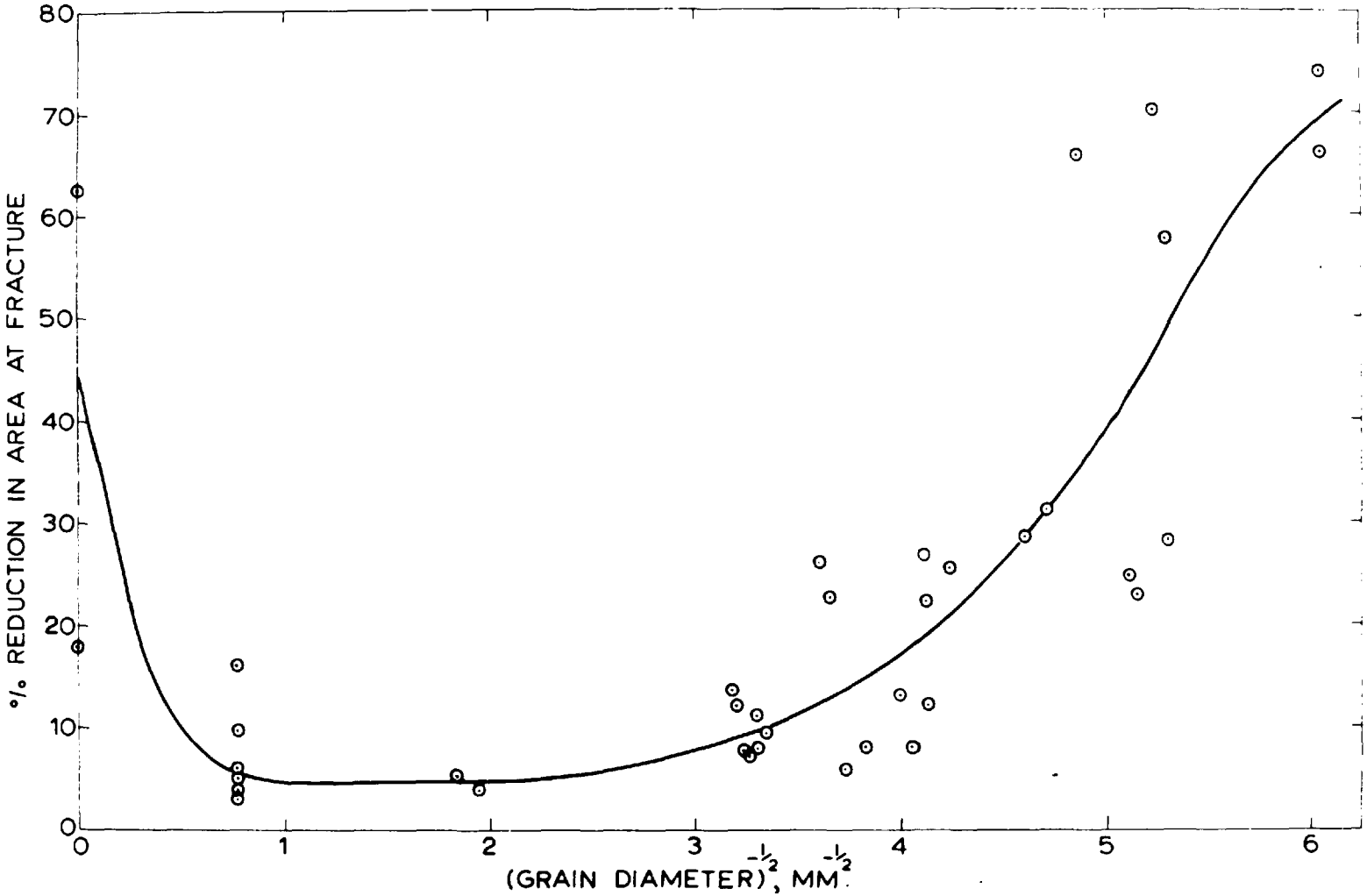

THE EFFECT OF GRAIN SIZE ON THE REDUCTION IN CROSS-SECTIONAL AREA AT FRACTURE OF MOLYBDENUM AT 293°K AND A STRAIN-RATE OF $0{\cdot}88\times10^{-4}$ sec^{-1} (INGOT 1).

FIG.9

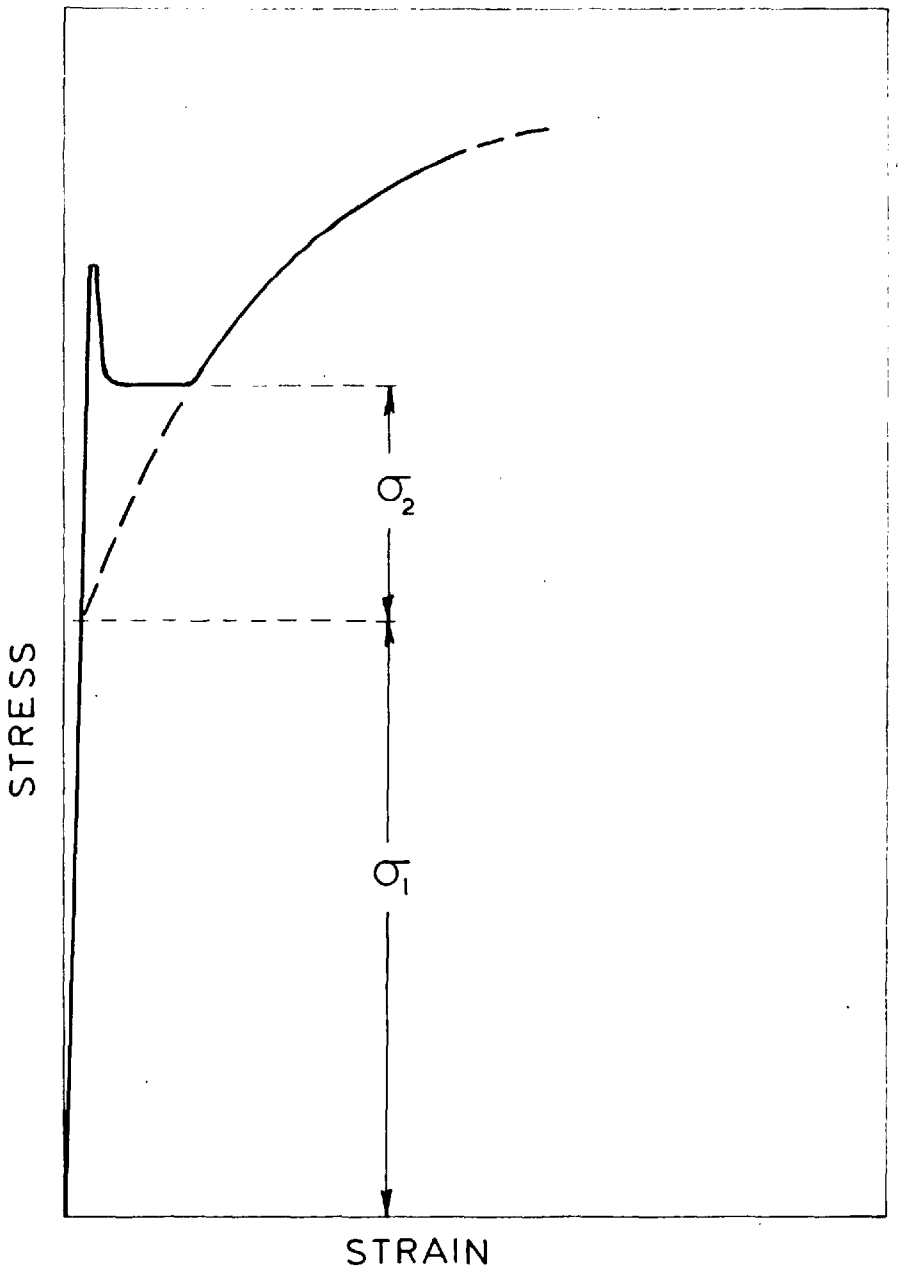

THE EXTRAPOLATION METHOD OF OBTAINING THE PETCH PARAMETERS FROM A SINGLE STRESS-STRAIN CURVE.

FIG.10

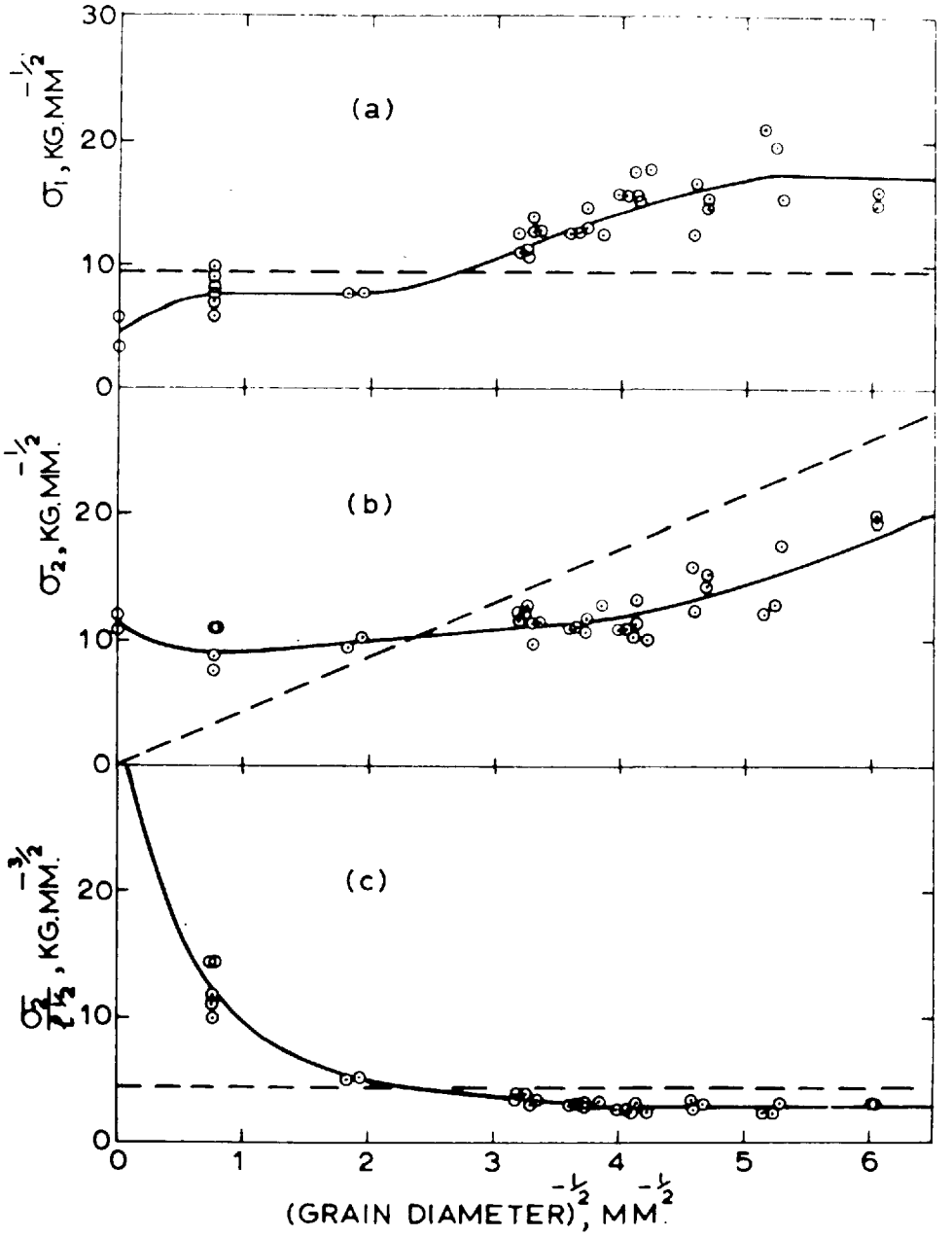

THE EFFECT OF GRAIN SIZE ON THE PETCH PARAMETERS FOR MOLYBDENUM DETERMINED BY EXTRAPOLATION OF STRESS-STRAIN CURVES OBTAINED AT 293°K AND A STRAIN-RATE OF $0{\cdot}88 \times 10^{-4}$ sec^{-1}. DASHED LINES INDICATE PARAMETERS TAKEN FROM THE PETCH PLOT.

FIG.11

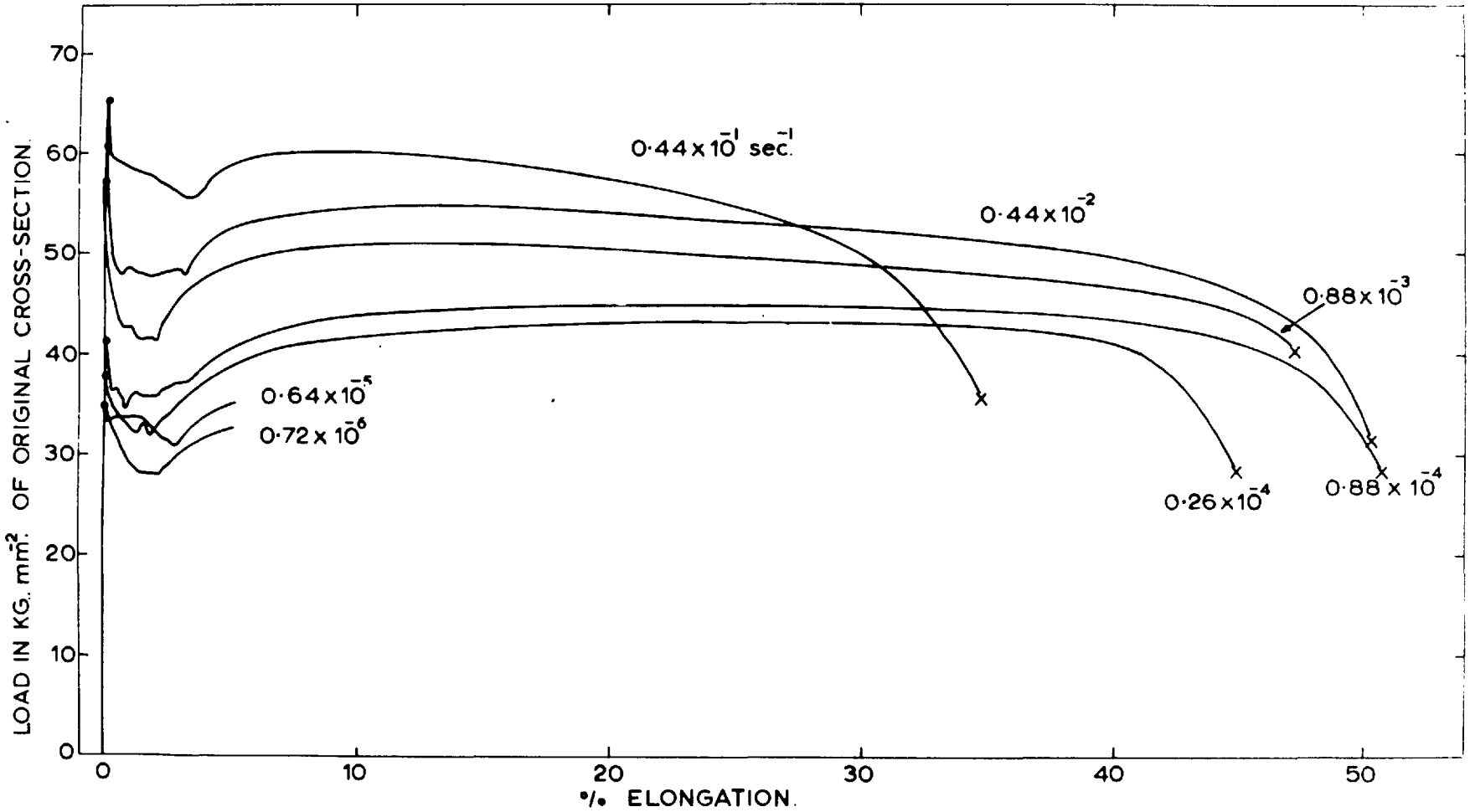

THE EFFECT OF STRAIN RATE ON THE LOAD-ELONGATION CURVE OF MOLYBDENUM WITH A GRAIN SIZE OF 0·027 mm. AT 293°K. (INGOT 2)

FIG.12

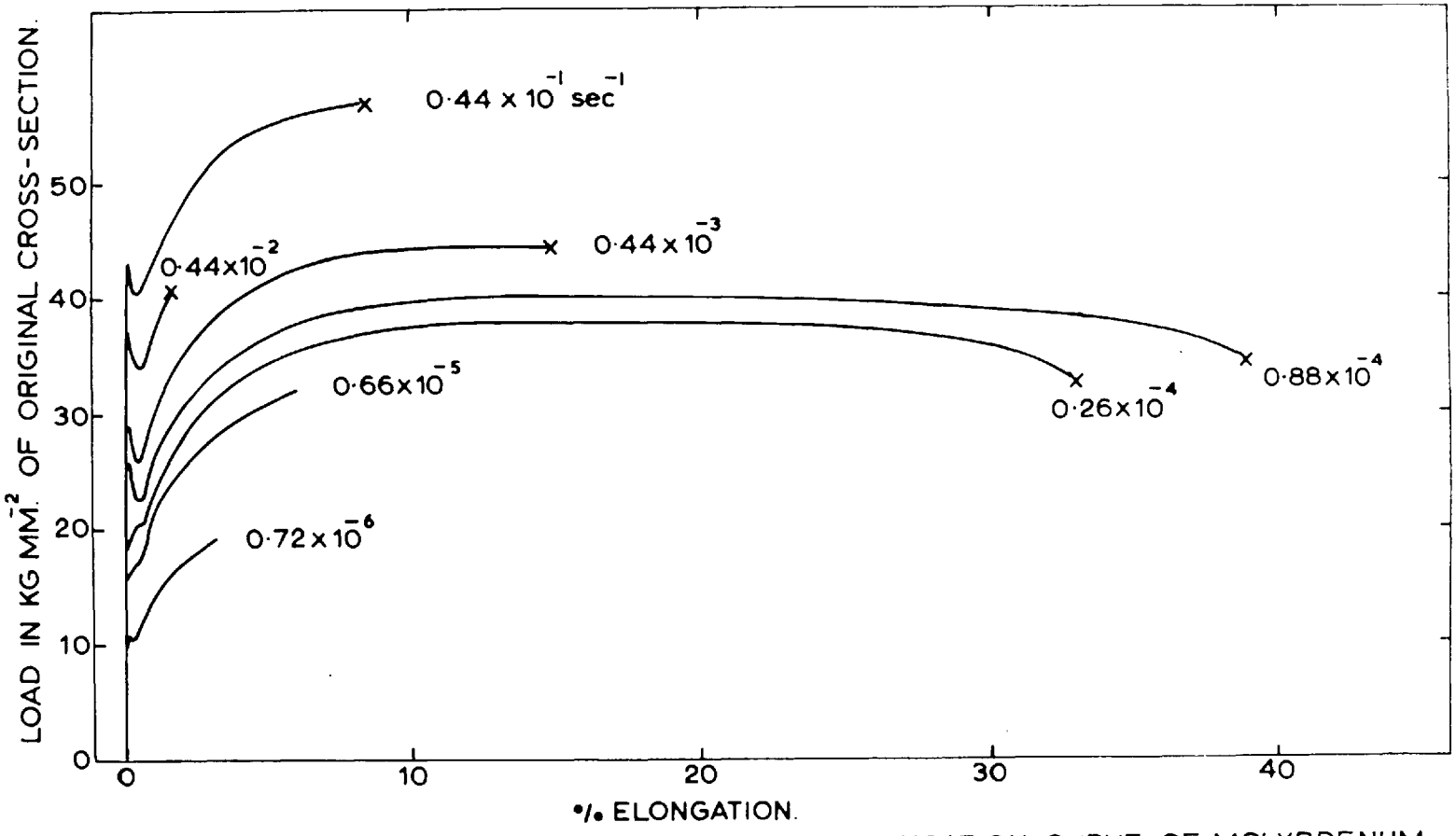

THE EFFECT OF STRAIN-RATE ON THE LOAD-ELONGATION CURVE OF MOLYBDENUM WITH A GRAIN SIZE OF 0·098mm AT 293°K (INGOT 2).

FIG.13

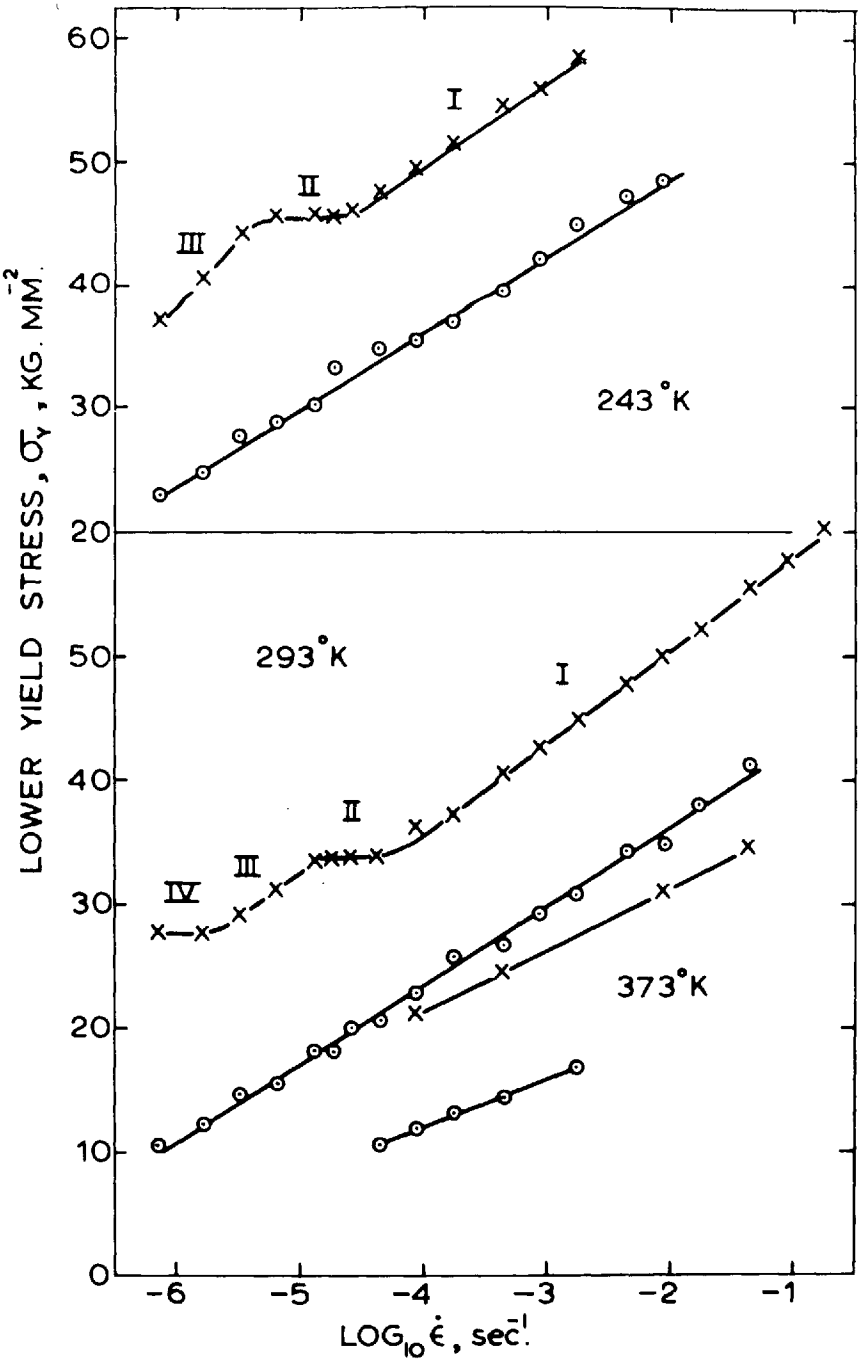

THE EFFECT OF STRAIN RATE ON THE LOWER YIELD STRESS OF MOLYBDENUM WITH A GRAIN SIZE OF 0·027mm (x) AND 0·098mm (o) (INGOT 2)

FIG.14

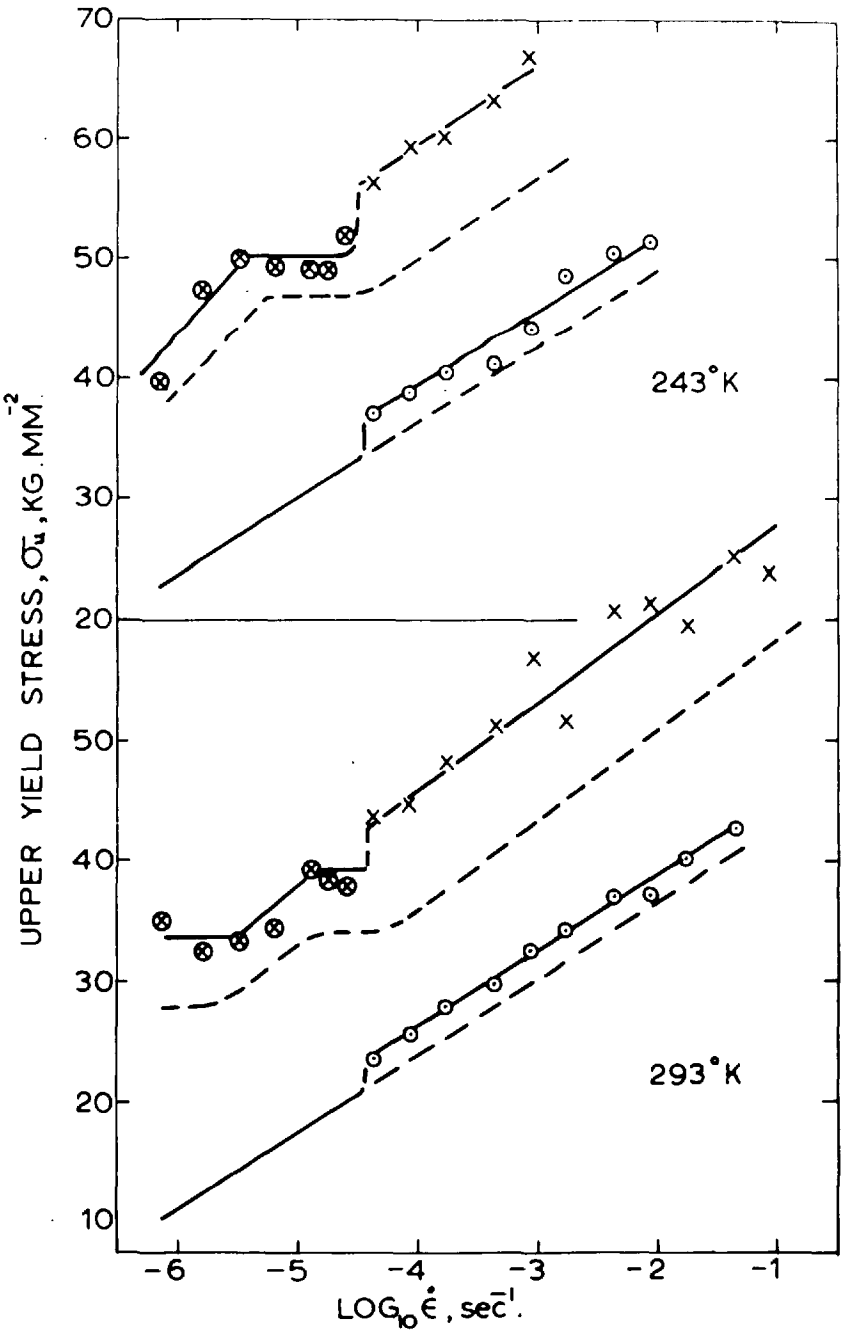

THE EFFECT OF STRAIN RATE ON THE UPPER YIELD STRESS OF MOLYBDENUM WITH A GRAIN SIZE OF 0·027mm (⊗X) AND 0·098mm (o). THE POINTS ⊗ REPRESENT TESTS CONDUCTED ON A HOUNSFIELD TENSOMETER (INGOT 2) DASHED LINES DENOTE LOWER YIELD STRESS DATA.

FIG.15

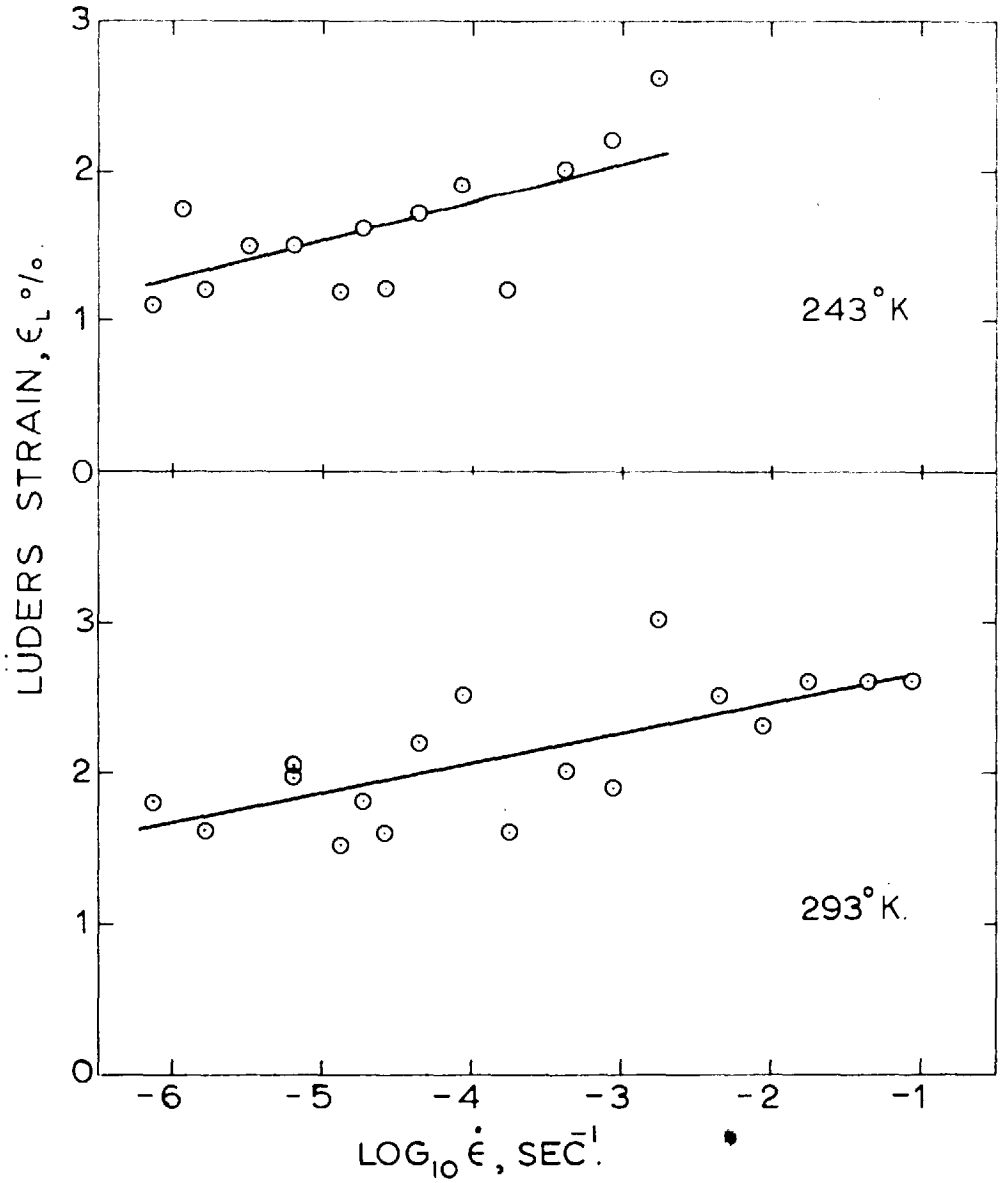

THE EFFECT OF STRAIN-RATE ON THE LÜDERS STRAIN OF MOLYBDENUM WITH A GRAIN SIZE OF 0·027 mm (INGOT 2).

FIG.16

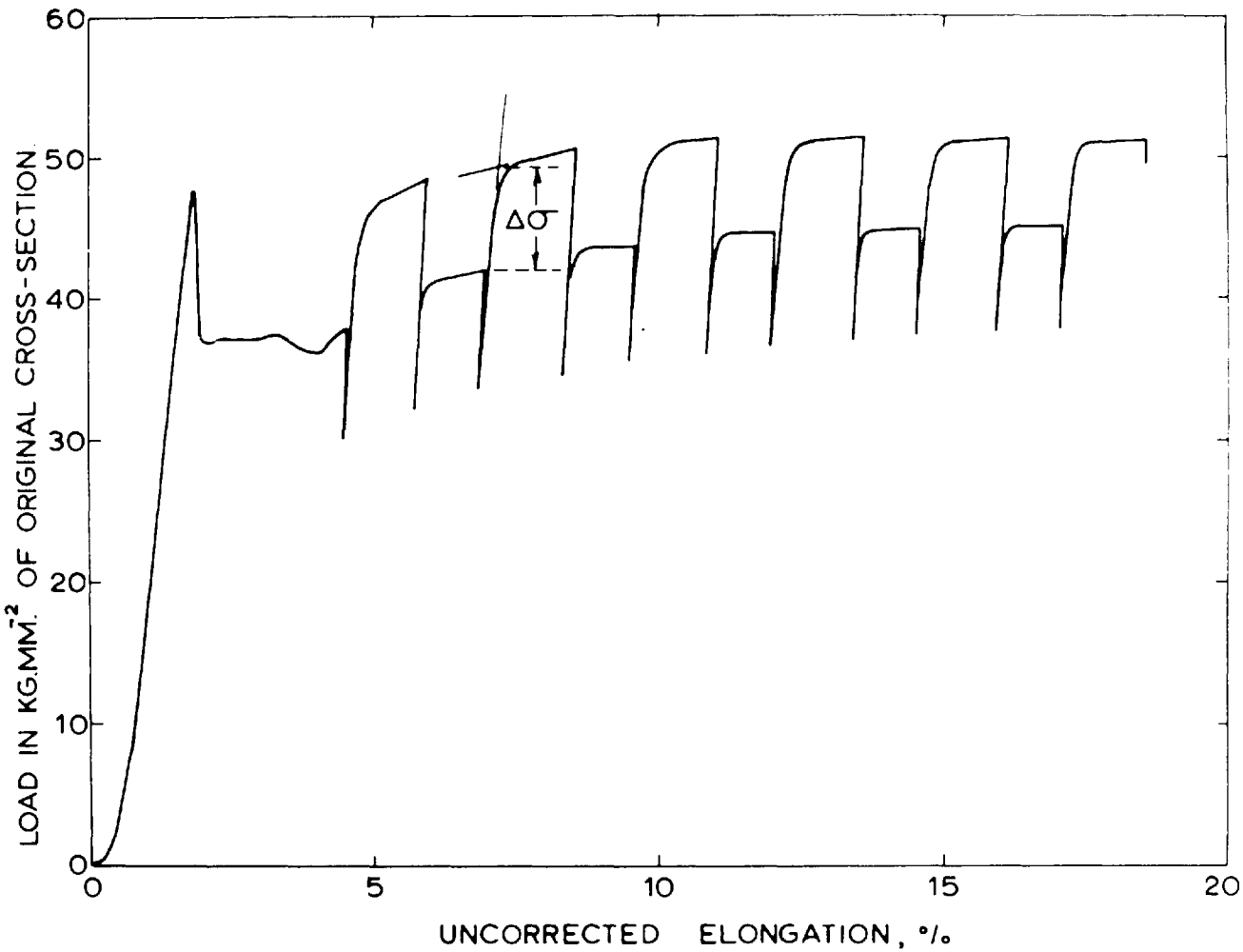

A TYPICAL LOAD-ELONGATION CURVE FOR MOLYBDENUM WITH A GRAIN SIZE OF 0·027 mm CYCLED BETWEEN $0{\cdot}88 \times 10^{-4}$ sec^{-1} AND $1{\cdot}8 \times 10^{-3}$ sec^{-1} AT 293° K

FIG.17

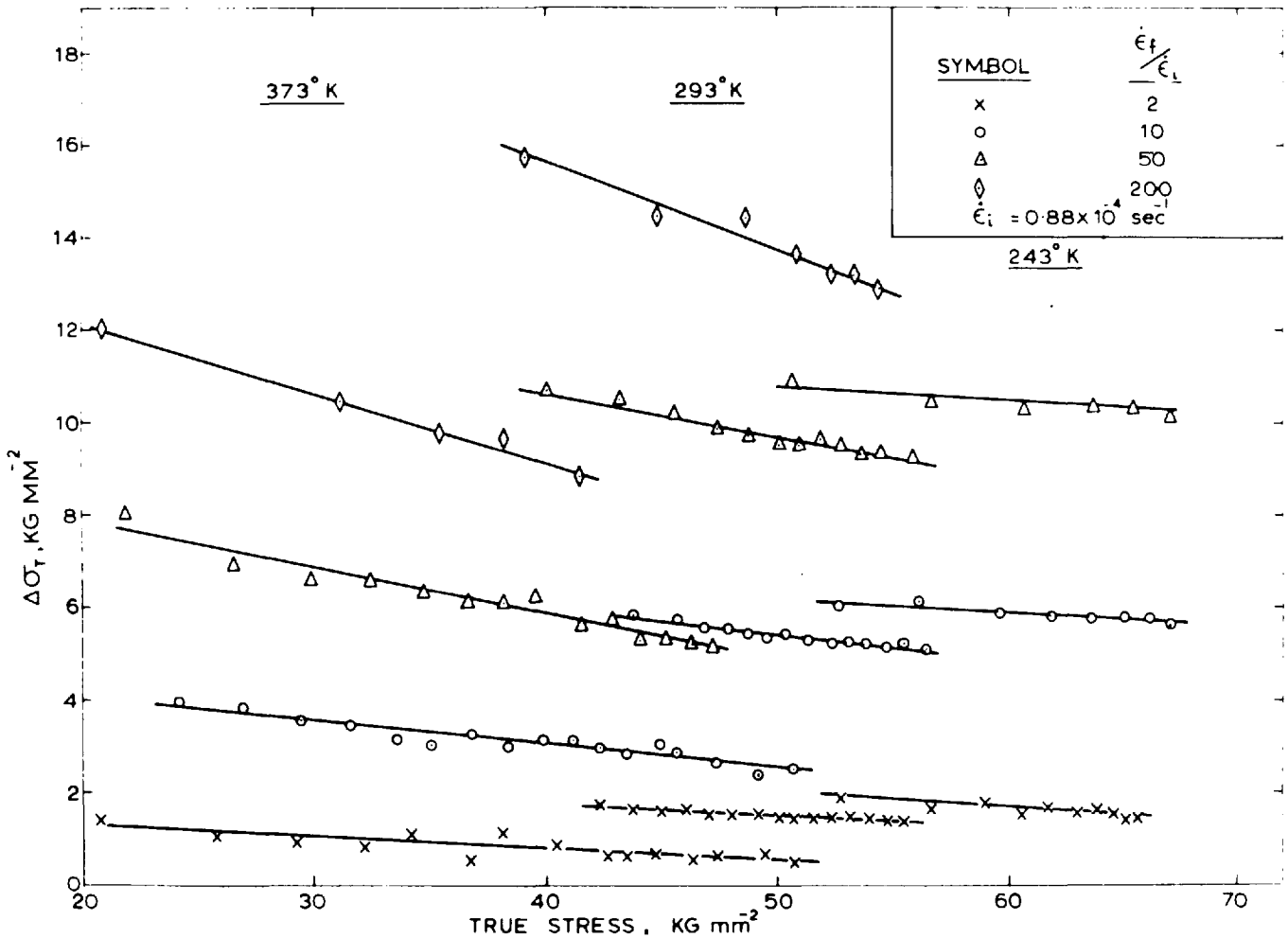

THE EFFECT OF STRESS ON THE REVERSIBLE CHANGE IN FLOW STRESS FOR MOLYBDENUM WITH A GRAIN SIZE OF 0·027mm FROM STRAIN RATE FACTOR CHANGE EXPERIMENTS (INGOT 2)

FIG.18

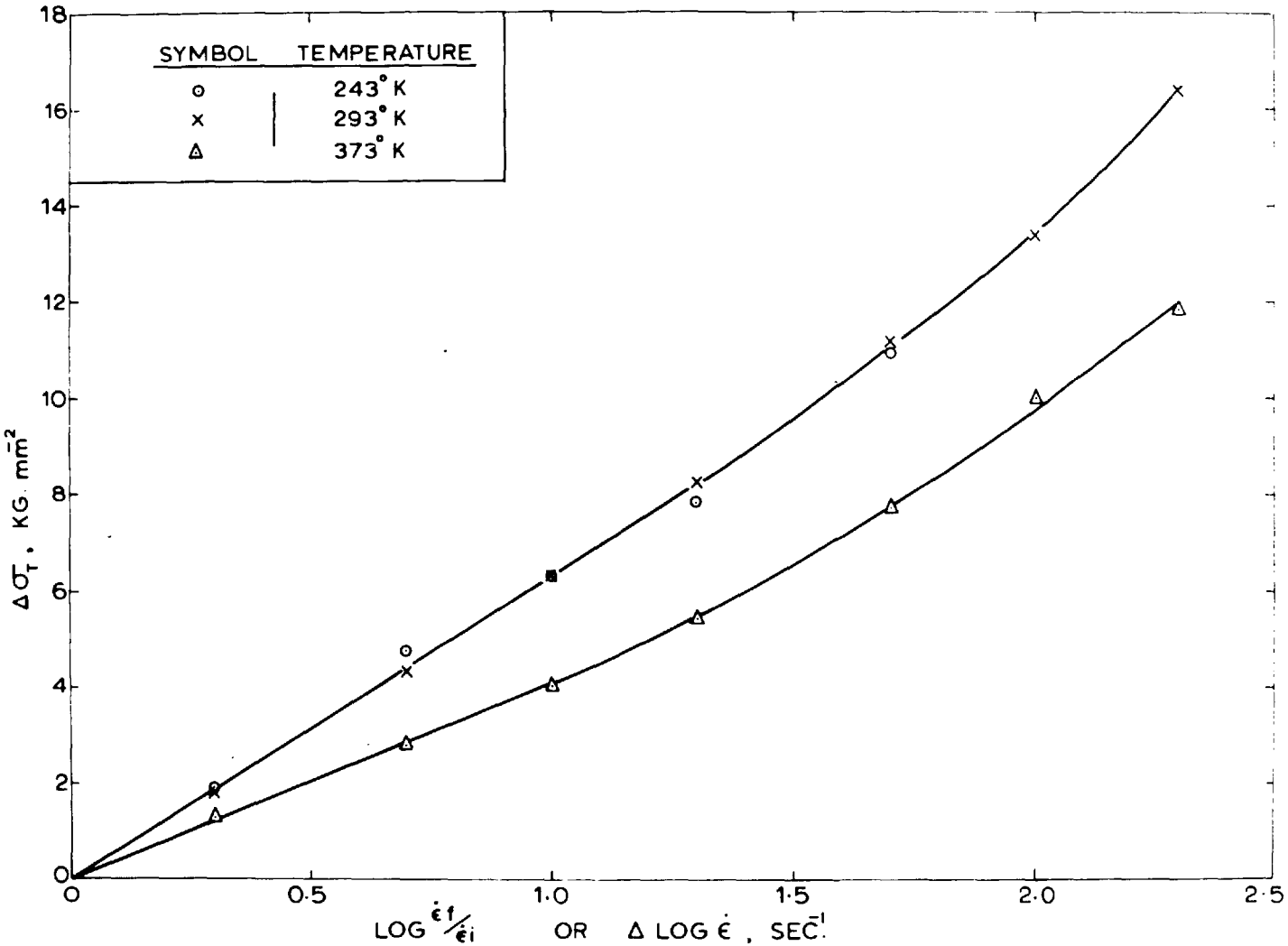

THE EFFECT OF STRAIN-RATE FACTOR ON THE REVERSIBLE CHANGE IN FLOW STRESS OF MOLYBDENUM WITH A GRAIN SIZE 0·027 mm (INGOT 2)

FIG.19

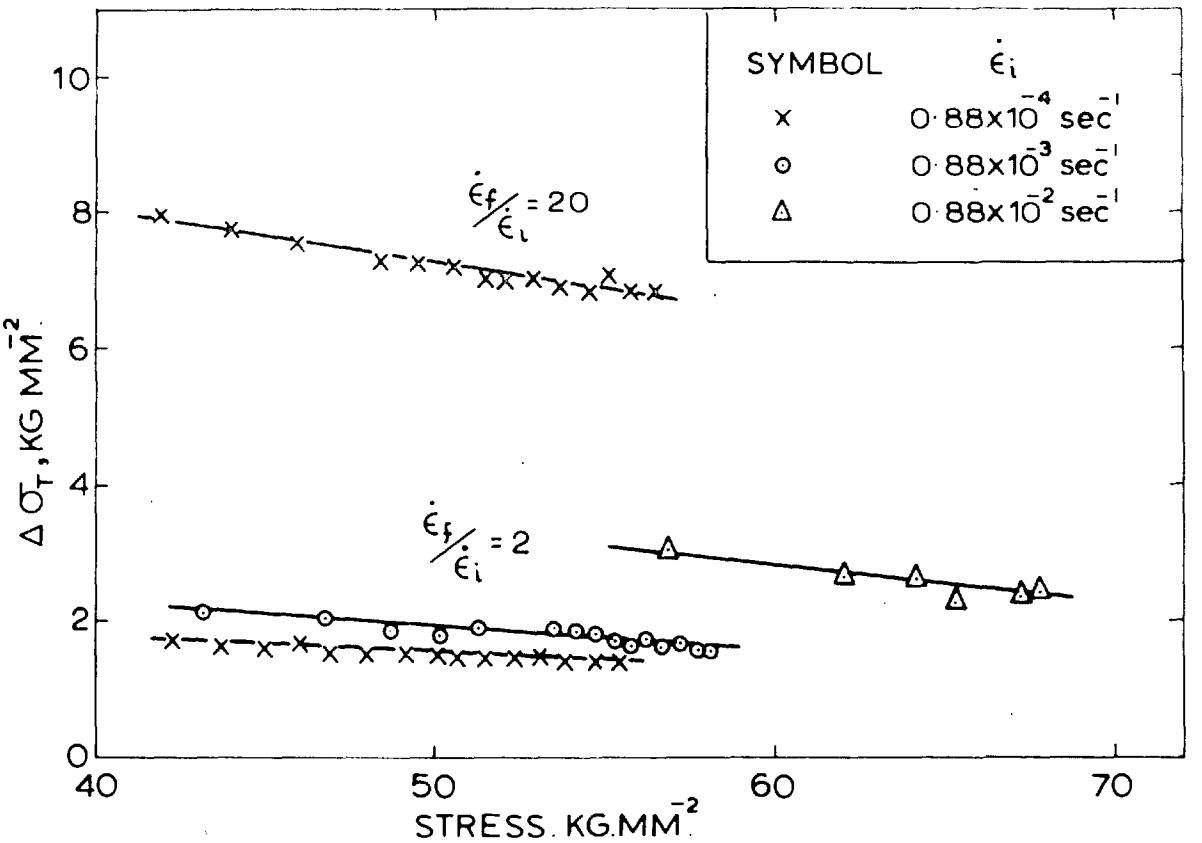

THE EFFECT OF STRESS ON THE REVERSIBLE CHANGE IN FLOW STRESS OF MOLYBDENUM WITH A GRAIN SIZE OF 0·027mm. FROM BASIC STRAIN-RATE CHANGE EXPERIMENTS AT 293°K FOR $\dot{\epsilon}_f/\dot{\epsilon}_i = 2$. THE RESULTS FOR $\dot{\epsilon}_f/\dot{\epsilon}_i = 20$ ARE GIVEN FOR COMPARISON. (INGOT 2).

FIG.20

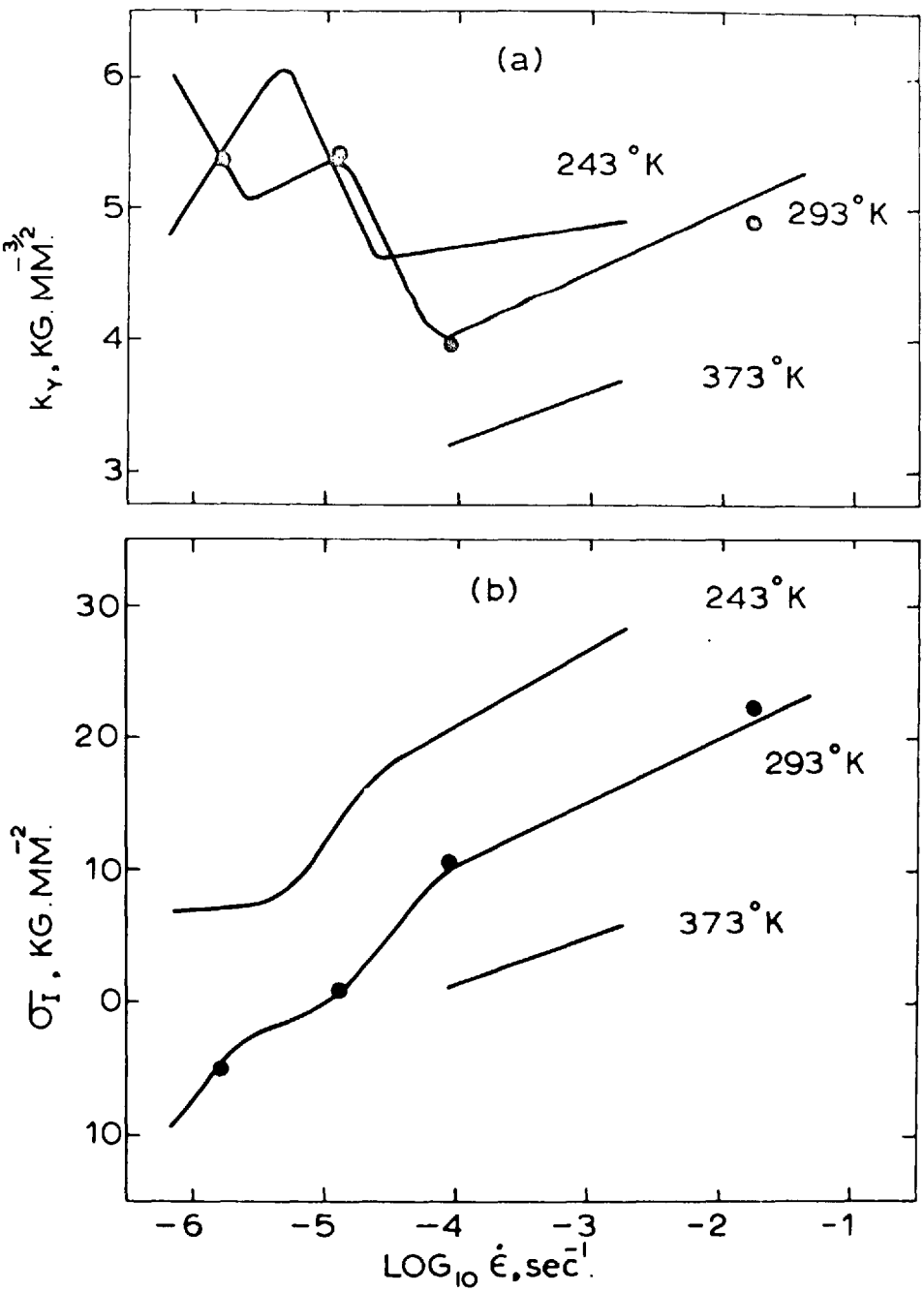

THE EFFECT OF STRAIN RATE ON THE PETCH PARAMERS (a) k_y (b) σ_i OF MOLYBDENUM. ACTUAL DATA POINTS SHOWN WERE OBTAINED FROM PETCH PLOTS. (INGOT 2).

FIG.21

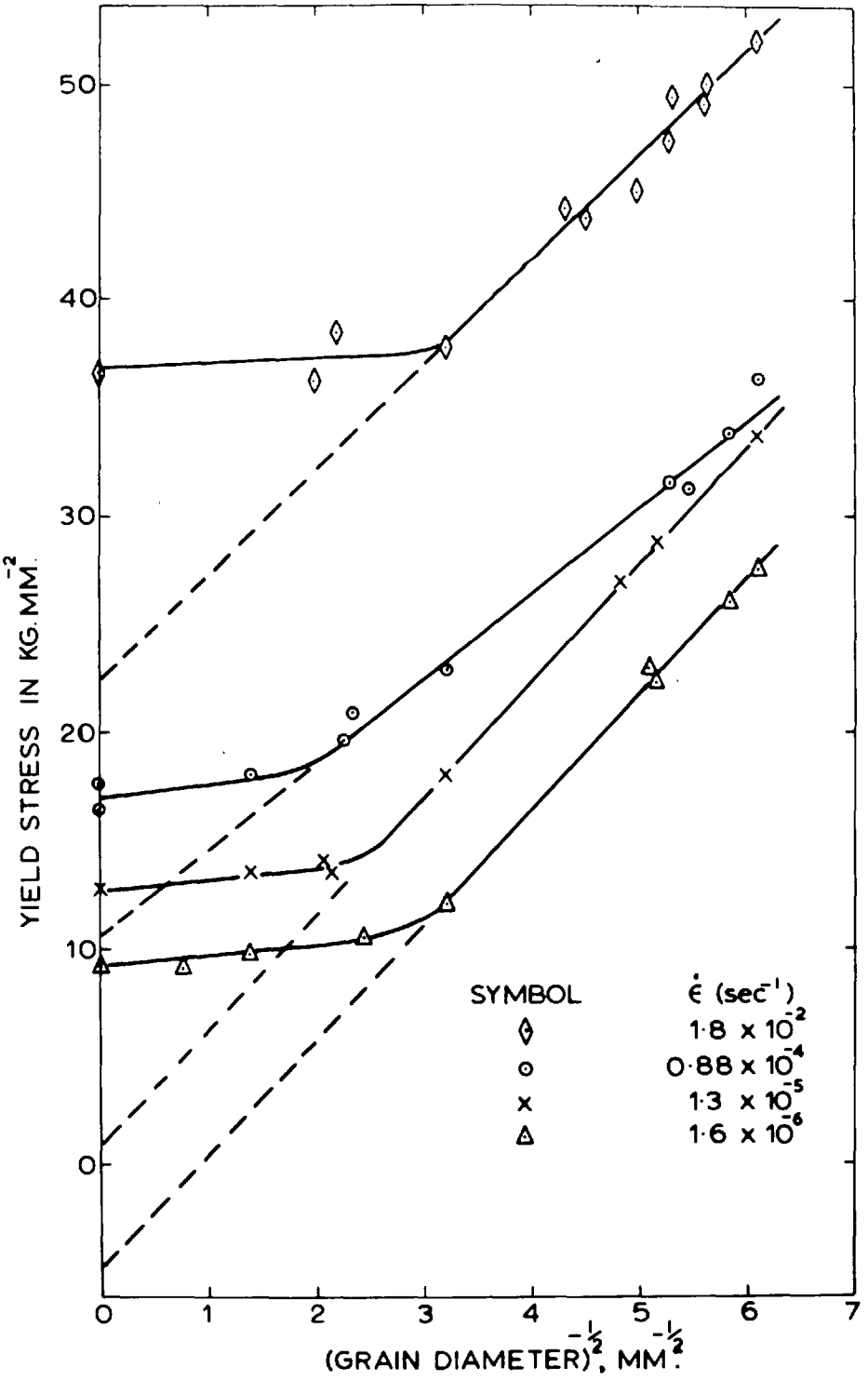

THE EFFECT OF STRAIN RATE ON THE PETCH RELATION OF MOLYBDENUM AT 293°K (INGOT 2).

FIG.22

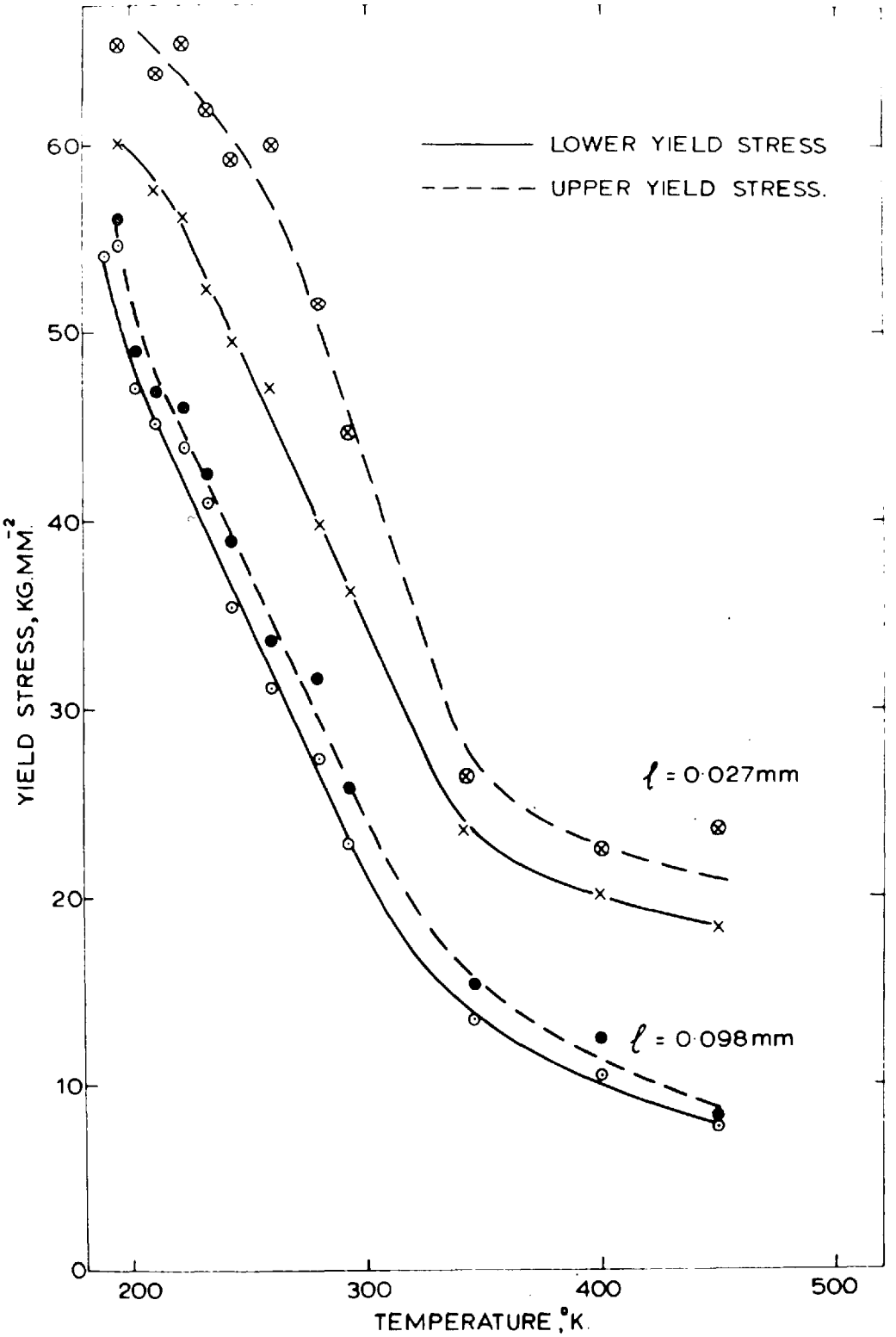

THE EFFECT OF TEMPERATURE ON THE YIELD STRESS OF MOLYBDENUM AT A STRAIN RATE OF $0{\cdot}88 \times 10^{-4}\ sec^{-1}$ (INGOT 2)

FIG.23

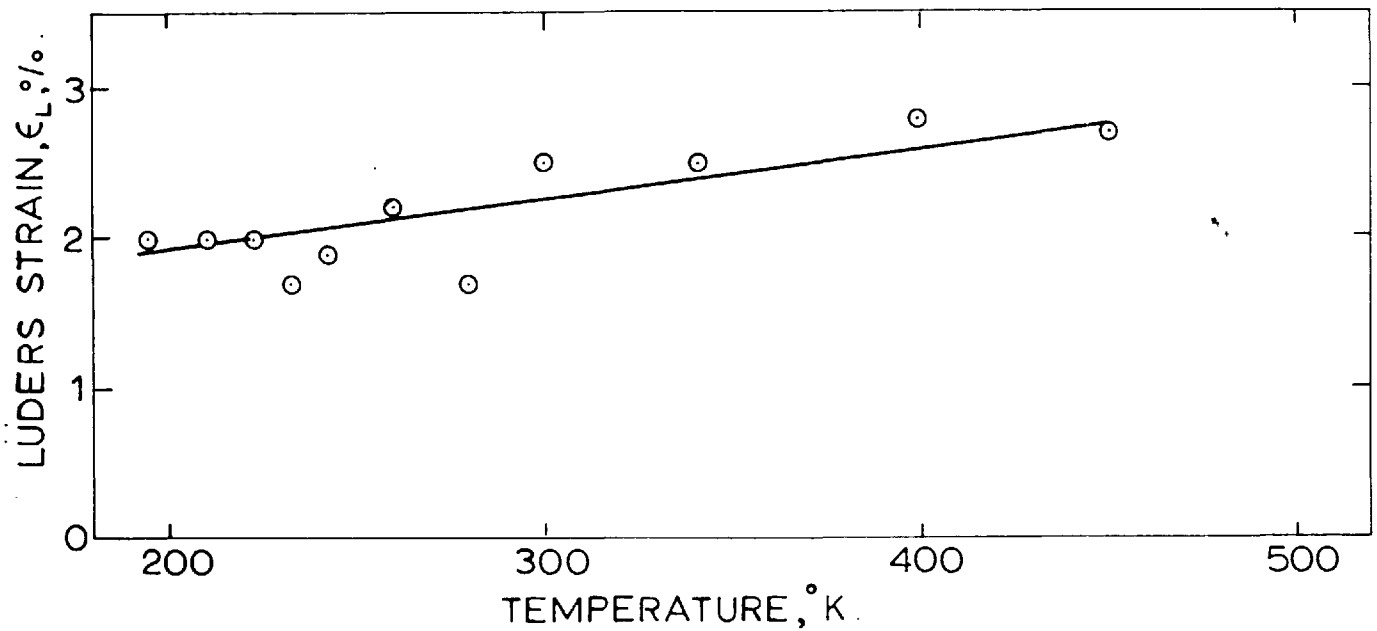

THE EFFECT OF TEMPERATURE ON THE LUDERS STRAIN OF MOLYBDENUM WITH A GRAIN SIZE OF 0·027mm. AT A STRAIN-RATE OF $0{\cdot}88 \times 10^{-4}$ sec^{-1} (INGOT 2)

FIG.24

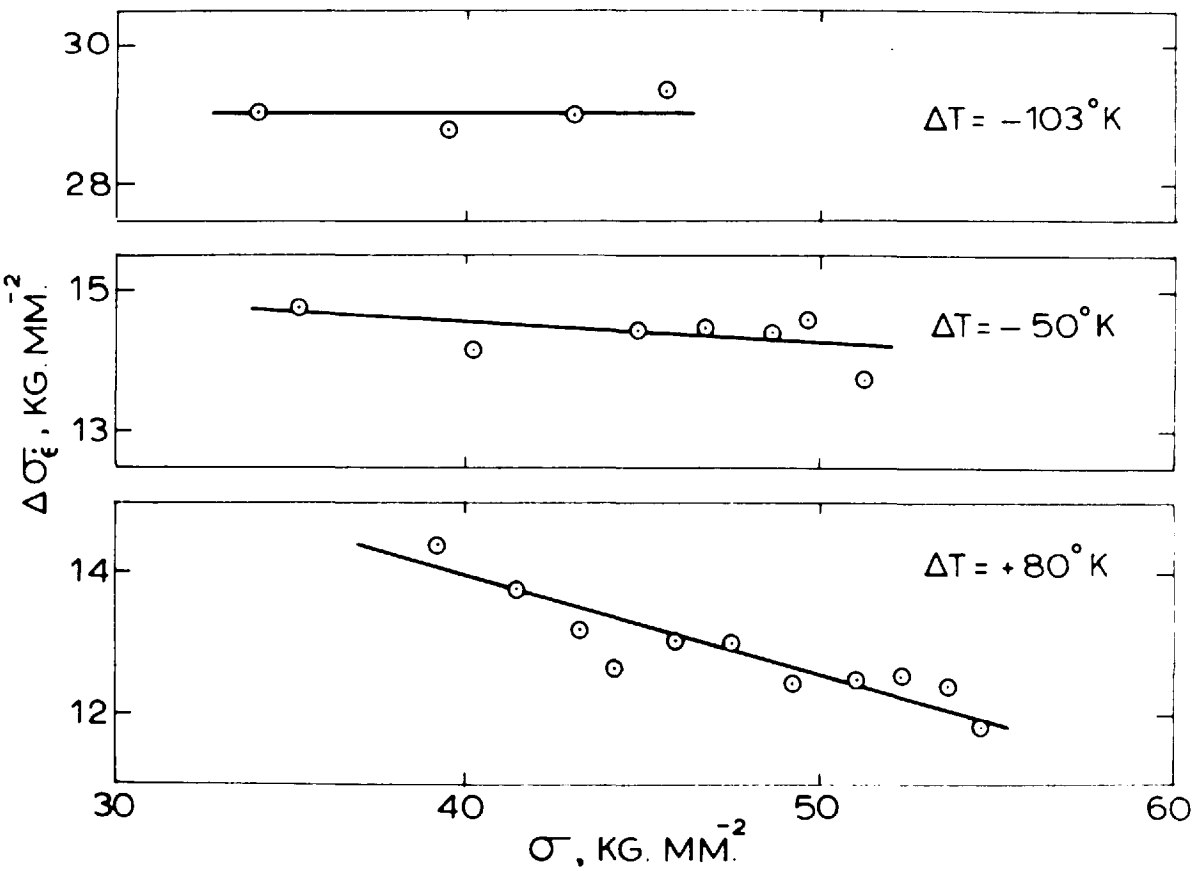

THE EFFECT OF STRESS ON THE REVERSIBLE CHANGE IN FLOW STRESS DUE TO A CHANGE IN TEMPERATURE FROM 293°K FOR MOLYBDENUM WITH A GRAIN SIZE OF 0·027mm AT A STRAIN RATE OF $0{\cdot}88 \times 10^{-4}$ sec^{-1} (INGOT 2)

FIG.25

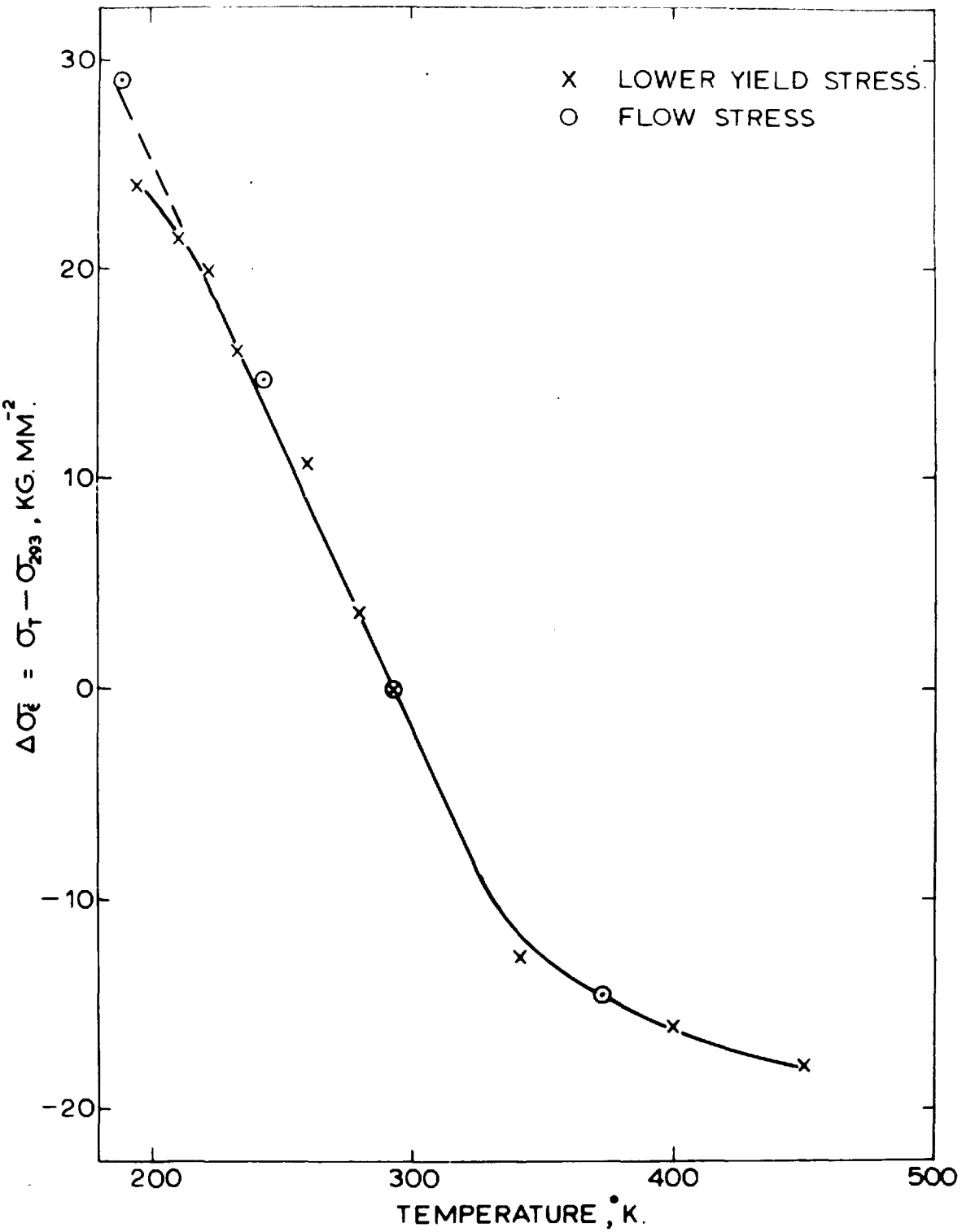

THE EFFECT OF TEMPERATURE ON THE LOWER YIELD AND FLOW STRESS OF MOLYBDENUM WITH A GRAIN SIZE OF 0·027mm AT A STRAIN RATE OF $0{\cdot}88 \times 10^{-4}$ sec^{-1} (INGOT 2).

FIG.26

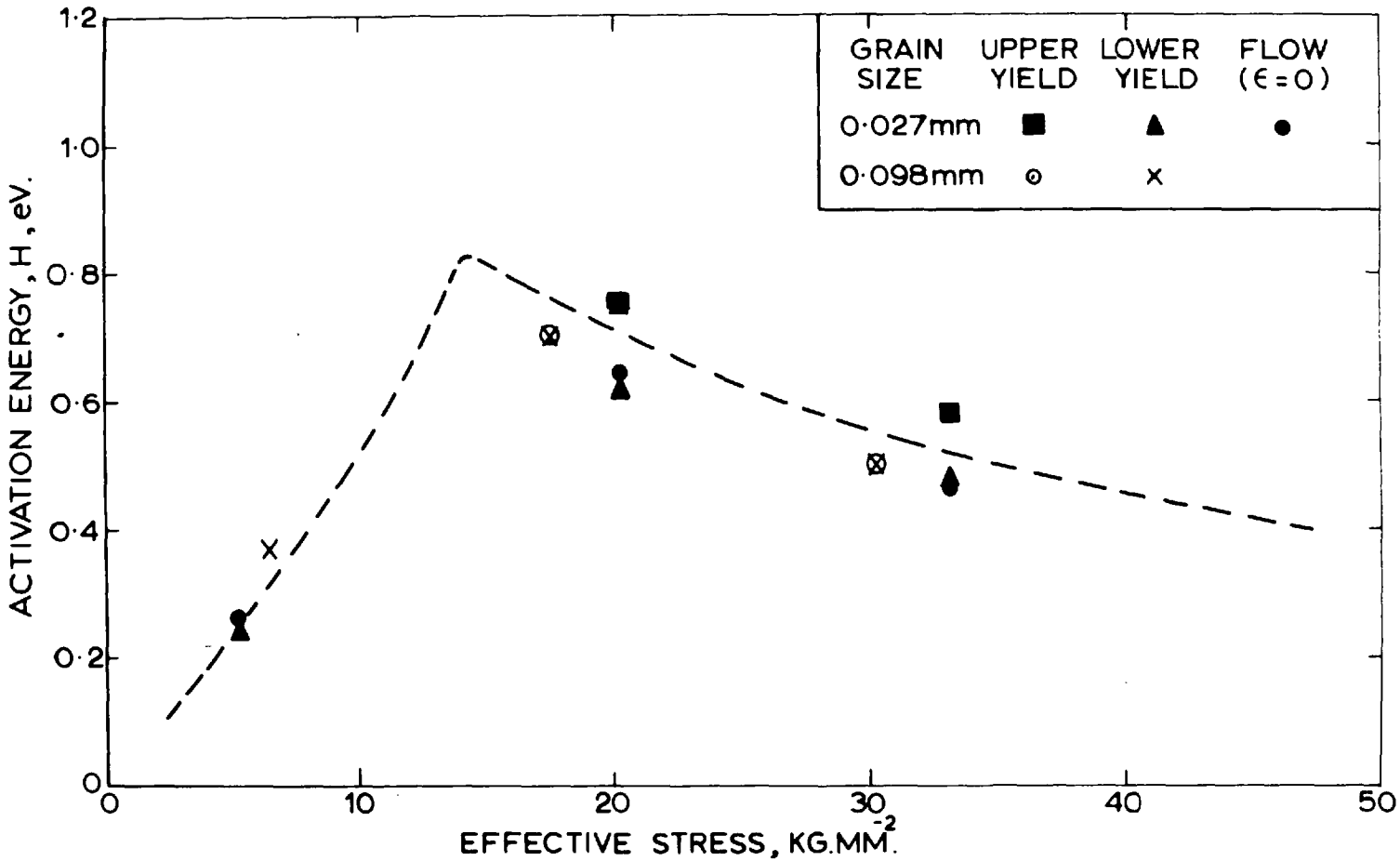

THE STRESS DEPENDENCE OF THE ACTIVATION ENERGY FOR THE YIELDING AND FLOW OF MOLYBDENUM (INGOT 2). THE DASHED CURVE PERTAINS TO EXTRAPOLATED DATA.

FIG.27

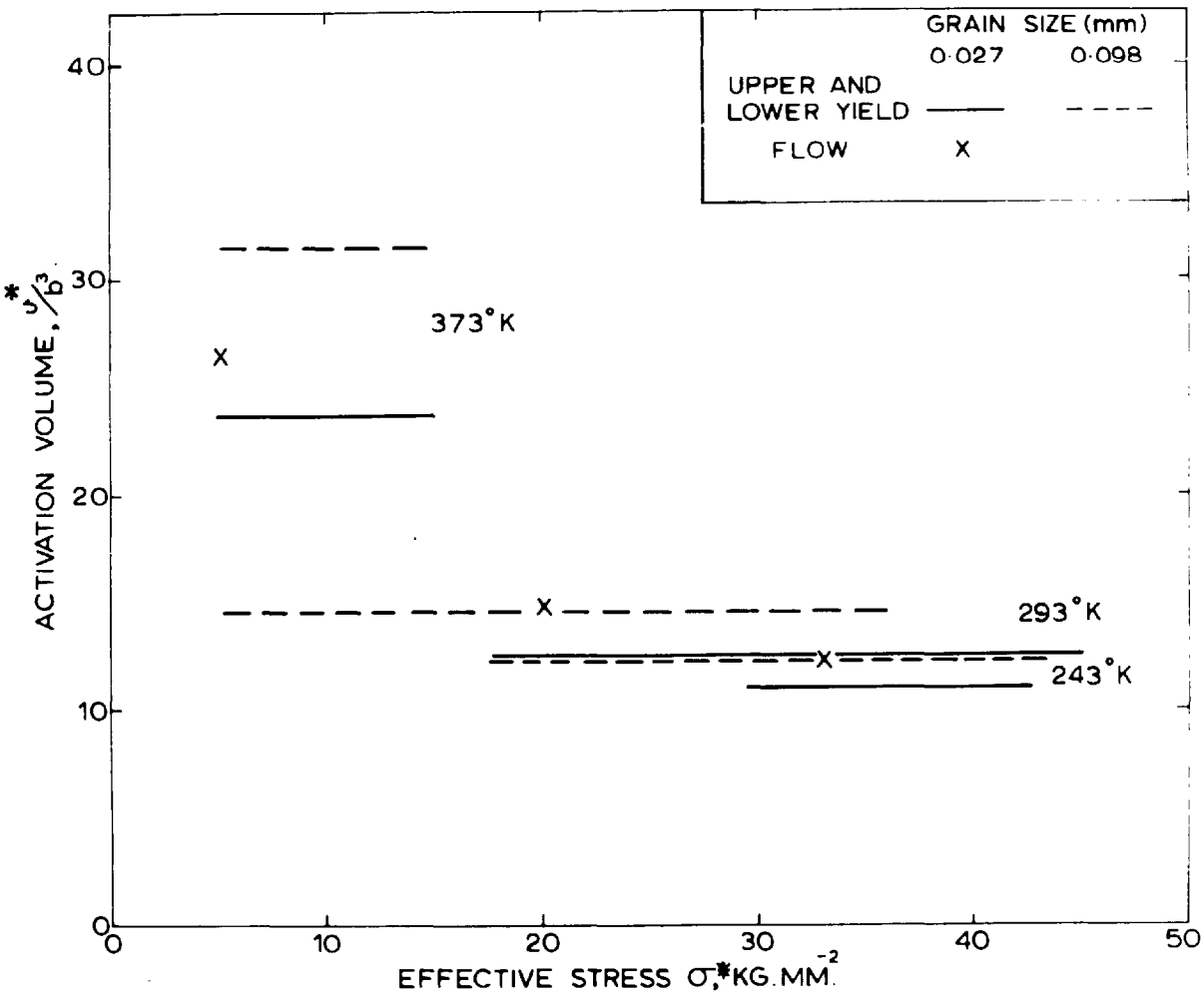

THE STRESS DEPENDENCE OF THE ACTIVATION VOLUME FOR THE YIELDING AND FLOW OF MOLYBDENUM.

FIG.28

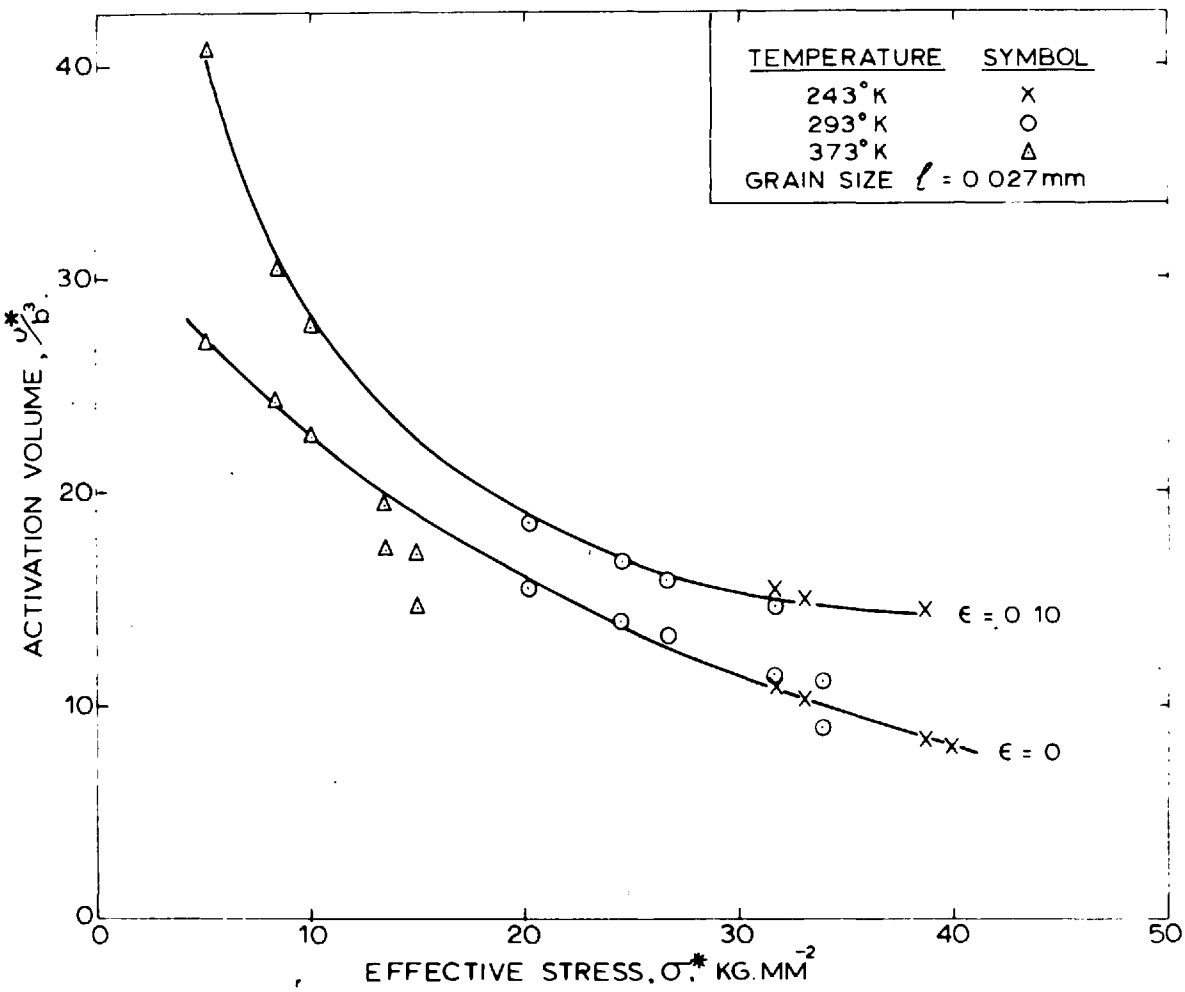

THE STRESS DEPENDENCE OF THE ACTIVATION VOLUME FOR THE FLOW OF MOLYBDENUM FROM BASIC STRAIN-RATE CHANGE EXPERIMENTS

FIG.29

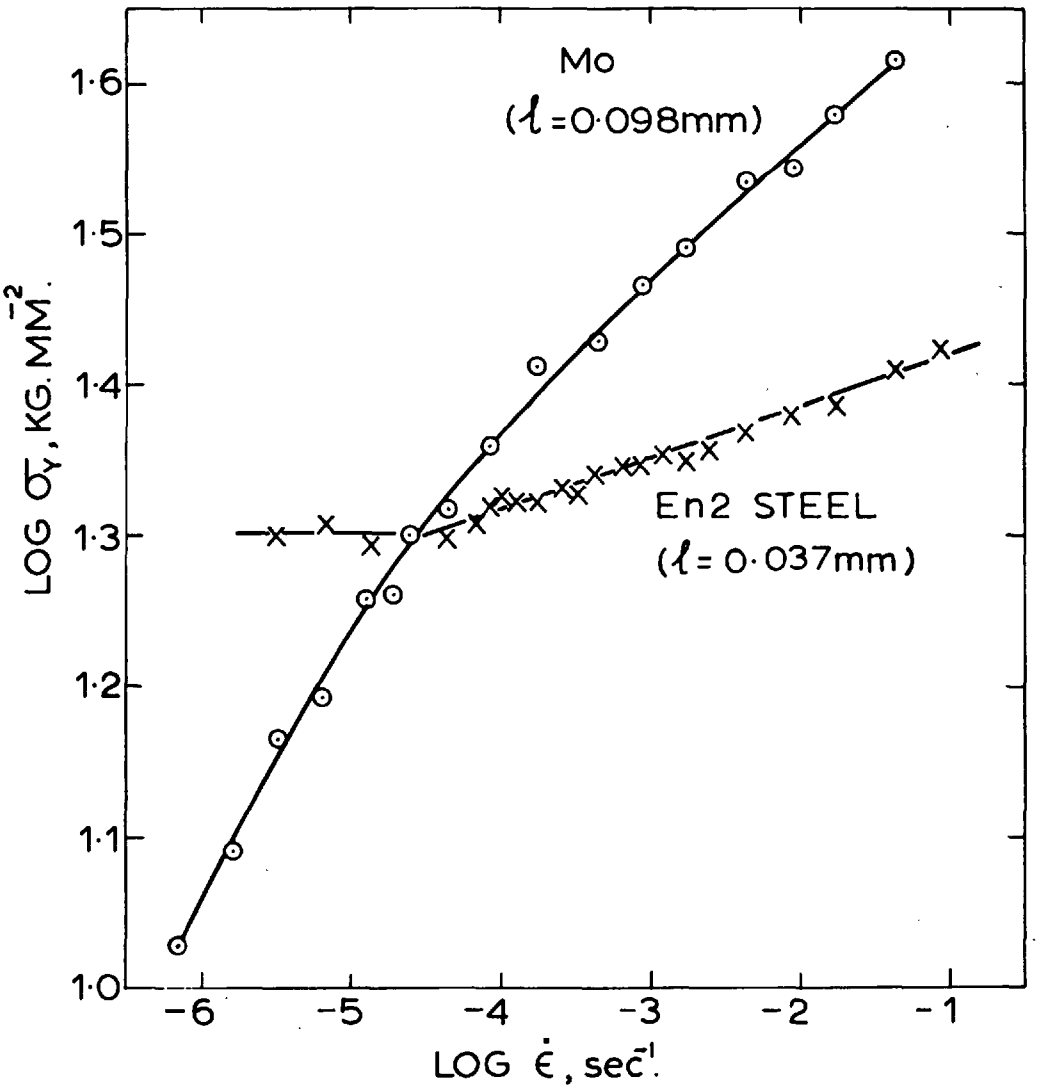

THE EFFECT OF STRAIN RATE ON THE LOWER YIELD STRESS OF MOLYBDENUM AND En2 STEEL AT 293°K.

FIG. 30

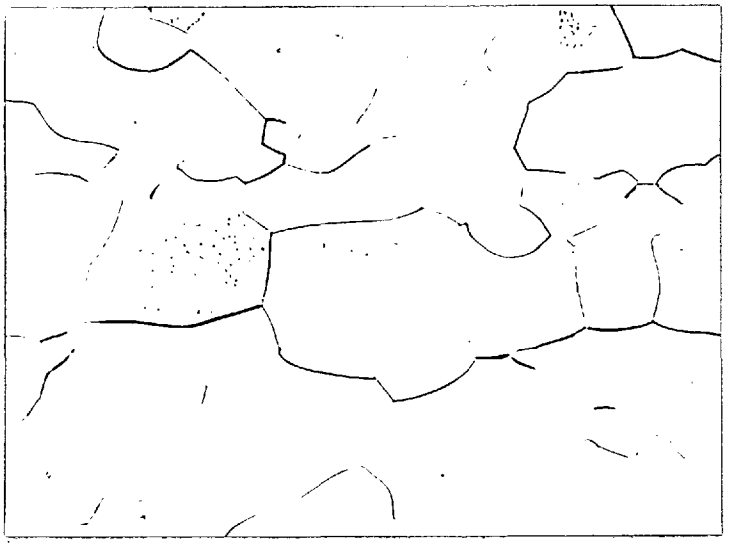

(a)

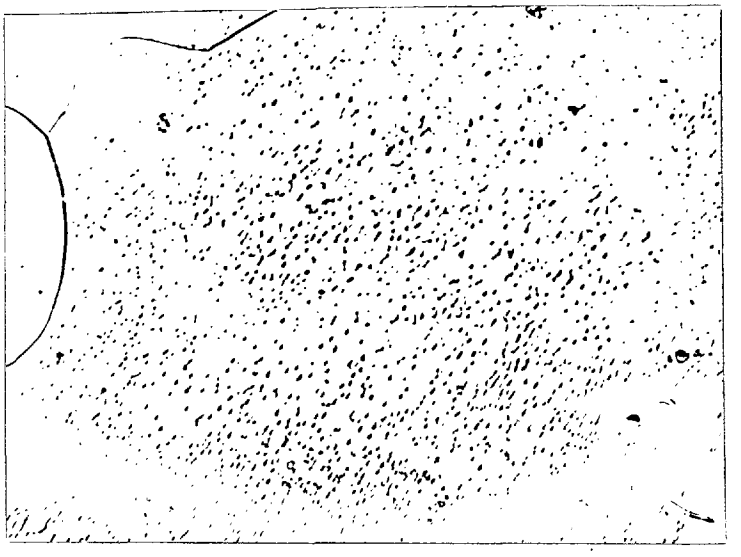

(b)

Dislocation substructure in annealed molybdenum with a grain size of (a) 0.027 mm. and (b) 0.098 mm., revealed by etch-pitting. X 500.

FIG. 31

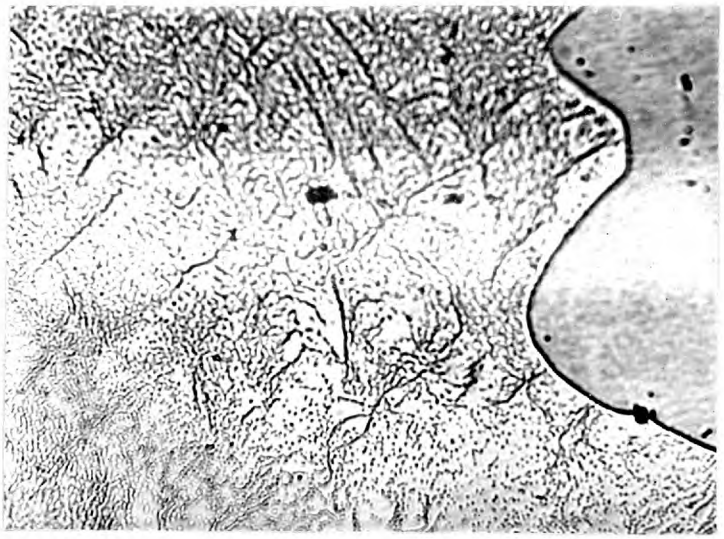

Dislocation substructure in molybdenum with a grain size of 0.098 mm. annealed at 1600°C for 1 hour subsequent to a pre-strain of 5%, revealed by etch-pitting. X 500.

FIG. 32